



Faculty of Health Science

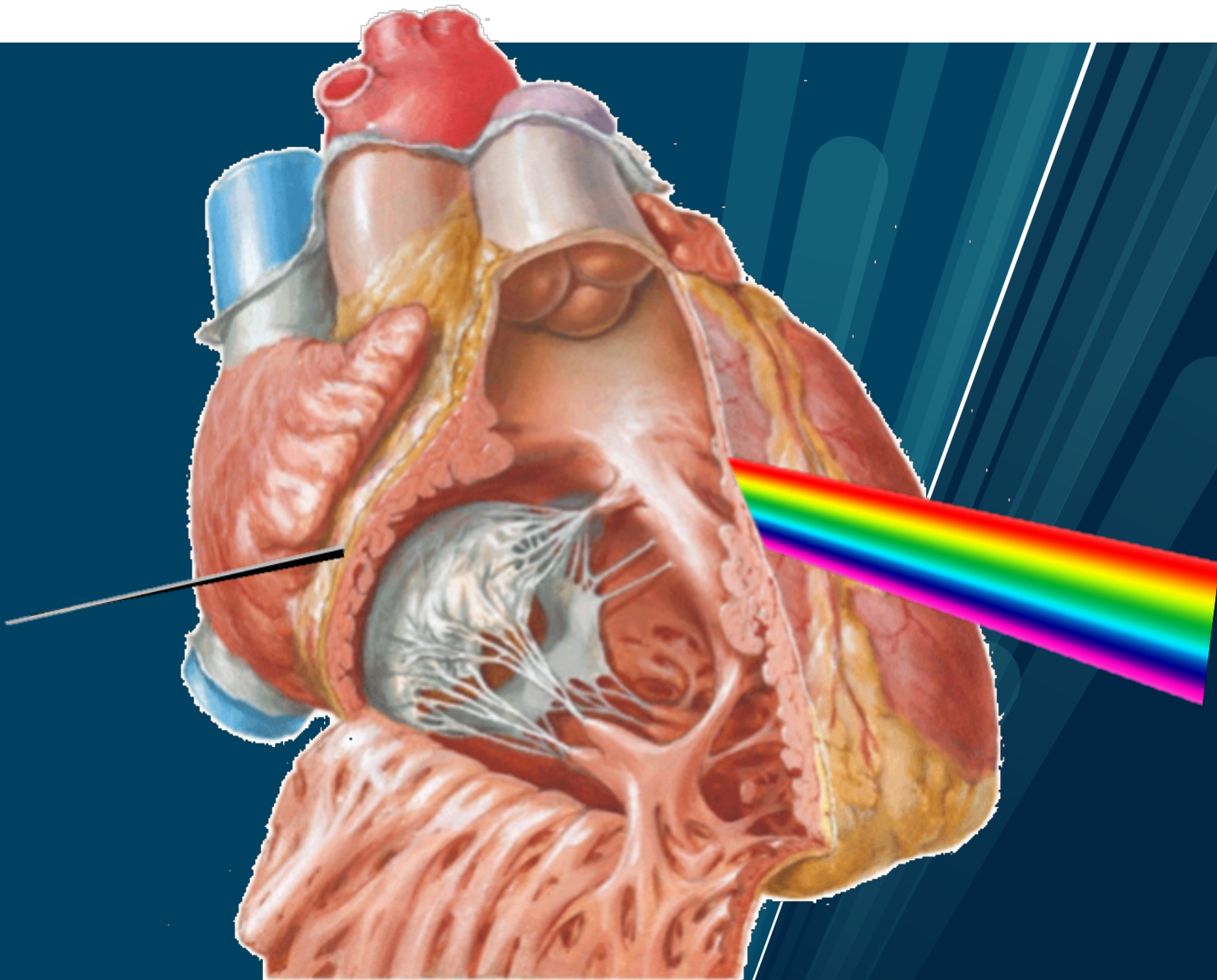
Department of Clinical Medicine

**Guanylate cyclase activators and stimulators. Potential cardiovascular therapeutics, with special focus on the right ventricle.**

Torvind Næsheim

A dissertation for the degree of Philosophiae Doctor May 2022

1







**Guanylate cyclase activators and stimulators.  
Potential cardiovascular therapeutics, with special  
focus on the right ventricle.**

Torvind Næsheim, Cand. Med



A dissertation for the degree of Philosophiae Doctor May 2022

The Arctic University of Norway  
Faculty of Health Science  
Department of Clinical Medicine





# Table of contents

<b>1</b>	<b>Acknowledgements</b> .....	<b>1</b>
<b>2</b>	<b>Selected abbreviations</b> .....	<b>2</b>
<b>3</b>	<b>List of papers</b> .....	<b>4</b>
<b>4</b>	<b>Abstract</b> .....	<b>5</b>
4.1	<i>Background</i> .....	5
4.2	<i>Aims</i> .....	5
4.3	<i>Methods</i> .....	5
4.4	<i>Results and conclusions</i> .....	5
<b>5</b>	<b>Introduction</b> .....	<b>7</b>
5.1	<i>Nitric oxide, NO</i> .....	7
5.1.1	NO-effects .....	7
5.1.2	NO-synthesis.....	8
5.1.3	NO-signaling .....	10
5.1.4	A clinical example: NO non-responders in pulmonary hypertension .....	11
5.1.5	The search for different means of stimulating sGC: sGC-stimulators and sGC-activators.....	11
5.2	<i>Right ventricular failure – potential benefits of sGC effects</i> .....	12
5.2.1	Pathophysiology of right ventricular failure .....	15
5.2.2	Management of RV failure .....	17
5.2.3	Therapy against reversible causes.....	19
5.2.4	Optimization of preload.....	19
5.2.5	Stimulation of cardiac contractility .....	19
5.2.6	Pulmonary arterial vasodilatation .....	22
<b>6</b>	<b>Material and methods</b> .....	<b>23</b>
6.1	<i>NO-blockers</i> .....	23
6.2	<i>Ganglion blocking by using Hexamethonium</i> .....	23
6.3	<i>Pharmacokinetics of Riociguat and Cinaciguat</i> .....	25
6.4	<i>Cardiovascular measurements</i> .....	25
6.4.1	Right ventricular afterload.....	25
6.4.2	Systolic ventricular function .....	26

6.4.3	Diastolic ventricular function .....	28
6.4.4	Echocardiography .....	29
6.4.5	Pressure-volume analysis of cardiac function .....	29
6.4.6	Conductance technique.....	30
6.4.7	Micro sonometric measurements of ventricular volumes .....	32
6.4.8	Cardiac output measurements .....	32
6.4.9	Ventriculo-arterial coupling .....	32
6.4.10	Cardiometabolic efficiency.....	34
6.4.11	Venous compliance and capacitance .....	38
6.4.12	Hepatic resistances.....	42
6.5	<i>Statistics</i> .....	43
<b>7</b>	<b>Aims of the studies</b> .....	<b>47</b>
7.1	<i>Paper 1</i> .....	47
7.2	<i>Paper 2</i> .....	47
7.3	<i>Paper 3</i> .....	47
7.4	<i>Paper 4</i> .....	48
<b>8</b>	<b>Results</b> .....	<b>49</b>
8.1	<i>Paper 1</i> .....	49
8.2	<i>Paper 2</i> .....	49
8.2.1	Hemodynamics in a closed chest model.....	49
8.3	<i>Paper 3</i> .....	51
8.3.1	Hemodynamics in an open chest model.....	51
8.3.2	Cardiometabolic efficiency.....	51
8.4	<i>Paper 4</i> .....	51
8.4.1	Hepatic flows and pressures .....	51
8.4.2	Liver compliance and capacitance .....	52
<b>9</b>	<b>Discussion</b> .....	<b>53</b>
9.1	<i>Discussion of the state of the literature</i> .....	53
9.1.1	Animal studies on Riociguat .....	53
9.1.2	Animal studies on Cinaciguat.....	55
9.1.3	Lessons learned from animal studies of Riociguat and Cinaciguat .....	56
9.1.4	Human studies on Riociguat.....	56
9.1.5	Human studies on Cinaciguat.....	58
9.1.6	Lessons learned from human studies of Riociguat and Cinaciguat .....	59

9.1.7	Summary of the current literature.....	60
9.2	<i>Discussion of the results from our studies</i> .....	60
9.2.1	General hemodynamics .....	60
9.2.2	Interplay with the NO-system.....	61
9.2.3	Cardiac effects of SGC-stimulators and activators .....	62
9.2.4	Cardiometabolic efficiency.....	63
9.2.5	Liver circulation and venous hemodynamics .....	65
<b>10</b>	<b>Strengths and limitations</b> .....	<b>67</b>
10.1	<i>Strengths</i> .....	67
10.2	<i>Limitations</i> .....	67
	<b>Conclusions</b> .....	<b>69</b>
10.3	<i>Paper 1</i> .....	69
10.4	<i>Paper 2</i> .....	69
10.5	<i>Paper 3</i> .....	69
10.6	<i>Paper 4</i> .....	69
<b>11</b>	<b>Future perspectives</b> .....	<b>71</b>
<b>12</b>	<b>References</b> .....	<b>73</b>
<b>13</b>	<b>Papers</b> .....	<b>93</b>
13.1	<i>Paper 1</i> .....	95
13.2	<i>Paper 2</i> .....	107
13.1	<i>Paper 3</i> .....	123
13.2	<i>Paper 4</i> .....	137

## Figures and Tables

Figure 1	Principal end organ effects of different concentrations of nitric oxide.....	8
Figure 2.	Principal effector sites for Nitric Oxide, sGC-stimulators and sGC-activators and the interaction with redox-state. ....	12

Figure 3 Mechanisms of right ventricular failure including therapeutic options. ....	16
Figure 4 Therapeutic options in right ventricular failure. ....	18
Figure 5 Principal effects of vasoconstrictors, vasodilators and inotropes in right ventricular failure..	21
Figure 6. Effector site of Hexamethonium and its interaction with the autonomous nervous system..	24
Figure 7. Simultaneous pressure and volume measurements of the right ventricle during deloading through occlusion of the inferior vena cava.. ....	27
Figure 8. Preload recruitable stroke work . ....	28
Figure 9. Ventriculo-arterial coupling between left ventricle and the aorta.....	33
Figure 10. Instrumentation to obtain data for cardiac metabolic efficiency.....	35
Figure 11. Data from study 2 with comparison of the difference in stroke work and potential energy between baseline and medication with Riociguat or L-NAME.....	36
Figure 12. Relationship between measured oxygen consumption and total work of the heart with comparison of baseline and Riociguat and Riociguat and L-NAME.....	37
Figure 13. Instrumentation for measurement of hepatic flows, pressures and resistance. ....	39
Figure 14. Measurements done during occlusion of hepatic venous flow.. ....	40
Figure 15, Plots of liver blood volume increment again mean hepatic thickness and hepatic lobulus venous pressure and estimated liver blood volume .....	41
Figure 16. Comparison of univariate anova, multivariate anova and mixed models. ....	44
Figure 17. Principal example where simple linear regression would yield a negative correlation between the x- and y-axis although each individual shows a positive correlation with different slopes and different intercepts.....	45
Table 1 Association between right heart and left heart pathology and consequence for prognosis.....	14
Table 2. Data from study 2.....	50
Table 3. Animal studies on riociguat.....	54
Table 4. Animal studies on cinaciguat. ....	56
Table 5. Human studies on riociguat .....	58
Table 6. Human studies on cinaciguat.....	58



# 1 Acknowledgements

The practical work of this thesis has been carried out at the Department of Clinical Medicine at the Faculty of Health Science at the Arctic University of Norway between 2011 and 2017 and have been financed by the Arctic University of Norway. I have had the opportunity of combining preclinical research with clinical work at the Department of Anesthesiology and Intensive Care as well as at the Department of Emergency medicine at the University Hospital of North Norway.

My main interest in clinical medicine is hemodynamics in critical ill patients. As a cardiothoracic anesthesiologist I have had ample opportunities to observe all aspects of deranged circulation in patients both in the operation theatre as well as in the intensive care unit. The problems of right ventricular failure have always intrigued me. Often, I have encountered and tried to solve these clinical puzzles in cooperation with professor Truls Myrmel, so he was aware of my curious soft spot. When professor Myrmel approached me with a suggestion of conducting a series of large animal experiments into the abyss of right ventricular function and failure, it was impossible for me to decline. His well-known stamina when facing the unexplainable and unsolvable has been an everlasting inspiration for me both in clinical work and academia.

The next prerequisite and inspiration in this process has been Ole-Jakob How. I have been leaning heavily on his vast knowledge on animal models and scientific thinking. His ability to refine airy, general questions into testable hypothesis and further into publications has been invaluable. Furthermore, the staff at the surgical research laboratory have contributed with practical assistance and have lifted my spirits on grey days. A special thanks to Knut Steinnes for his patience when helping me with the setup of the animal lab and producing illustrations for my publications. Thank you for all constructive discussions with and practical assistance from my research colleagues Jens Petter Bakkehaug and Anders Kildal.

I also owe thanks to my clinical colleagues at UNN, and especially the small group of cardiothoracic anesthesiologists, for putting up with my partial mental and physical absence these years.

My partner, Anna Bågenholm, started her PhD-journey well after me and, to her outspoken delight, finished well in advance of me. She has been an inspiration through the whole process and have pushed me to keep an eye on the goal in a world packed with distractions.

## 2 Selected abbreviations

### Table of Abbreviations

ANOVA	Analysis of variance
ANP	Atrial natriuretic peptide
ATP	Adenosine triphosphate
CF	Cystic fibrosis
cGMP	Cyclic guanosine monophosphate
CI	Cardiac index
CO	Cardiac output
CTEPH	Chronic thromboembolic pulmonary hypertension
CVP	Central venous pressure
EDP	End diastolic pressure
EF	Ejection fraction. The volumetric difference between diastole and systole
ENOS	Endothelial nitric oxide synthetase
ESP	End systolic pressure
ESPVR	End systolic pressure-volume-relationship
ESV	End systolic volume
ET	Endothelin
GMP	Guanosine mono phosphate
GTP	Guanosine tri phosphate
ICU	Intensive care unit
LAD	Left anterior descending coronary artery
LVAD	Left ventricular assist device
MAP	Mean arterial pressure
MPAP	Mean pulmonary arterial pressure



MR	Magnetic resonance imaging
NO	Nitric oxide
NOS	Nitric oxide-synthetase
PA	Pulmonary artery
PAH	Pulmonary arterial hypertension
PDE	Phosphodiesterase
PE	Pulmonary embolism
PEEP	Positive end expiratory pressure
PI	Pulsatile index
PRSW	Preload recruitable stroke work
PVA	Pressure volume area
PVR	Pulmonary vascular resistance
RA	Right atrium
RCA	Right circumflex artery
RCT	Randomized controlled trial
RV	Right ventricle
SGC	Soluble guanylate cyclase
SGCA	Soluble guanylate cyclase activator
SGCS	Soluble guanylate cyclase stimulator
SNP	Sodium nitroprusside
SV	Stroke Volume
SW	Stroke Work
VAC	Ventriculo-arterial coupling
VSMC	Vascular smooth muscle cells

### 3 List of papers

Næsheim T, How O-J, Myrmel T. Propulsion of blood through the right heart circulatory system. *Scandinavian Cardiovascular Journal* [Internet]. Informa UK Limited; 2017 Nov 30;52(1):4–12.

Næsheim T, How OJ, Myrmel T. Hemodynamic Effects of a Soluble Guanylate Cyclase Stimulator, Riociguat, and an Activator, Cinaciguat, During NO-Modulation in Healthy Pigs [published online ahead of print, 2020 Jul 14]. *J Cardiovasc Pharmacol Ther*. 2020;1074248420940897.

Naesheim T, How OJ, Myrmel T. The effect of Riociguat on cardiovascular function and efficiency in healthy, juvenile pigs. *Physiol Rep*. 2020 Sep;8(17):e14562

Næsheim T, How O-J, Myrmel T: The effect of Riociguat and Cinaciguat on liver blood flow in healthy anesthetized pigs during NO-modulation. Manuscript to be submitted.

## **4 Abstract**

### **4.1 Background**

Soluble guanylate cyclase, sGC, is a major contributor to the signal transduction in the cardiovascular system, and dysfunction in the NO-sGC-cGMP signaling plays an important role in cardiovascular disease. This system is sensitive to a wide variety of pathological conditions spanning from substrate shortage to sGC-insensitivity to nitric oxide (NO), during pathological oxidative states. SGC-activators (sGCA) and -stimulators (sGCS) bypass the need of NO for sGC-activation. Furthermore, both compounds stimulate sGC despite high oxidative states and represent an alternative pathway to induce cGMP-production and a potential target to restore cGMP-signaling during pathological conditions.

### **4.2 Aims**

Pharmacological principles acting through the NO-sGC-cGMP-pathway have been extensively utilized in cardiac failure therapy. This includes NO-donors and PDE inhibitors. These drugs have limitations in pathological conditions, both regarding effect and tolerability. Direct sGC stimulation and activation represents a promising principle to overcome these challenges. We therefore addressed cardiovascular effects of the guanylate cyclase stimulator Riociguat and the guanylate cyclase activator Cinaciguat using large animal models.

### **4.3 Methods**

Healthy pigs were instrumented for systemic and pulmonary hemodynamic measurements. The hemodynamic effects were investigated in a closed chest model through a dose finding study. We then made repeated measurements during administration of sGCA and sGCS with additional manipulation of NO-tone using nitroglycerin (NO-infusion) and L-NAME (N-nitro-L-arginine methyl ester, a NO-blocker). Subsequently, we assessed the effects of sGCA and sGCS on cardiac energy metabolism in an open chest model. Finally, we evaluated the influence of these drugs on venous vascular compliance and liver blood flow in a closed chest, open abdomen model.

### **4.4 Results and conclusions**

Our experiments confirm the principal pharmacological properties of Riociguat and Cinaciguat as potent systemic arterial vasodilators without pulmonary selectivity or inotropic

effects. The direct cardiac effects are limited to a minor diastolic alteration possibly related to changes in vascular loads. No major effect on venous vascular tone could be discerned in our large animal model. Importantly, while Riociguat acts in concert with NO and is modulated by NO-tone, Cinaciguat works independent of the NO-system and blocks the physiological NO-tone in the vascular system.

## **5 Introduction**

### **5.1 Nitric oxide, NO**

#### **5.1.1 NO-effects**

NO is a ubiquitous molecule in vertebrates and normal NO-signaling is important to cellular and organ homeostasis<sup>1</sup>.

NO primarily acts as a vasodilator, but NO will also inhibit platelet activation and leucocyte activation. Furthermore, NO interacts with the respiratory chain<sup>2</sup> and has direct effects on cardiac contractility<sup>3</sup>. In the central nervous system, NO affects neurotransmission in glutaminergic nerves<sup>4</sup> and is involved in macrophage function<sup>5</sup>. S-nitrosothiol species have been implicated in controlling oxygen delivery to tissues, and modulating both the function and activity of transcription factors, enzymes, and ion channels<sup>6</sup>.

Increased activation of NOS is part of various pathological responses. High levels of NO are seen during inflammation and vasoplegia and can have neurotoxic effects in stroke and neurodegenerative conditions<sup>7</sup>. Lack of NO, on the other hand, is integral to hypertension and atherosclerosis<sup>8</sup> (Figure 1).

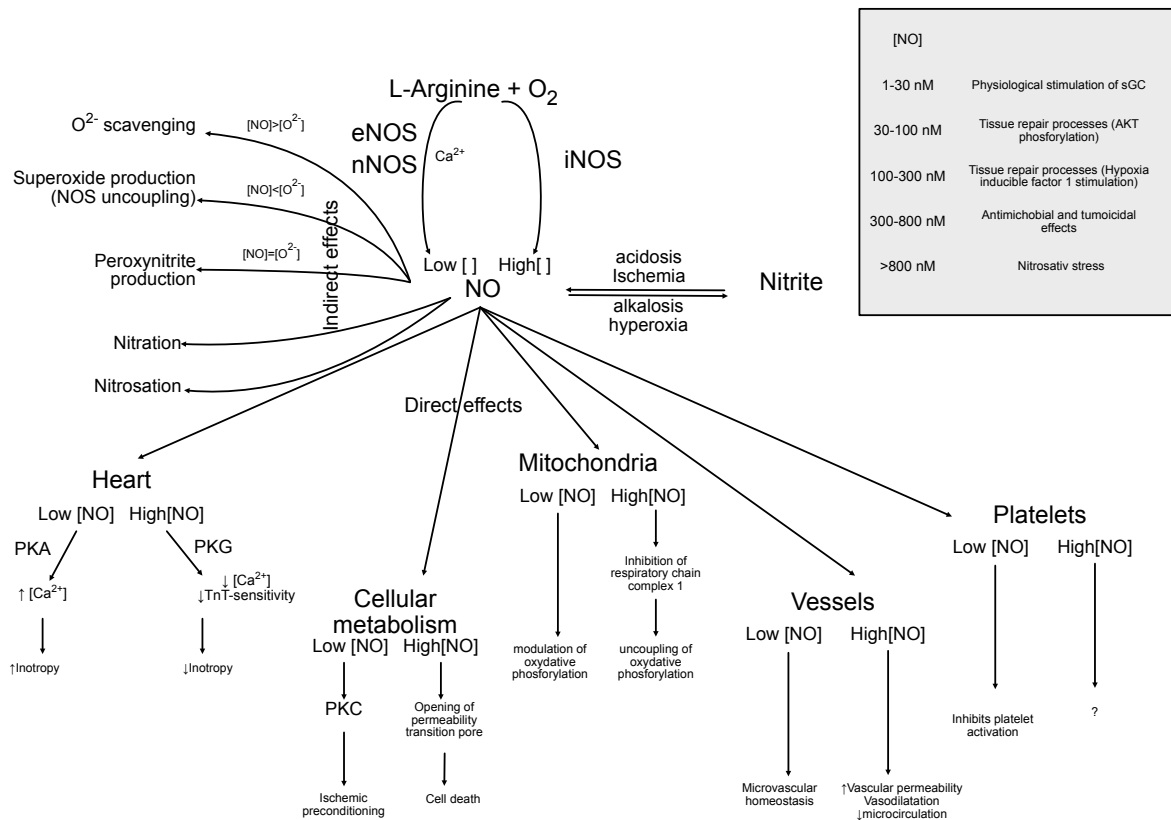


Figure 1 Principal end-organ effects of different concentrations of nitric oxide, NO. eNOS is endothelial nitric oxide synthetase, nNOS is neuronal nitric oxide synthetase, iNOS is inducible nitric oxide synthetase, PKA is phosphokinase A, PKC is phosphokinase C, PKG is phosphokinase, AKT is v-AKT-oncogene, or protein kinase B.

### 5.1.2 NO-synthesis

NO is formed by a two-step oxidation from L-arginine, catalyzed by NO-synthetase (NOS) (Figure 1). NOS exists in three isoforms. L-arginine is available through the diet but is also synthesized from citrulline<sup>9</sup>. Nitrite has recently been shown to be a reservoir of NO in the circulation, and may in fact be the most important such source of NO. NO production dependent on availability of L-arginine, activity of NOS enzymes and availability of necessary cofactors<sup>10</sup>

NO can also be formed at the tissue level, during ischemic conditions, via a nonenzymatic pathway:  $e^- + 2H^+ + NO_2^- \rightarrow NO + H_2O$ . The capacity of this pathway is comparable to the enzymatic pathways<sup>10</sup>

Bioavailability and regulation of NO is under influence of transcriptional and post-translational control (phosphorylation, acetylation, protein-protein regulation, s-nitrosylation and S-glutathionylation) as well as red-ox regulation. The half-life in blood is short (< 1 sec) due to quick inactivation via hemoglobin, superoxide or oxidation <sup>11</sup>

Endothelial NOS (eNOS) is localized to the endothelium of blood vessels, cardiomyocytes, platelets, and erythrocytes. eNOS is activated by shear stress and stretch through transmembrane components of glycocalyx or by increased intracellular calcium <sup>12</sup>. eNOS-NO-signaling in red blood cells is responsible for downstream effects of NO and vasodilating effects in hypoxic tissues <sup>12</sup>. In addition, eNOS is involved in stretch-induced increased in contractility (Anrep-effect) <sup>13</sup> and can also influence basal contractility and  $\beta$ -adrenergic responses in a dose-dependent biphasic pattern <sup>14</sup>.

Neuronal NOS (nNOS) is primarily located to the neuronal system. Stimulation of nNOS tips the balance in the autonomic nerve system in the direction of increased parasympathetic tone <sup>12</sup>. However nNOS is also found in cardiac myocytes, where it is localized in the sarcoplasmic reticulum and modulates calcium influx <sup>15</sup>.

eNOS and nNOS activity have been shown to have cardioprotective properties during ischemia-reperfusion. The mechanisms of protection include reduced adrenergic sensitivity, reduced Ca<sup>2+</sup> overload, and inhibition of oxygen radical production. These effects offers both acute protection of the myocardium and leads to changes in remodeling during chronic conditions of pathology. On the other hand, excessive NO production during ischemia may exacerbate tissue injury through NOS uncoupling and increased oxygen radical production. In addition, reduced eNOS and nNOS activity seems to increase the risk of cardiac arrhythmias. High doses can cause uncoupling of oxidative phosphorylation and opening of a mitochondrial permeability transition pore with resulting cell death <sup>16,17</sup>.

Inducible NOS (iNOS) is primarily found in macrophages and connected to inflammatory responses. While eNOS and nNOS activation is dependent on intracellular calcium levels<sup>18</sup>, iNOS-activity is dependent only on the expression of enzyme levels, and has the capacity of high conversion rate to NO until exhaustion of available arginine and cofactors <sup>19</sup>.

In sepsis derangement of normal NO homeostasis contributes to microvascular heterogeneity and failure of oxygen delivery<sup>20</sup>. Increase levels of the endogenous NO-inhibitor ADMA is found in sepsis patients and can contribute to this picture<sup>21</sup>. In sepsis and trauma patients

lowered levels of arginine and citrulline have been found, pointing to reduced NO production as well<sup>22</sup>.

In pulmonary injury, iNOS and nNOS inhibition can improve gas exchange, lung compliance and lung edema<sup>23</sup>

### 5.1.3 NO-signaling

NO stimulates metal complexes as alkyl radicals and guanylate cyclase, cytochromes and lipid radicals. Indirect effects exist in the form of nitration, nitrosation and reactions with oxidative radicals. Interaction with oxygen radicals is dependent on both oxidative stress and NO-concentration. Indirect effects result in Ca<sup>2+</sup> regulation or post-translational changes to intracellular proteins<sup>24</sup>

NO binds reversibly and with a short half-life (0,2 s) to the red-ox sensitive enzyme soluble guanylate cyclase (sGC) and catalyzes the conversion of guanosine tri phosphate (GTP) to cyclic guanosine mono phosphate (cGMP) (Figure 2). The membrane bound form of guanylate cyclase is not stimulated by NO but is stimulated by atrial natriuretic peptide (ANP). sGC consists of a heme-binding  $\beta$ -unit and a larger  $\alpha$ -unit. NO binds to the heme-unit on the  $\beta$ -unit (Figure 2). sGC exists in three red-ox configurations. In the physiological state sGC contains Fe<sup>2+</sup> bound to the heme moiety. Through oxidation the iron ions are first oxidized to Fe<sup>3+</sup> and at the highest oxidation step the heme-group and iron ion is lost. The affinity for NO is the highest in the most reduced form of sGC and NO cannot stimulate sGC in its most oxidized form<sup>25,26</sup> (Figure 2).

Cyclic GMP downstream stimulates phosphokinase G (PKG) leading to vasodilatation, antiproliferation, antifibrosis and antiinflammation<sup>27</sup>. The levels of cGMP are regulated by phosphodiesterases (PDEs) which catalyzes the breakdown of cGMP and cyclic adenosine monophosphate cAMP selectively or non-selectively. Protein kinase G (PKG) exist in spatially diversified isoforms with PKG-1 $\alpha$  being the dominant isoform in VSMC and cardiomyocytes, causing vasodilatation and lusitropy through a Ca<sup>2+</sup>-lowering mechanisms (mostly reuptake into the sarcoplasmic reticulum via the SERCA channel) and lowering myofilament Ca<sup>2+</sup> sensitivity<sup>28</sup>.

In addition to the effects mediated by sGC, direct binding of NO to a thiol group on other proteins (s-nitrosylation) forming S-nitrosothiol (SNO) have cardiovascular effects



independent of cGMP, for instance on Ca<sup>2+</sup> handling and sensitivity. SNO even modulates the activity of sGC <sup>29</sup>.

Nitrosative stress and inactivation due to oxidation of sGC are the main mechanisms of NOS-NO dysfunction. Stimulation of all NOS isoforms in the absence of substrate for NO-formation will lead to uncoupling, with synthesis of oxygen radicals <sup>30,31</sup>.

#### **5.1.4 A clinical example: NO non-responders in pulmonary hypertension**

The effect of NO-administration to patients in need of pulmonary vasodilatation is variable. In a clinical study of inhaled NO as therapy against pulmonary arterial hypertension (PAH) in 26 patients with acute right heart failure, only 14 responded by reduction of pulmonary vascular resistance (PVR) and/or increase in cardiac output (CO). The diagnosis did not differ between the groups <sup>32</sup>. One explanation for this observed difference in reactivity of the pulmonary vascular bed to inhaled NO may be different red-ox states of sGC in the different patients. A high degree of oxidative stress, and deactivation of sGC by oxidation could account for reduced effect of NO in the non-responders.

#### **5.1.5 The search for different means of stimulating sGC: sGC-stimulators and sGC-activators**

To overcome the limitations of NO as a sGC-stimulator, scientists at Bayer Healthcare screened 20.000 compounds for their ability to stimulate or activate oxidized isoforms of sGC. Stimulators work in concert with NO on sGC with an intact heme group, while activators, as a principle, only work in the absence of the heme group. After several iterations the activator Cinaciguat and stimulator Riociguat were chosen for their potential clinical utility <sup>33</sup>. New classes of stimulators and activators are being intensively researched with substance patent applications from Astella, Bayer, Cyclerion, Merck and others <sup>34</sup>. Patent applications have been filed for a wide variety of diseases including cardiopulmonary and cardiorenal diseases, urological diseases, systemic sclerosis, cystic fibrosis, Duchenne muscular dystrophy, osteogenesis imperfecta, metabolic diseases, , fibrotic disease, cognitive dysfunction, sensoric disease and achalasia <sup>34</sup>.

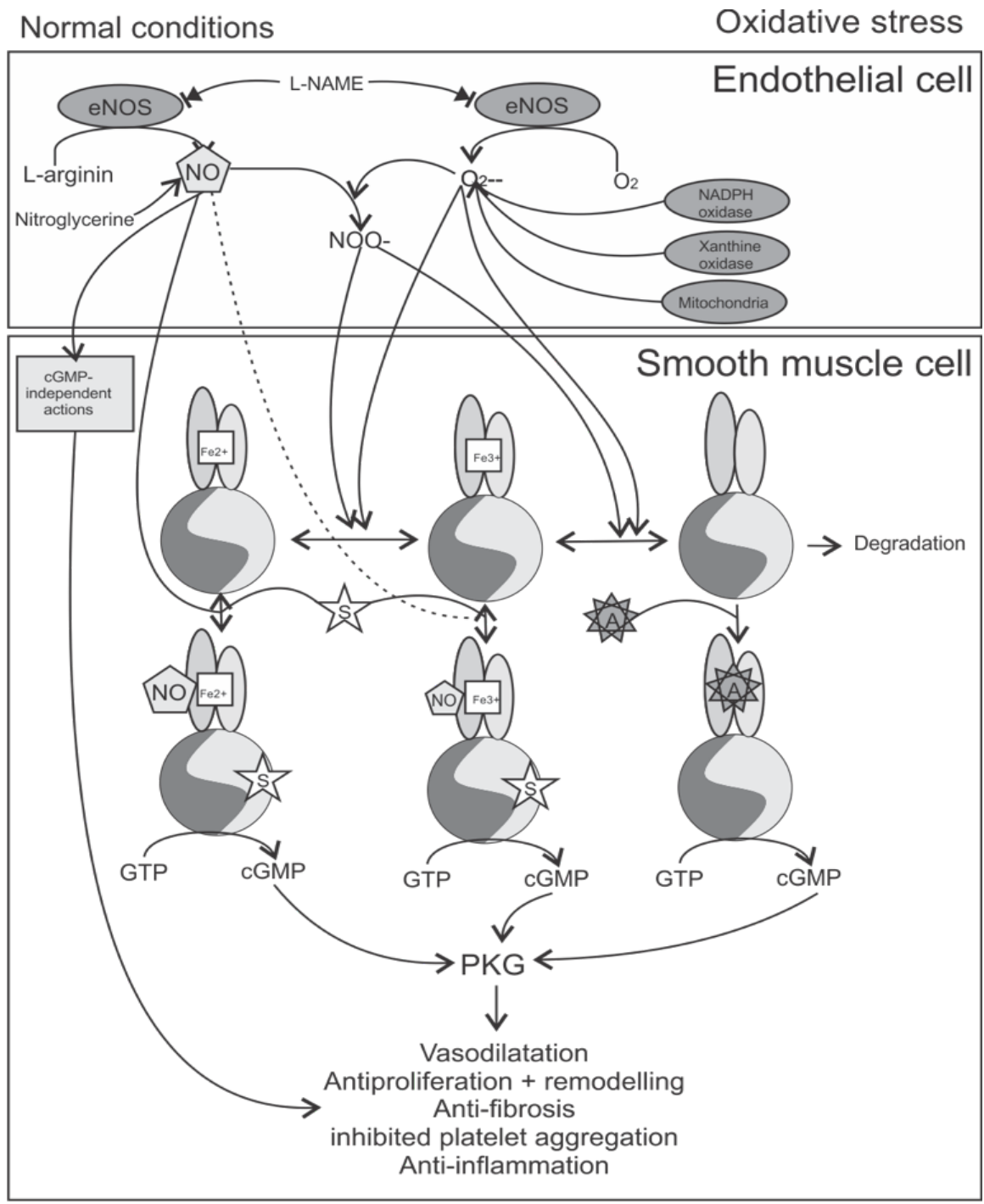


Figure 2. Principal effector sites for Nitric Oxide (NO), sGC-stimulators (S) and sGC-activators (A) and the interaction with redox-state. PKG is phosphokinase G, eNOS is endothelial nitric oxide synthetase. Inspired by reference <sup>35</sup>.

### 5.2 Right ventricular failure – potential benefits of sGC effects

Failure of the right ventricle is known to worsen the prognosis of patients with symptomatic heart failure <sup>36</sup> as shown in Table 1. The primary mechanism in the development of right

ventricular failure is an increase in right ventricular workload, which is a consequence of constriction and stiffening of the pulmonary vasculature, thromboembolism, hypoxic vasoconstriction or left ventricular failure<sup>37</sup>. Transmission of blood through the right heart is therefore highly dependent on vascular tone and therefore on the NO-physiology.

Other causes of right heart failure are contractile failure due to ischemia or inflammation, volume overload due to right sided valve failure or increase in venous return and displacement of the interventricular septum after mechanical unloading of the left ventricle<sup>38</sup>.

<i>Left heart pathology</i>	<i>Incidence of concomitant right ventricular dysfunction</i>	<i>Hazard Ratio for mortality in case of right ventricular dysfunction</i>	<i>Reference</i>
<i>Inferior myocardial infarction</i>	43%	3,2 (2,4-4,1)	Mehta 2001 <sup>39</sup>
<i>Acute decompensated CHF</i>	48%	3,7 (2,0-6,7)	Frea 2015 <sup>40</sup>
<i>HFrEF</i>	48%	2,98 (2,02-4,39)	Iglesias-Garriz 2012 <sup>41</sup>
<i>HFpEF</i>	28-68% depending on criteria for RV failure	1,16-1,45 (p<0,001) depending on criteria for RV failure	Gorter 2016 <sup>42</sup>
<i>Myocarditis</i>	4%	1,6 (1,07-2,4)	Caforio 2007 <sup>43</sup>
<i>Post LVAD insertion</i>	38,9%	3,7 (1,02-13,0)	Dang 2006 <sup>44</sup>

<i>Left heart pathology</i>	<i>Incidence of concomitant right ventricular dysfunction</i>	<i>Hazard Ratio for mortality in case of right ventricular dysfunction</i>	<i>Reference</i>
<i>Post heart transplant</i>	56,7% postoperatively, 16,6% at one year	NS	Bozbas 2013 <sup>45</sup>
<i>Postcardiotomia with postoperative hypotension</i>	40%	20.4 (4.2-98.8)	Reichert 1992 <sup>46</sup>
<i>Precardiotomia in cardiac surgery patients with LVEF &lt; 25%</i>	17%	30d: 152 (6,4-3600) 2 years: 135 (6,3-2900)	Maslow 2002 <sup>47</sup>

*Table 1 Association between right heart and left heart pathology and consequence for prognosis. CHF is chronic heart failure. HFrEF is heart failure with reduced EF, ejection fraction, HFpEF is heart with preserved EF, LVAD is left ventricular mechanical assist device, LVEF is left ventricular EF.*

The primary goal in therapy of right ventricular failure is the reduction of pulmonary artery pressure by treatment of thromboembolism, unloading of the left ventricle, therapy of pulmonary disease and pharmacological dilatation of pulmonary arterioles. At the same time the systemic perfusion pressure (MAP – CVP), which also constitutes the perfusion pressure for the myocardium, must be preserved <sup>48</sup>. The ideal vasodilator for right ventricular failure will therefore induce selective pulmonary vasodilation.

Most known vasodilators, including NO-therapy, have both systemic and pulmonary vasodilatory properties. The main task of this thesis has been the assessment of the sGC stimulators and activators on the integrated circulatory system with a particular focus on the right heart function and systemic circulation. In the following I will describe the main mechanisms of action of guanylate cyclase stimulators and activators and describe their potential clinical use in right ventricular failure

### **5.2.1 Pathophysiology of right ventricular failure**

The right ventricle has a limited capacity to compensate for increase in afterload. In animal experiments the healthy right ventricle can adapt to increase in MPAP (mean pulmonary arterial pressure) up to 30 mmHg with change in contraction pattern and increase in contractility. Above this level the right ventricle returned to baseline contractility and CO decreases<sup>49,50</sup>

While pulmonary hypertension is the leading cause of right ventricular failure, a multitude of conditions can put strain on the right ventricle. Regardless of the trigger of failure, these conditions typically link together in a vicious cycle to propel a progressive fall in cardiac output. The driving force in this cycle is the imbalance between oxygen demand and supply in the right ventricular myocardium as shown in Figure 3.

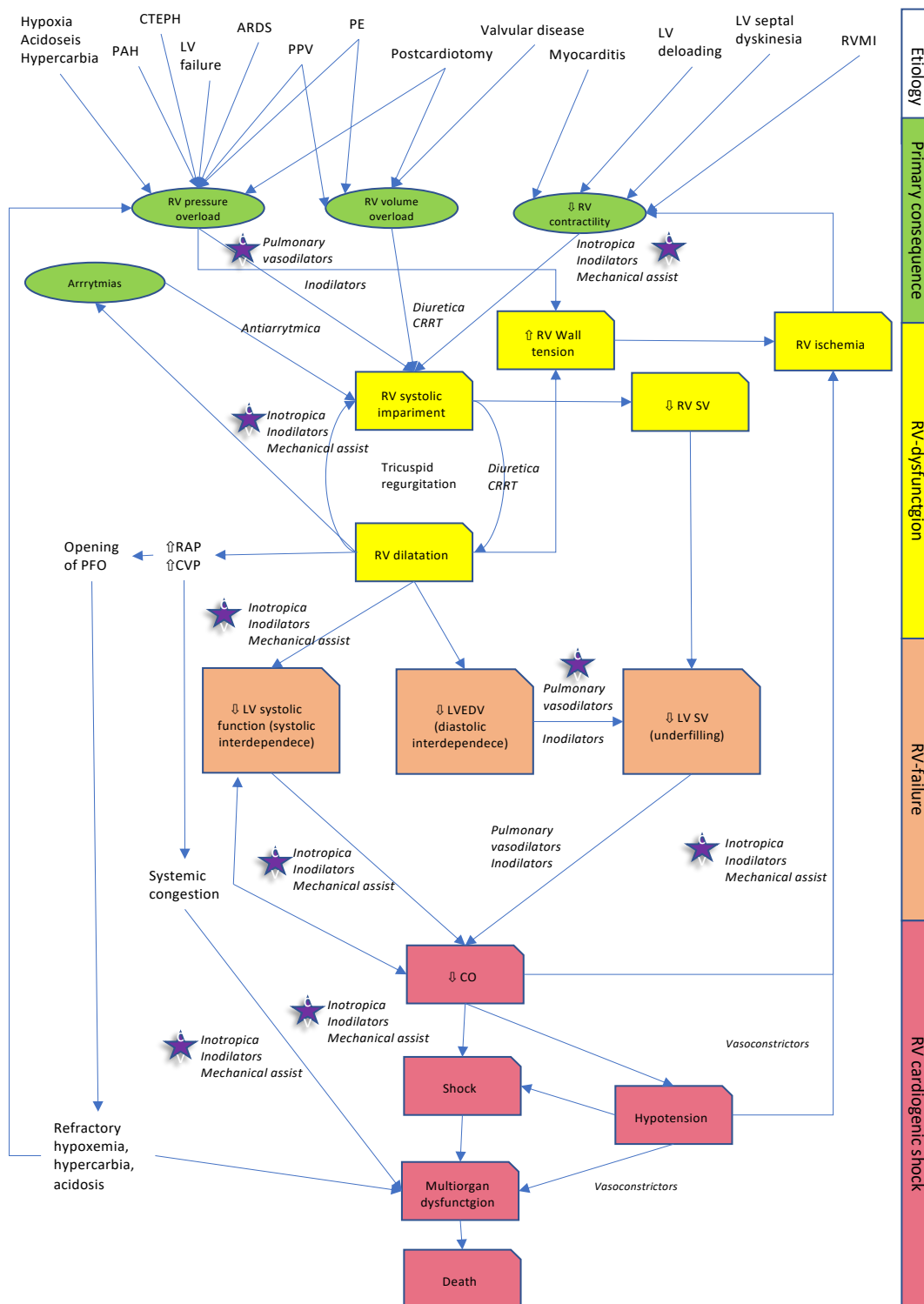


Figure 3 Mechanisms of right ventricular failure including therapeutic options in italics. Purple stars represent the potential targets of sGCA and SGCS. LV is left ventricle, RV is right ventricle, PAH is pulmonary arterial hypertension, CTEPH is chronic thromboembolic pulmonary hypertension, ARDS is acute respiratory distress syndrome, PPV is positive pressure ventilation, PE is pulmonary embolism, RVMI is right ventricular myocardial infarction, CRRT is continuous renal replacement therapy, SV is stroke volume, CO is cardiac output, PFO is

patent foramen ovalis, RAP is right atrial pressure, CVP is central venous pressure. Redrawn and expanded from reference <sup>51</sup> with permission.

### **5.2.2 Management of RV failure**

Guidelines for management of right ventricular failure have been published by The Heart Failure Association and the Working Group on Pulmonary Circulation and Right Ventricular Function of the European Society of Cardiology in 2016 <sup>48</sup> and by American Heart Association in 2018 <sup>52</sup>. These guidelines describe a sequential approach starting by identifying reversible causes and then treatment of these causes. Next step is optimization of volume status and systemic afterload, where sGCS and sGCA have theoretical effects. If hypoperfusion persists inotrope medication and pulmonary vasodilators are introduced. Potent, selective pulmonary vasodilators, however, are currently scarce and this is a potential niche for sGCS and sGCA. As a last resort mechanical circulatory support is instituted.

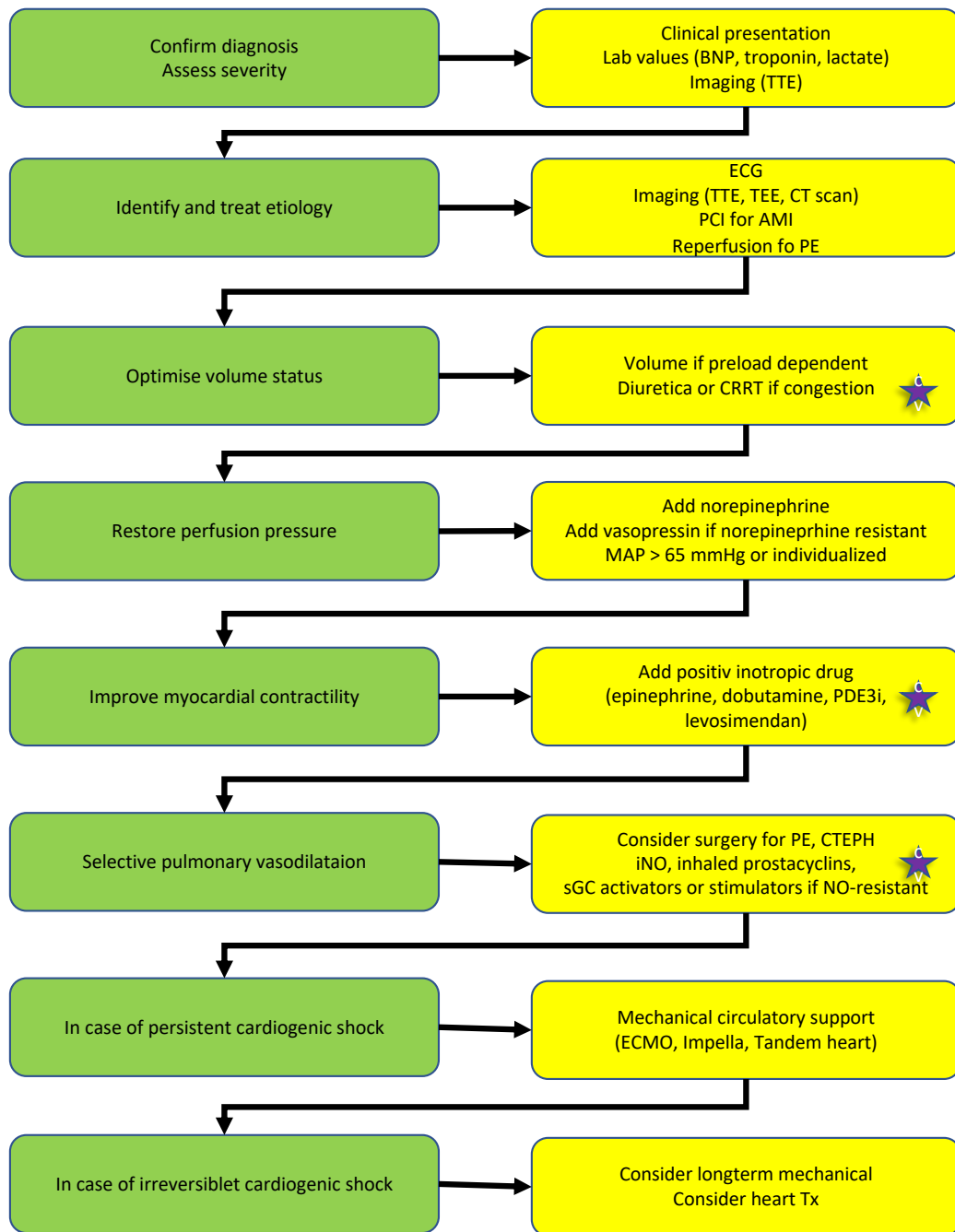


Figure 4 Therapeutic options in right ventricular failure. Purple stars at the potential beneficial uses of sGCS and sGCA. Adapted from reference <sup>52</sup> .



### **5.2.3 Therapy against reversible causes**

Reversal of hypoxia, hypercarbia and acidosis and optimization of lung pressures and volumes will induce pulmonary vascular vasodilatation and decrease right ventricular overload<sup>53</sup>. When these measures are insufficient to reverse pulmonary hypertension pulmonary vasodilators, including sGCA and sGCS, might be warranted.

Acute pulmonary embolism can be treated with systemic heparinization, thrombolysis, mechanical clot removal or extracorporeal circulation<sup>54</sup> depending of the degree of circulatory impairment<sup>55</sup>. The immediate mortality is high if untreated, but improves after clot removal<sup>56</sup>. sGCS and SGA may have a role in partial reversal of pulmonary hypertension as a bridge to resolution of emboli.

Chronic thromboembolic pulmonary hypertension is characterized by organized thrombi occupying a large proportion of the pulmonary arteries. Treatment is surgical with removal of clots<sup>57</sup>. If surgery is contraindicated or inefficient pulmonary vasodilators can give symptom reversal<sup>58-63</sup>. The sGCS Riociguat (Adempas) is approved for this indication<sup>64</sup>.

### **5.2.4 Optimization of preload**

Volume overload of the right ventricle will cause increase right ventricular wall tension, increase valvular regurgitation, decrease contractility, and displace the intraventricular septum. The sum of this is a decrease in cardiac output, and a decreased perfusion pressure (mean arterial pressure minus central venous pressure)<sup>65-69</sup>. Venous vasodilation may contribute to achieve euvolemia and acceptable systemic venous pressures in patients with right ventricular failure<sup>53</sup>, again a potential target for sGCA and sGCS.

### **5.2.5 Stimulation of cardiac contractility.**

Inotropic medication, like Dopamine, Dobutamine, Epinephrine, Levosimendan and Phosphodiesterase inhibitors all increase right ventricular contractility (Figure 5). The role of sGCS and sGCA as inotropic agents is still undetermined and warrants investigation.

Both NO and cGMP show a positive inotropic response in lower concentrations, but inhibits contractility at higher (supraphysiological) levels, possibly through interaction with a cGMP-inhibitable cAMP-phosphodiesterase. Higher levels of cAMP open L-type Ca-channels and lead to increase intracellular calcium. In higher concentrations of cGMP this channel is

inhibited and in addition  $\text{Ca}^{2+}$  sensitivity have been shown to decrease<sup>3</sup>. Therefore, the effects of sGCA and sGCS may be dependent of the resulting cGMP-levels.

The mismatching of contractility and pulmonary arterial input impedance is also of importance in development of right ventricular failure and can identify patients with advanced right ventricular failure<sup>70</sup>. The effect of sGCS and sGCA on pulsatility and vascular stiffness may have therapeutic implications in addition to their blood pressure lowering effects<sup>71-73</sup>.

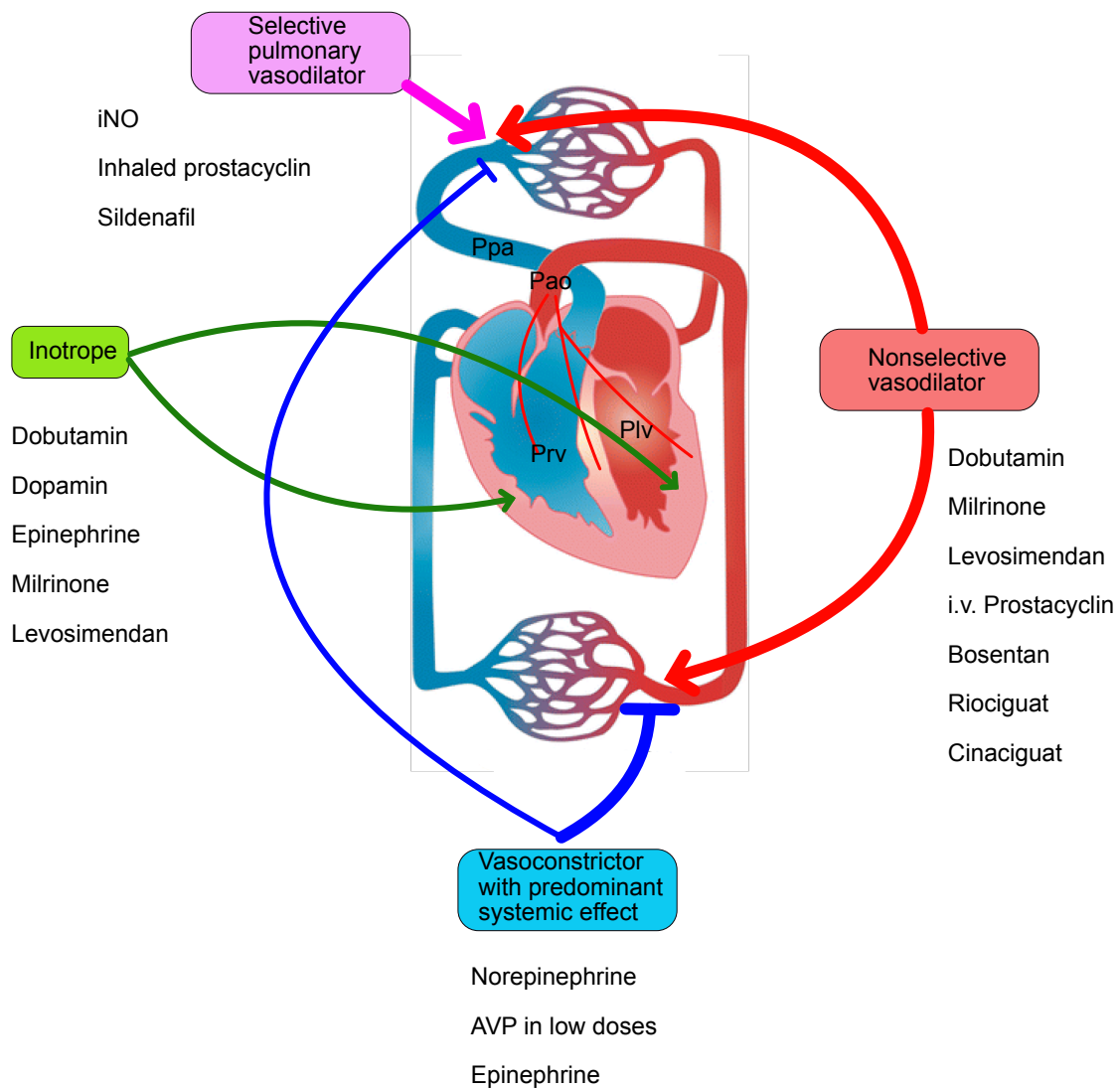


Figure 5 Principal effects of vasoconstrictors, vasodilators and inotropes in right ventricular failure. INO is inhaled nitric oxide, AVP is arginine vasopressin. Ppa is the pressure in the pulmonary artery. Pao is the pressure in the aorta. Prv is the pressure in the right ventricle and Plv is the pressure in the left ventricle. Pathways ending in arrows at vessels induce vasodilatation and arrow ending in the myocardium induce inotropy. Pathways with obtuse endings induce vasoconstriction. The width of the pathways suggests the effect size.

## 5.2.6 Pulmonary arterial vasodilatation

Pulmonary vasodilatation can reduce right ventricular afterload and improve overall hemodynamics. However pulmonary vasodilators are often hampered by concomitant systemic vasodilatation and disruption of normophysiological hypoxic vasoconstriction in nonventilated parts of the lung. The terminal effect on the systemic circulation and outcome may therefore be unpredictable <sup>74</sup> (Figure 5). Furthermore pulmonary arterial vasodilatation can induce pulmonary capillary congestion when used in a setting of left ventricular backwards failure and should be avoided in non-pre-capillary PAH <sup>75,76</sup>.

Inhaled NO and prostacyclin have the highest initial selectivity for the pulmonary vasculature and have modest acute systemic effects. This selectivity is time limited since both drugs have downstream systemic effects when used long term <sup>77</sup>. The effect of NO is also, as earlier described, dependent on the red-ox-state of SGC <sup>25,26</sup> and drugs with effects through its action on NO-levels will therefore be hampered by the high oxidative state often found under pathological conditions. Guanylate cyclase stimulators and activators bypass the need for NO-sGC-binding and may be an attractive strategy in the face of reduced NO-vasodilatory response.

The effects of inotropes, inodilators and vasoconstrictors in right heart failure were systematically reviewed by Price et al 2010 <sup>78</sup>. Later narrative reviews and consensus recommendations have echoed these recommendations<sup>52,79–81</sup>.

## **6 Material and methods**

### **6.1 NO-blockers**

Since overactivation of the NO-system induces intolerable systemic hypotension, blocking of NOS is an attractive pharmacological treatment in vasoplegia. While several substances have been developed through computer aided screening of large substance libraries, the most common inhibitors are arginine analogs which compete with L-arginine for the catalytic binding site on NOS <sup>82</sup>. In experimental studies such compounds have been shown to cause a concentration dependent inhibition of eNOS that can be reversed by increasing the concentration of L-arginine. The result of NOS-blockade is a dose-dependent increase in blood pressure and accompanying bradycardia <sup>83</sup>. N<sup>G</sup>-nitro-L-arginine (L-NAME) is one example of a L-arginine analogue that induces potent, reversible, inhibition of acetylcholine induced relaxation. L-NAME has been the drug of choice in our laboratory for NO-blockade, and dose-response studies have shown an increasing vasoconstriction and hypertensive effect in swine up to doses of 15-20 mg/kg <sup>84</sup>. In the present studies, we have used NO-blockade to create a defined NO-tone as a frame for studying SGC stimulators and activators. Thus, L-NAME has been used to explore the effects of Riociguat and Cinaciguat isolated from NO to explore the direct effects of these substances as well as their interaction with NO.

### **6.2 Ganglion blocking by using Hexamethonium**

We have employed hexamethonium to block autonomic reflexes during our experiments.

The heart is innervated by both the sympathetic and parasympathetic nervous system, and it is receptive to circulating catecholamines.

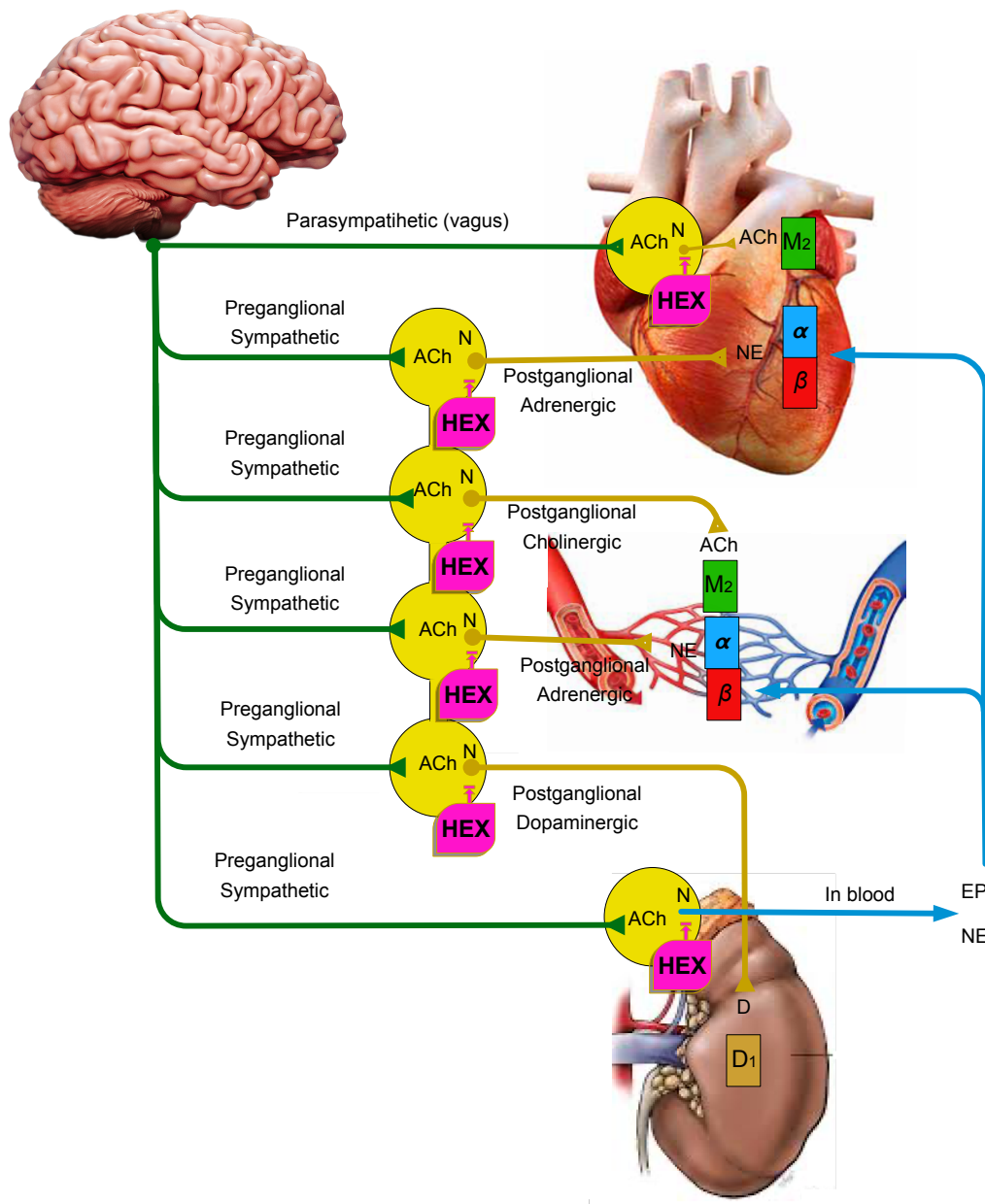


Figure 6. Effector site of Hexamethonium (HEX) and its interaction with the autonomic nervous system. ACh is acetylcholine, N is nicotinic receptor, NE is norepinephrine, EPI is epinephrine, D is dopamine, D<sub>1</sub> is dopaminergic receptor, M<sub>2</sub> is muscarinic receptor, β is beta adrenergic receptor, α is alpha adrenergic receptor. Yellow circles are ganglia. Modified from reference<sup>85</sup> with permission.

Hexamethonium is a nicotinic receptor (nAChR) antagonist working as a non-depolarizing autonomic ganglionic blocker effectively blocking both sympathetic and parasympathetic transmission. The end organ effect depends on the resting balance between the two autonomous systems. Brown studied defense reactions in cat and the effect of Hexamethonium and acetylcholine<sup>86</sup>. He found that Hexamethonium gave a sub-complete block of the cardio-vasoactive response of preganglionic stimulation and addition of atropine

abolished the same response. In hemodynamic studies in intact animals Hexamethonium have been used to attenuated sympathetic activation during interventions and measurements. This makes it easier to single out the exact effect of cardio-vasoactive drugs, since these effects can be masked by autonomous homeostatic reflexes <sup>87</sup>.

In our experiments the use of Hexamethonium is a dilemma and trade-off. The consequence of vasodilation in these pigs is a pronounced reflectory tachycardia. This is of course a physiological response but make several of the assessed parameters difficult to interpret. For instance, tachycardia will alter the contractile state of the myocardium and influence cardiac output. As we have used several test-drugs, these responses could be different for the various groups and thus make the interpretation of the data difficult. We therefore chose to keep the heart rate under control during the experiments although it is not optimal for translational interpretation.

## **6.3 Pharmacokinetics of Riociguat and Cinaciguat**

Cinaciguat is tested in humans, and the pharmacokinetics can be described in a two-compartment model with delay between plasma concentration and compartment concentration between 0,3 and 0,9 hours. Maximum plasma concentrations were reached after 30 minutes of infusion. The interindividual variability was moderate <sup>88</sup>. Constant effect compartment concentrations for the period of the experiment therefore can be expected after an observation period of 30 minutes and requires a continuous infusion of medication to achieve stable levels for the duration of the experiment.

Riociguat have been tested in humans after intravenous or oral administration<sup>89</sup>. The half-life in plasma was found to be 12 hours in humans <sup>90</sup>. Therefore, bolus intravenous injection of Riociguat is expected to give a steady state pharmacokinetic for the duration of our experiments.

## **6.4 Cardiovascular measurements**

### **6.4.1 Right ventricular afterload**

Right ventricular (RV) afterload can be defined as the RV wall stress during systole. By La Place law this wall stress is proportional with the transmural pressure for the right ventricle,

and the internal radius of the ventricle and inversely proportional to the RV wall thickness. Due to the complex structure of the right ventricle and its interaction with the left ventricle, this method is not as well suited as well for the right as the left ventricle. Therefore, it is more appropriate to regard the right systolic ventricular wall stress to be the sum of resistive and pulsatile components of the blood stream out of the right during ejection. Pulmonary vascular resistance calculated as mean pulmonary arterial pressure and mean stroke velocity does not account for the pulsative component of the blood stream (1/2-1/3 of the hydraulic power). The high degree of branching of the pulmonary vascular tree gives rise to abundant reflected waves that will affect both antegrade pressures and flows in the pulmonary artery, and the relationship between PVR and pulmonary input impedance will change with pathological stiffening of the vasculature during development of pathology. Total right ventricular afterload can better described by transforming the flows and pressures from the time- to frequency domain via a Fourier transformation<sup>91</sup>. This however demands simultaneous high-fidelity flow and pressure measurements and is not achievable in a closed-chest model. In our acute experiments in healthy we have therefore chosen to use PVR as a marker of right ventricular load.

#### **6.4.2 Systolic ventricular function**

In experimental models indices derived from pressure- and volume analysis can be used to drive indices of right ventricular systolic function<sup>91</sup>. Karunanithi and coworkers have compared preload recruitable stroke work (PRSW), end-systolic pressure-volume-relationship (ESPVR), and  $dp/dt$  max-end-diastolic relations to search for the best index of contractility. The criteria for a robust contractility index are high reproducibility, pre- and afterload independence, inotropy sensitivity and chronotropy independence. These authors observed that ESPVR was highly load sensitive, while PRSW was relatively load insensitive and showed a high degree of reproducibility<sup>92</sup>. In our studies we have therefore chosen PRSW as the principal index of cardiac function for both the left and right ventricle.

Ees (elastance) is achieved by sampling data during vena cava inferior occlusions. This maneuver induces an acute shift in parallel volume during conductance catheter measurements (PV-catheter, especially right ventricular volume) and will give different results when using PV-catheters compared to sonometric crystals for volume estimates<sup>93,94</sup>.



Ees is curvilinear over a wide range of volumes <sup>95</sup>. During deloading the assumption that Ees is linear will, therefore, not be correct <sup>96</sup> PRSW have a lower sensitivity but higher specificity for detecting changes in contractility compared to maximum dP/dt during contraction <sup>94</sup>.

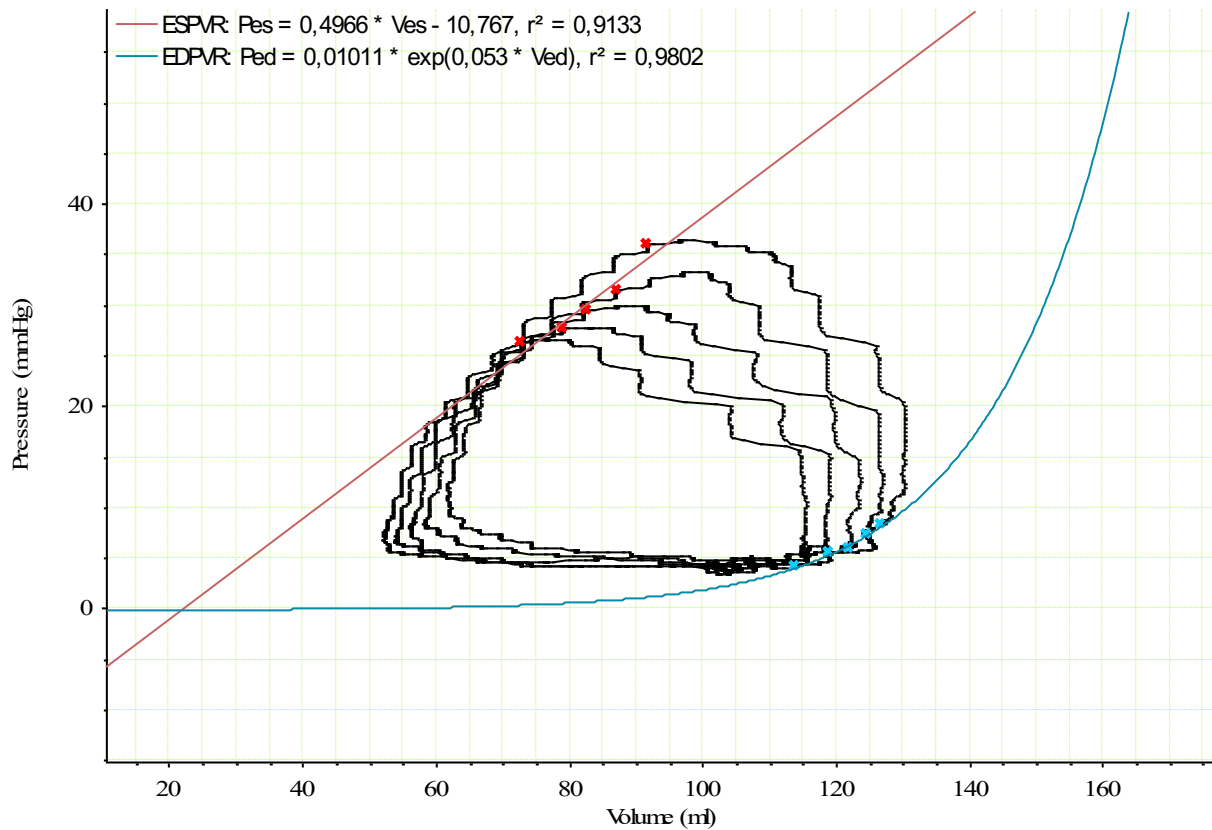


Figure 7. Example from one pig with simultaneous pressure and volume measurements of the right ventricle during deloading through occlusion of the inferior vena cava. ESPVR (used for elastance, Ees assessments) is the linear relationship between end-systolic pressures and volumes.

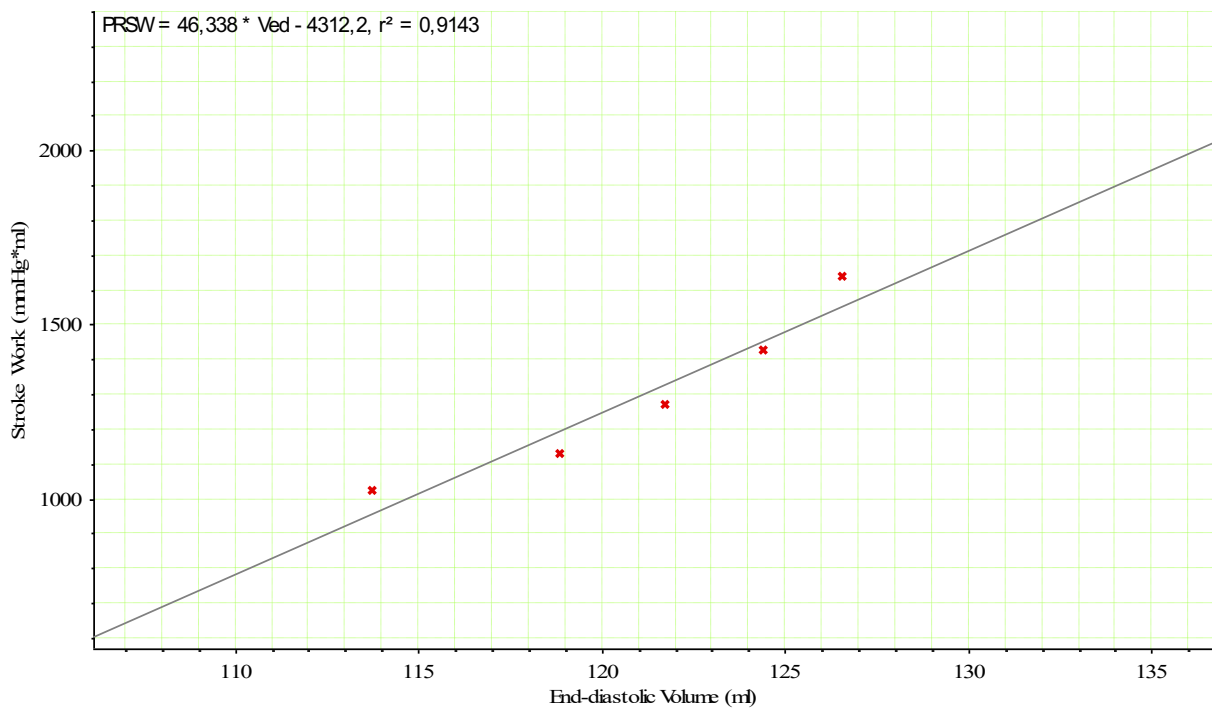


Figure 8. Example from the same pig as in the last figure. Here the area of each work-diagram (the pressure-volume product) is plotted against the corresponding end-diastolic volumes to achieve the plot of preload recruitable stroke work (PRSW).

### 6.4.3 Diastolic ventricular function

Diastole consists of an early, energy dependent, active relaxation phase and a late passive filling phase. Passive filling starts when right atrial pressure exceeds the intracavitary pressure of the right ventricle. A rapid influx driven by the pressure gradient is followed by a period of zero flow as pressures between the atrium and ventricle equalizes. Atrial contraction then contributes with the remaining 15-30% of ventricular filling<sup>97</sup>.

The end-diastolic pressure (EDP) of the right ventricle is the pressure at the moment of tricuspid valve closure. While EDP will be increased in diastolic dysfunction, this index is highly dependent on preload, afterload, and heartrate. The value of EDP increases if it is obtained over a range of different end-diastolic volumes, construction the end-diastolic pressure-volume-relationship, EDPVR. This index gives a description of the passive stiffness of the myocardium.

The active relaxation can be evaluated by using the pressure-decay  $dP/dt_{min}$ .  $Dp/dt_{min}$  is the steepest slope of the pressure/time curve of the right ventricle.  $DP/dt_{min}$  decreases with decreased diastolic dysfunction. This index is, however, also fallible to ventricular loading<sup>98</sup>

Tau, the time constant of isovolumetric relaxation, is another measure of diastolic function. Tau can be calculated as an exponential or logistic curve fitting of the pressure curve and represents the time for the pressure at  $dp/dt$  min to fall by 64% (Weiss, exponential) or 47% (Matsubara, logistic)<sup>99</sup>, of which the logistic approach have proven to be the least load sensitive<sup>100</sup>. We have chosen logistic Tau as our main indicator of active diastolic ventricular function.

#### **6.4.4 Echocardiography**

Echocardiography is noninvasive, cheap and have a high value for estimation of left ventricular function. In right ventricular failure however, the diagnostic value of 2D echocardiography is more debatable.

Two-dimensional echocardiography has limitations with regard to the complex three-dimensional structure of the right ventricle. Even so, the two-dimensional area of the right ventricle and the long axis movement have been shown to give information on the right ventricle function<sup>101–103</sup>. Blood and tissue doppler imaging can be used to further evaluate aspects of the mechanical function<sup>104</sup>. Three-dimensional echocardiography have the potential of more accurate right ventricle volumetric quantification, but the availability of hardware and software for this application is still limited<sup>105–108</sup>. An further advancement is the use of 3D-speckel tracking which promises more accurate description of right ventricular motion<sup>109</sup>

In the current studies more invasive, and more reproduceable methods, as micro sonometry and conductance, with higher time resolution have been chosen, but echocardiography has still been useful to calibrate the volumetric measurement of the other methods during our studies.

#### **6.4.5 Pressure-volume analysis of cardiac function**

The “cardiac work diagram”, as suggested by Starling in 1895<sup>110</sup> is a way to describe the hydraulic work of the heart. Simultaneous recordings of pressure and volume of the heart chamber are plotted in a pressure/volume diagram, resulting in a closed figure starting at the end-systolic point with the lowest pressures and volumes when the mitral valve opens. The next corner of the figure is the end-diastolic point when the mitral valve recloses. The area of the figure is the pressure/volume product of the hydraulic work of the ventricle, named stroke work (SW). SW is the external mechanical work performed by the ventricle. The width of the

figure is the volume of cardiac ejection, Stroke Volume (SV). Peak pressure is the Systolic Blood pressure in the aorta. In addition to this the placement of the figure on the x-axis signifies the end-systolic and end-diastolic volumes (Figure 9).

Suga explored the relationship between left ventricular pressures and aortic flow and developed a canine model where he could regulate the end-diastolic volumes of the left ventricle. He found that the resulting pressure/volume points at aortic closure (which he named Ees, end systolic elastance) fell on a straight line and that the slope of this line increased with increase in contractility and decreased with reduced contractility. The X-axis intercept of the line through the Ees-points obtained at different end-diastolic volumes is named  $V_0$ , which is a theoretical unstressed volume where the left ventricular pressure is zero. Sagawa and coworkers have expanded the pressure-volume framework to the right ventricle through their experiments in isolated canine hearts. <sup>91</sup>.

#### 6.4.6 Conductance technique

The conductance method of describing time varying left ventricular volumes was first suggested by Baan <sup>111</sup>. The method is based on differential conductivity of electricity in blood and myocardium. He used a 7 fr catheter with eight equally spaced circular electrodes, spanning the long dimension of the ventricle (Figure 10). A constant current was applied from electrode 1 to 8, and the remaining electrodes was used to measure voltages between electrode pairs. The voltage between electrodes is dependent of the impedance of the surrounding structures. The blood is then viewed as a variable resistor with constant height (distance between electrodes) and variable cross-sectional area. Resistance between two electrodes is linearly correlated to the volume of this disk. The ventricular wall also contribute to the impedance and this contribution must be subtracted to gain the true segmental ventricular volume. For one segment the formula is

$$V = \frac{1}{\alpha} \times \rho \times L^2 \times (G - G^P)$$

Where  $V$  is instantaneous volume of the segment of the ventricle,  $\alpha$  is a correction factor against a known volume measured by another method,  $\rho$  is specific conductance of blood,  $L$  is the distance between pairs of electrodes,  $G$  is the measured conductance (1/resistance) and  $G^P$  is the parallel conductance from the ventricular wall.

To obtain the volume of the whole ventricle all the segmental volumes are summarized.

To use this formula the specific conductance of blood must be calculated in-vitro. Parallel conductance is measured by injection of hypertonic saline. The crossing between the regression line for the resulting conductance during washout and the line with slope 1 is the parallel volume. Alternatively, as used in our studies, the resulting conductance for all segments is calibrated against end-diastolic volume and stroke volume measured by echocardiography at each phase of the study.

Conductance catheters have also been used in right ventricular studies <sup>112-114</sup>. While there is a high agreement between the conductance method in the right ventricle and other more direct measurements of volume under physiological conditions, a degree of nonlinearity is observed during deloading of the heart by IVC-occlusion <sup>115</sup>, and to a lesser degree within a cardiac cycle <sup>116</sup>. Extreme pressure-volume values will also not follow the linear tendency of normophysiological values <sup>95</sup>.

The experience from extensive hemodynamic studies in the lab is that volumetry with conductance is subject to significant drift during an experiment and repositioning because of displacement or wall artifacts is often necessary<sup>117</sup>. The value of PV-catheters, in our opinion, is the simultaneous measurements of relative ventricular volume and pressure, while absolute volumetry is more demanding and includes a stable position of the catheter, a homogenous field of electricity around each electrode, stable resistivity of the blood and a stable parallel volume. All this prerequisites for correct volumetry with PV are questionable for the duration of the experiment <sup>111</sup> Therefore, recalibration makes the setup more accurate and eliminates the unpredictable drifting in the registration. Instead of using the method of hypertonic saline injection to acquire absolute volumes with the PV-catheter we used echocardiography at end-diastole and stroke volume from thermodilution to convert relative volumes from the PV-catheter to absolute values. Echocardiography was done with clinical grade echocardiography equipment (Philips I33), and we found that a right-sided parasternal view gave good image quality (good definition of the endocardial border in the anterior and posterior walls of the left ventricle) in all animals.

The advantage of the conductance catheter is that it may be used in a closed-chest animal model.

#### **6.4.7 Micro sonometric measurements of ventricular volumes**

An alternative to conductance is using micro sonometric crystals placed in the myocardium to measure critical dimensions in both ventricles to be able to calculate biventricular instantaneous volumes. An ellipsoidal shell-subtraction model can be used to estimate the volume of the right ventricle. In this model the volumes of both ventricles are considered an ellipsoid, and the volume of the left ventricle a second ellipsoid. The difference between these two is the right ventricular volume <sup>118</sup> (Figure 10). This model does not account for the thickness or variability of the interventricular septum and can be predicted to overestimate the absolute values of the right ventricular volumes. Agreement between the two methods is high, but with significant inter-animal variations <sup>119</sup>.

Micro sonometry is a more direct measurement of ventricular volumes compared to conductance but requires an open chest model and pericardiotomy to apply the crystals.

#### **6.4.8 Cardiac output measurements**

Thermodilution is regarded golden standard for CO-estimation <sup>120</sup> and was used in our closed chest studies to calibrate the PV-catheter together with end-diastolic volumes from echocardiography. Pironet and coworkers have compared the pressure-volume catheter with aortic flow probe, the PiCCO monitor and thermodilution <sup>121</sup>. They found that while all methods were highly repeatable, the methods showed poor agreement. The two methods that correlated highest were thermodilution and aortic flow probe. In our lab we use pulmonary artery flow probe as golden standard in open chest models and thermodilution in closed-chest models.

#### **6.4.9 Ventriculo-arterial coupling**

Ventriculo-arterial coupling (VAC) describes the transfer of energy from the heart to the vascular system. Optimal coupling exists when a minimum of energy is lost to heat, oscillations, and friction. To achieve such efficient energy transfer the physical properties of the heart and circulation must be matched: The internal impedance of the heart must match the input impedance of the arterial system <sup>122</sup>.

One way to describe VAC is through the framework of Suga and Sagawa. As described earlier Suga found that  $E_{max}$  is a representation of the contractility of the ventricle. The slope

of  $E_{max}$  at different loads (the end-systolic pressure volume relationship) is called end-systolic elastance,  $E_{es}$ . The line from the crossing of  $E_{es}$  and the end systolic volume to the end-diastolic volume on the x-axis of the cardiac work-diagram is a representation of the arterial elastance,  $E_a$ . Both elastances describes the way hydraulic work is given and received and the relationship between them represents the hydraulic matching between the ventricle and the arterial system.

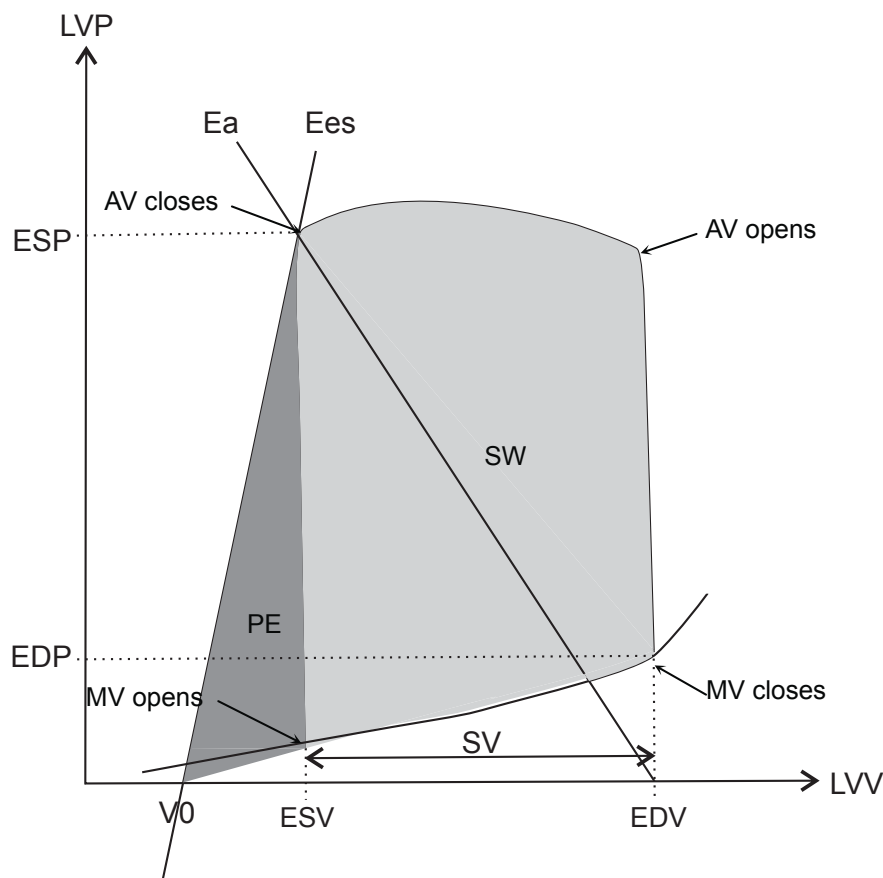


Figure 9. Ventriculo-arterial coupling between left ventricle and the aorta. LVP is left ventricle pressure, LVV is left ventricle volume. EDP is the end diastolic pressure, ESP is the end systolic pressure, EDV is the end diastolic volume, ESV is the end systolic volume, SV is stroke volume. The light gray area is stroke work, SW, and the dark grey area is potential energy, PE. Together SW and PE represents the pressure volume area, PVA. MV is mitral valve, AV is aortic valve.  $E_a$  is arterial elastance and  $E_{es}$  is ventricular elastance. The intercept of  $E_{es}$  and the X-axis is  $V_0$ .

When both  $E_{es}$  and  $E_a$  are drawn onto the cardiac work-diagram, the relationship between ventricular and arterial elastance can be visualized. The product of SV and ESP is the hydraulic work of the left ventricle, SW. PE, the area under the  $E_{es}$ -curve from  $V_0$  to ESV is

the potential energy. Together SW and PE are the total mechanical energy expenditure of the heart, the pressure-volume area, PVA. The mechanical efficiency of the heart is therefore  $SW/(SW + PE)$ . Of geometrical reasons the mechanical efficiency will be at its maximum when  $E_{es} = 2 \times E_a$ , and maximum stroke work will be achieved when  $E_a = E_{es}$ <sup>122</sup>.

#### **6.4.10 Cardiometabolic efficiency**

Cardiometabolic efficiency describes the relationship between cardiac work and oxygen consumption and can be divided into hydraulic work and non-hydraulic work<sup>123,124</sup>. In his search to decipher the sources of oxygen consumption in the heart, Suga<sup>124</sup> suggested that the total energy of contraction could be divided into external work, SW and potential energy, PE being spent on tensioning elastic elements of the heart. The amount of elastic energy spent will depend on the stretch of these elements and will be related to the ventricular size. Suga proposed that the triangular area under the  $E_{max}$ -line represents the PE. In support of this theory, he observed that measures PVA and oxygen consumption  $MVO_2$  correlated linearly over a wide variety of loads. The slope of this curve signifies the oxygen cost of contractility, and the y-axis intercept is suggested to be the basal metabolism of the heart and the cost of excitation-contraction coupling (Figure 12). Cardiac metabolic efficiency defined as the oxygen consumption at a given PVA can then decrease either by an increase in slope or increase in y-intercept of this curve. Suga found that factors associated with ATP-dependent  $Ca^{2+}$ -handling influenced the y-intercept while the slope varied by acid-base status and core temperature<sup>125</sup>.

The oxygen cost of non-hydraulic work is called the unloaded oxygen consumption and as stated is suggested to be basal cardiomyocyte metabolism and excitation-contraction coupling. Furthermore, the hydraulic work in the heart must be transferred to hydraulic work in the arterial system as described in the previous paragraph.

In the  $MVO_2/PVA$  and work-diagram frameworks it is possible to derive both the unloaded oxygen cost of the heart as well as the mechano-metabolic efficiency, defined as the oxygen cost of contractile work. This relationship is shown to be linear over a wide variety of loads, while stroke work efficiency will be dependent on volume- and pressure<sup>123,124</sup>. The difference between stroke work and PVA will increase with increasing loads.



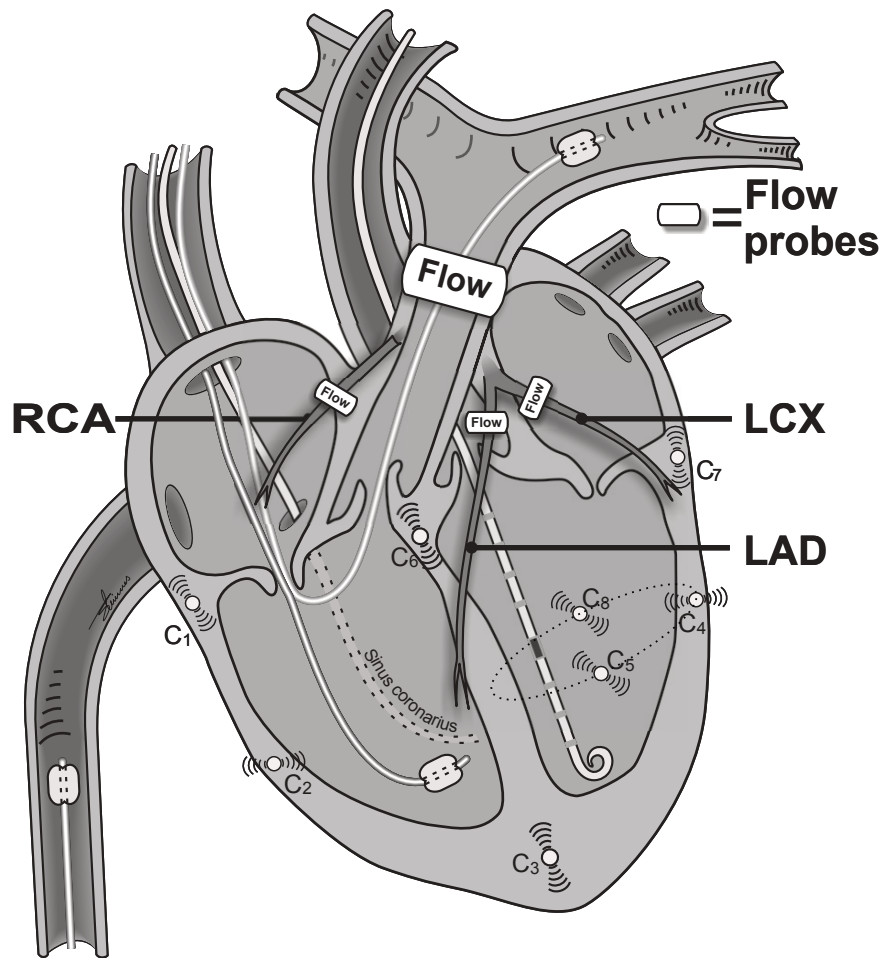


Figure 10. Instrumentation to obtain data for cardiac metabolic efficiency. C# are micro sonometric crystals, Flow are time-transit flow probes. RCA is the right coronary artery, LCX is the left circumflex artery and LAD is the left anterior descending artery. Schematic drawing of the sonometric crystals positions used for assessing right and left ventricular volumes (see equation 1 and 2). The placements of the crystals are in the subendocardial position. Crystal nr 8 is placed in the posterior wall of the left ventricle adjacent to crystal nr 5 in the anterior wall. “Flow” are time-transit flow probes, RCA is right coronary artery, LCX is left circumflex coronary artery, LAD is left anterior descending artery, C1 to C8 are sonometric crystals placed in the sub endocardium. Balloon catheters in the right ventricle and pulmonary artery. Conductance catheter is placed along the long axis in the left ventricle.

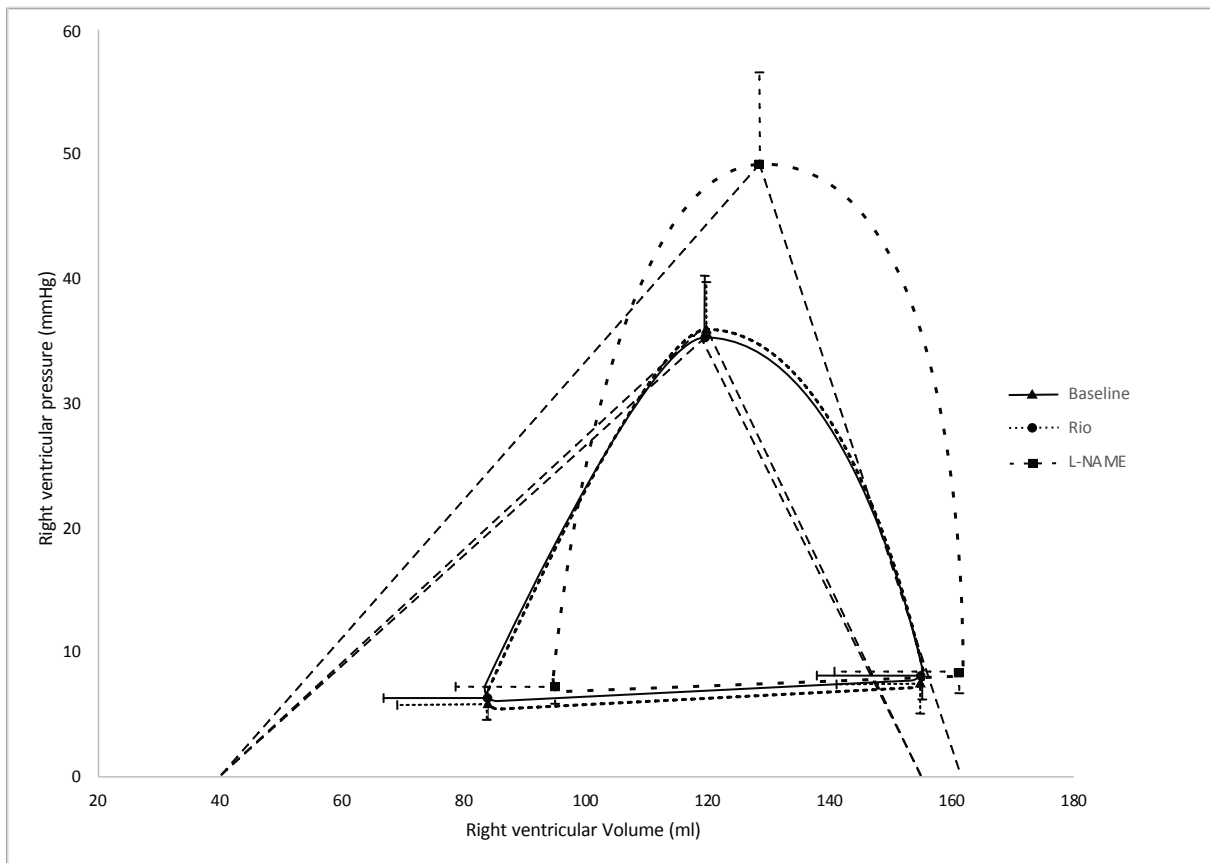


Figure 11. Data from study 2 with comparison of the difference in stroke work and potential energy between baseline and medication with Riociguat (Rio) or L-NAME.

Increase in inotropy will also affect the relationship between SW and PVA and therefore the oxygen cost of SW. Inotropy induces leftwards, and upwards changes of the end-systolic pressure/volume relationship and PE will therefore be decreased while stroke work will increase. PVA can remain unchanged, and the typically observed increase in oxygen requirement for a given PVA must therefore be because on increase unloaded metabolism in the cardiomyocytes.

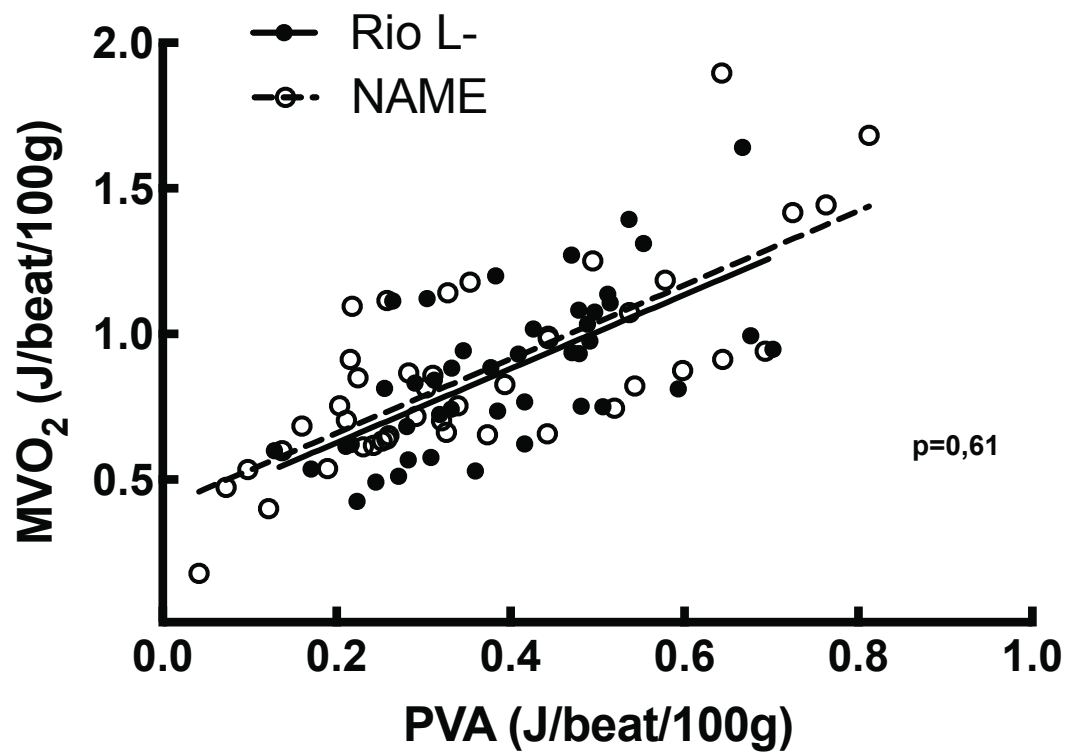
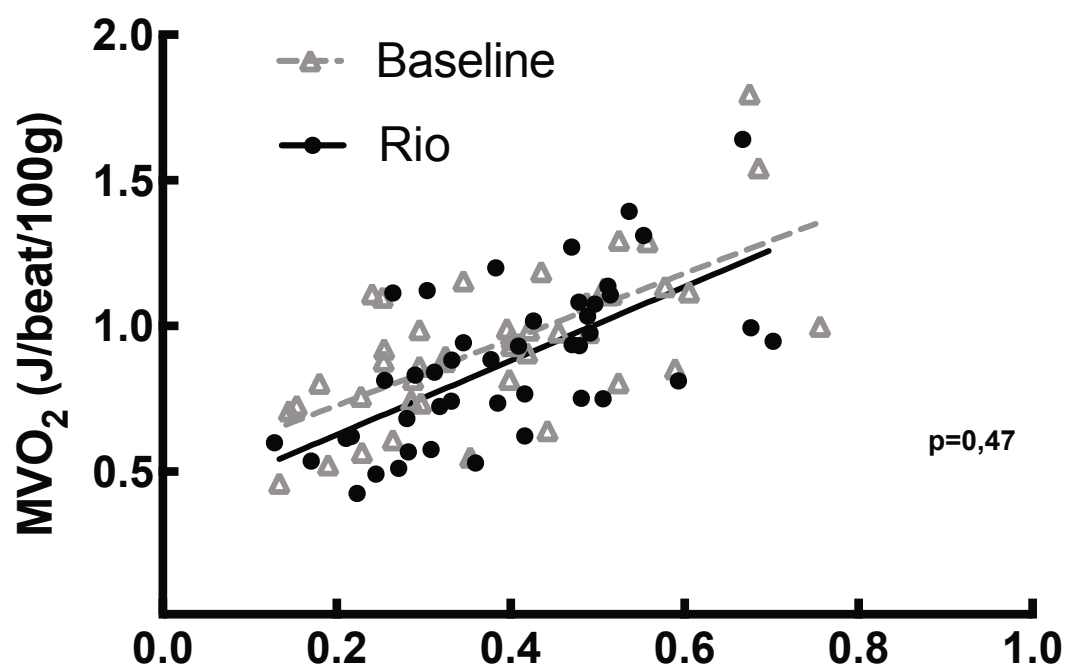


Figure 12. Data from study 2. Relationship between measured oxygen consumption ( $MVO_2$ ) and total work of the heart with comparison of baseline and Riociguat and Riociguat and L-NAME.

### 6.4.11 Venous compliance and capacitance

The venous system holds approximately 70% of the blood volume and is under sympathetic influence. Equivalent to the vasoconstriction in the arterial system, sympathetic stimulus induces reduction in venous compliance and capacitance, effectively increasing venous filling pressures without changing the total fluid balance<sup>126</sup>.

Vascular capacitance is the ratio between a distending pressure and a given volume in a segment of blood vessels<sup>127</sup>. Vascular capacity is the total blood volume in the circulation at a given pressure. This can be divided into an unstressed, and stressed fraction of which the unstressed volume is the systemic blood volume at zero pressure, and the stressed volume is the difference between the total blood volume at a given pressure and the unstressed volume. Only the stressed volume will influence hemodynamics. The size of the unstressed volume (60-70% of the total blood volume) is influenced by the capacity of its holding vessels, inflow and the transmural pressure of these vessels. Unstressed volume can be converted into stressed volume through venoconstriction<sup>128</sup>. The splanchnic vascular bed constitutes the largest proportion of unstressed blood<sup>129</sup>. The spleen and liver are important reservoirs for auto-transfusion in acute hypovolemia<sup>130</sup>.

Compliance describes the slope of the volume/ transmural pressure-relationship in a vascular bed<sup>127,131</sup>, and can be influenced by sympathetic stimulation or nitroglycerin<sup>126</sup>

Smiseth and coworkers have developed a framework for evaluation of venous compliance and capacitance through instantaneous measurements of distending liver pressures, found to be best represented by liver lobular venous pressures and relative liver blood volume<sup>132-135</sup>.

Our instrumentation included vascular pressure catheters in aorta (MAP), vena porta (Ppv) and vena hepatica (Phv). In addition, a miniature pressure catheter (2fr) was introduced through the vascular catheter in vena hepatica and positioned at the point where the 6 fr catheter in the same vessel was found to be wedged before retraction (Phlv). Flow probes were placed on arteria hepatica (Qha) and vena porta (Qpv). Anteroposterior pairs of microsonometric crystals were sutured in a subcapsular position at the thickest part of the left liver lobulus.

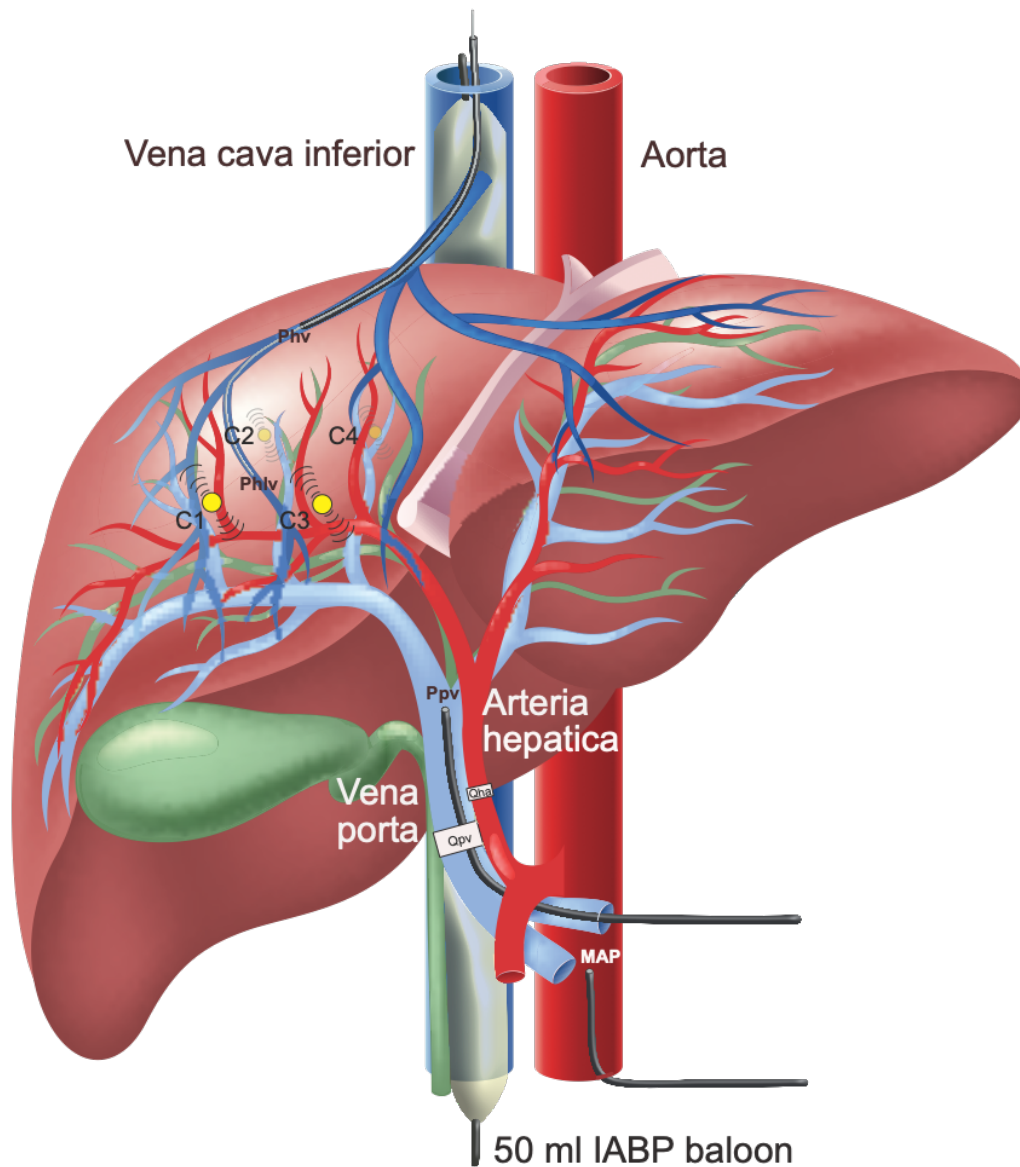


Figure 13. From study 3: Instrumentation for measurement of hepatic flows, pressures and resistance. Microsonometric crystals C1 to C4 for volumetric measurements for estimation of hepatic compliance and capacitance. Phv is the pressure in a hepatic vein. Phlv is the venous pressure in a hepatic lobulus, Ppv is the vena porta pressure, Qha is flow in arteria hepatica, Qvp is flow in vena porta. MAP is mean arterial pressure.

The liver blood volume is derived from sonometric measurements of hepatic thicknesses calibrated against liver blood volume increase during occlusion of the liver veins. With the help of flow probes on vena porta and arteria hepatica liver inflow can be integrated during liver vein occlusion.

The constant between hepatic dimensions and the integral of hepatic inflow during venous occlusion (liver compliance),  $k$  was calculated by linear regression of  $k_n$  for the duration of venous occlusion.  $D_n$  is the mean of the two liver dimensions at timepoint  $n$ ,  $D_0$  is the mean of

the two liver dimensions at baseline of the experiment. 17,5 is the arbitrary liver blood volume in ml kg<sup>-1</sup> at baseline.

$$k_n = \frac{D_n - D_0}{\int_0^n (Q_{pv} + Q_{ha})}$$

The instantaneous liver blood volume per kg at the timepoint n (LBV<sub>n</sub>) was calculated as, where W is the pigs body weight at baseline.

$$LBV_n = 17,5 + \frac{\left(\frac{D_n - D_0}{k}\right)}{W}$$

The Y-intercept of the compliance-curve is the liver blood volume at zero pressure and is considered to be the unstressed liver blood volume.

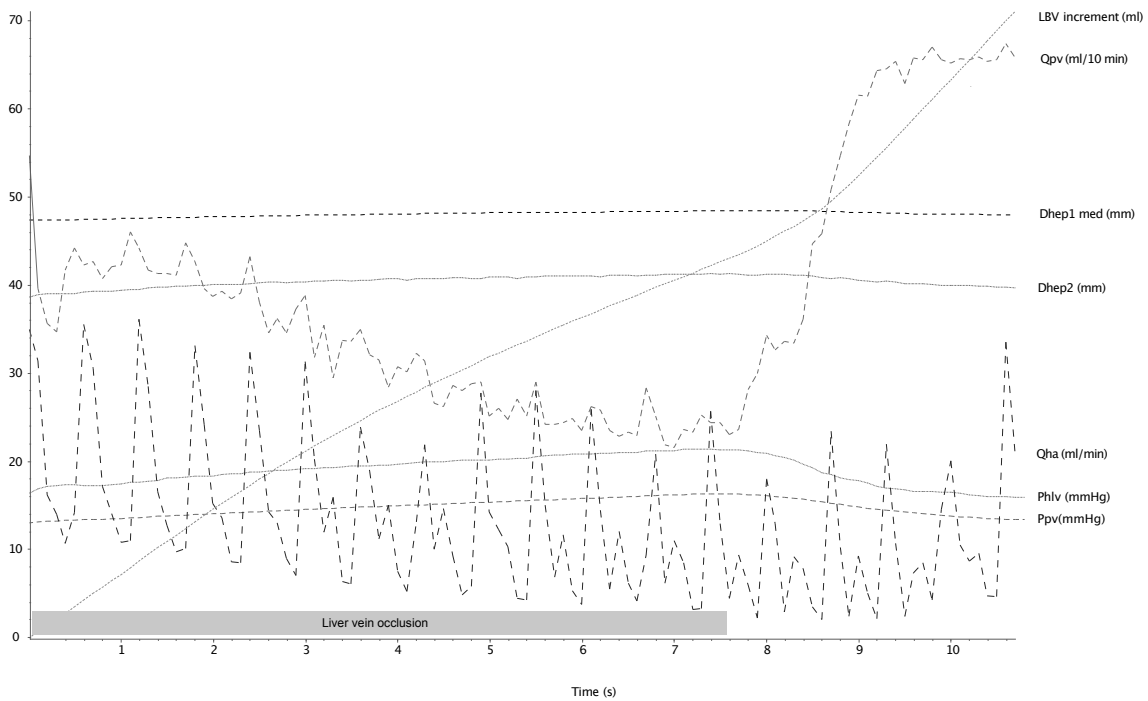


Figure 14. Data from measurements done during occlusion of hepatic venous flow. LBV increment is the sum of vena porta inflow (Qpv) and hepatic artery inflow (Qha). Phlv is the venous pressure in a hepatic lobulus and Ppv is the vena porta pressure. Dhep 1 and Dhep2 is the thickness of the liver measures with micro sonometric crystals in the region of the pressure measurement Phlv.

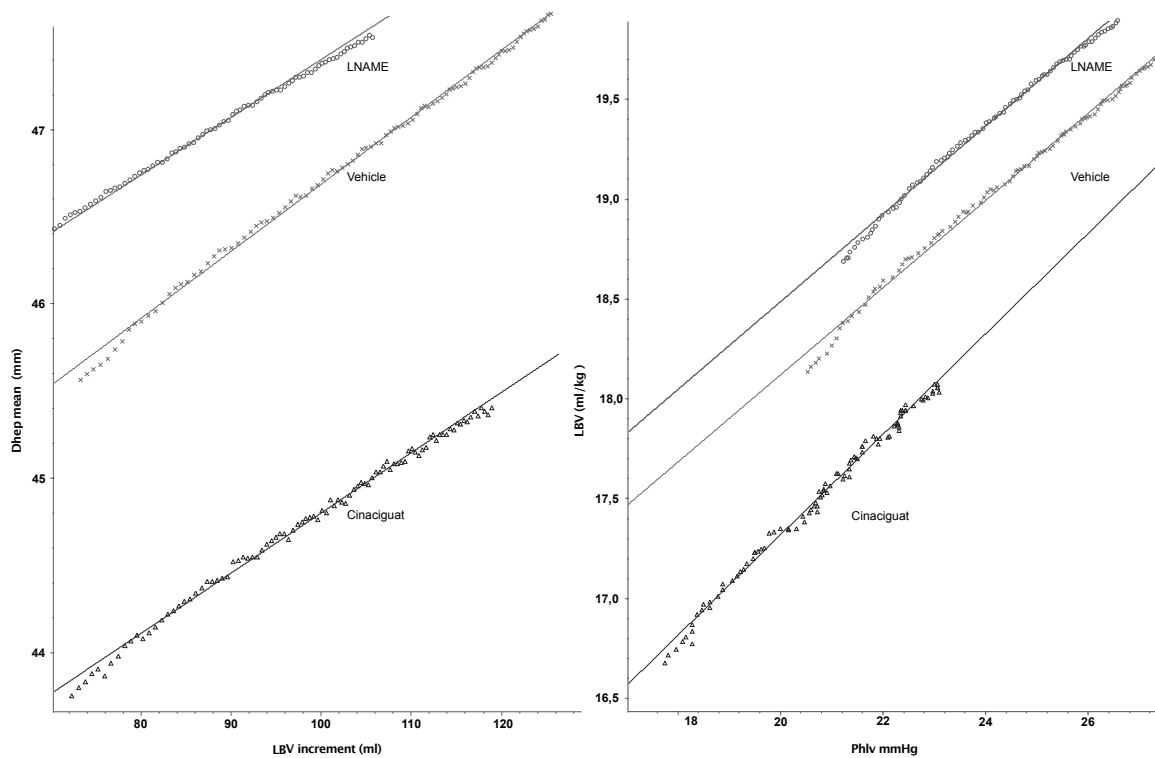


Figure 15, Plots of liver blood volume increment against mean hepatic thickness (*Dhep mean*) and hepatic lobulus venous pressure (*phlv*) and estimated liver blood volume (*LBV*)

Figure 15 shows example plot from one pig. Left panel is the plot of mean liver diameter between the two pairs of anteroposterior micro sonometric crystals and the integral of liver blood inflow during balloon occlusion of outflow with the IABP-balloon in vena cava inferior. From this plot the slope for each condition of the experiment is calculated by linear regression. This slope is then used as the calibration constant between increase in liver diameter and liver blood volume. In the right panel this constant is used to generate the plot between liver lobulus pressure and absolute liver blood volume.

The validity of this model have been questioned by Rothe and coworkers<sup>136</sup>. In their highly invasive cat-model they measured liver volume by plethysmography and spleen volume by weight and correlated changes during sympathetic nerve stimulation against ultrasound crystal dimension measurements. They found that the cubed dimensions of the spleen correlated well with weight changes, while the cubed thickness of the liver showed a low degree of correlation with liver volume. Furthermore, different crystal pairs on the same liver yielded high variability in the resulting slope and y-intercept of the cubic regression lines. Also repeated measurements of plethysmographic volumes and cubed crystal dimensions showed

high variability. The average means for both methods were the same. Rothes group speculates that the different results in liver and spleen can be explained by several factors. First The spleen expels a larger proportion of its control blood volume upon stimulation (70-80% compared with 50% for the liver). For the liver 50% reduction in blood volume corresponds to 12% decrease in total liver volume. This translates to only 4% decrease in liver thickness<sup>136</sup>. Because of the small changes in dimensions, positioning and fixation of crystals is critical. Furthermore, Rothe speculates that other large structures in the liver (large vessels and bile ducts) can become interpositioned between two ultrasound crystals and the ultrasound measurements will be then affected if these structures have a different volume response than the liver parenchyma.

Smiseth et. al. did show high reproducibility in their results by using their method despite the pitfalls discovered by Rothe. Also, Rothe acknowledged that mean values of liver volumes obtained by micro sonography correlates acceptably with more invasive methods.

In our study the relative changes in crystal dimensions and volumes have been calibrated at each measuring point by integrating the inflow in vena porta and the hepatic artery after occluding the liver veins. The measured change in liver blood volume showed high degree of linear correlation with the measured intralobular vein pressures and with the crystal dimension, however the change in crystal dimensions were minimal and within uncertainty of measurement. Therefore, the calculation of compliance based on liver inflow and vein pressure have a higher degree of precision than the calculation of absolute liver blood volume and capacitance based on this volume.

#### **6.4.12 Hepatic resistances**

Total hepatic resistance is calculated as

$$THR = \frac{P_{pv} - P_{hv}}{Q_{pv} + Q_{ha}}$$

Portal venous resistance is calculated as

$$PVR_{Hep} = \frac{P_{pv} - P_{hv}}{Q_{pv}}$$

Hepatic arterial resistance is calculated as

$$AVR_{Hep} = \frac{MAP - P_{hv}}{Q_{ha}}$$



Liver compliance, Compliance, was calculated as the linear regression between liver volume change and liver lobular pressure change during liver vein occlusion.

$$Compliance_n = \frac{\int_0^n (Q_{pv} + Q_{ha})}{Pvhl_n - Pvhl_0}$$

## 6.5 Statistics

Animal experiments often include repeated measurements in individual animals. Measurements may be separated in time and interventions. The conventional methodology for analyzing such data is univariate or multivariate analysis of variance (ANOVA or MANOVA).

ANOVA demand that pairs of observations made in one animal at different times all have the same covariance regardless of the time factor and that the covariance between animals is the same at all time points. It is to be expected that measurements in one animal correlates higher than measurements between animals, and that measurements taken close in time correlates higher than measurements taken far apart. Using incorrect standards of mean increases the risk of type 1 statistical errors (falsely rejecting the null hypothesis) and results in inefficient use of repeated data.

MANOVA accounts for variation between animals and is better for analyzing trends over time but requires balanced data with observations at all time points. If data is missing, that subject will be omitted from further analysis, and this results in critical data loss when the sample size is small<sup>137</sup>.

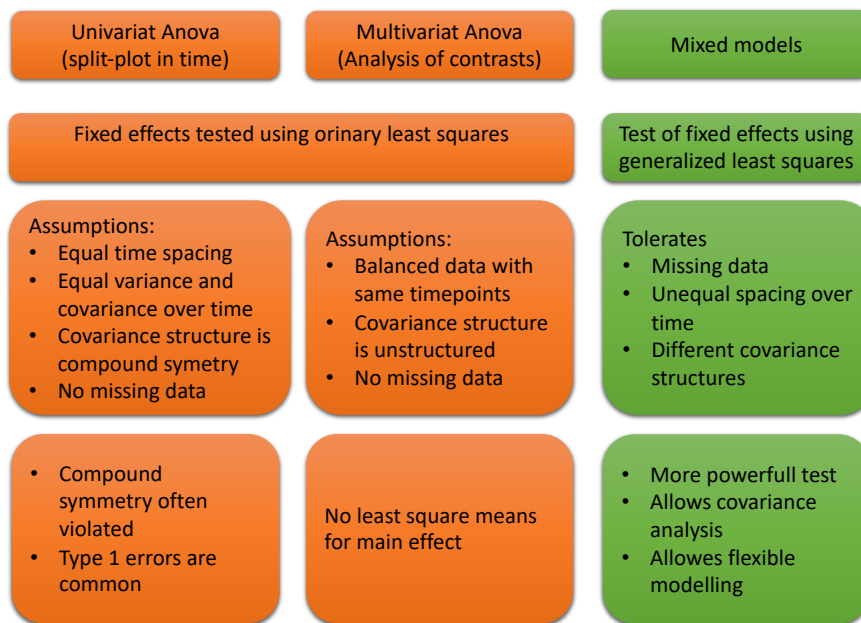


Figure 16. Comparison of univariate anova, multivariate anova and mixed models.

Mixed models make fewer assumptions regarding the covariance structure in repeated data and offers the possibility of assessing different covariance structures and compare the goodness of fit between models. Furthermore, mixed models include subjects despite missing data on one or more measurement points (avoids listwise deletion). Unbalanced longitudinal datasets (measurements at different time points) are also easily accommodated in a linear mixed model. These advantage gives superior utilization of repeated data. The critical step in performing mixed models analysis is to choose the correct covariance structure, which results in the best model fit of the data. Several covariance structures must be tested and the simplest model, with the best goodness of fit, is chosen.

The random effect in an animal study will typically be the identification of the single animal while fixed effects are categorical factors representing treatment levels. In the analysis individual characteristics of the animal can then be separated from direct treatment effects <sup>138</sup>.

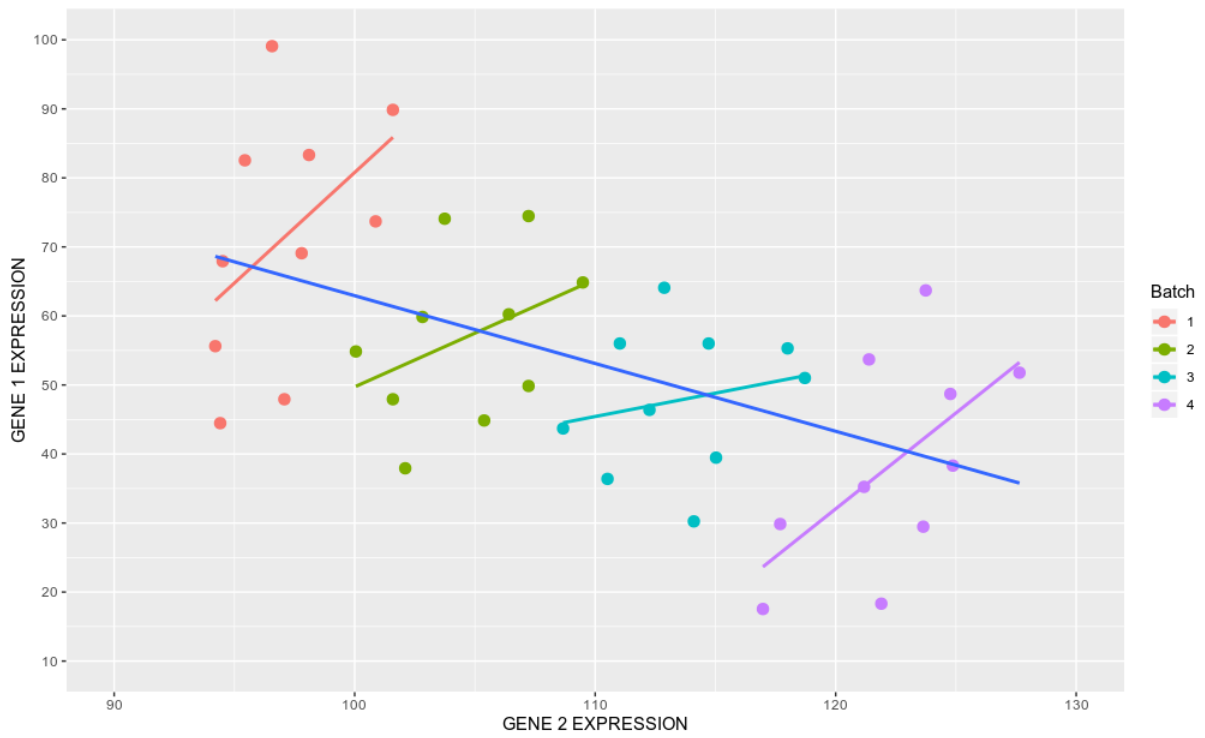


Figure 17. Principal example where simple linear regression would yield a negative correlation between the x- and y-axis although each individual shows a positive correlation with different slopes and different intercepts. From reference <sup>139</sup> with permission.



## **7 Aims of the studies**

### **7.1 Paper 1**

As a baseline for the planned animal studies on Riociguat and Cinaciguat we wanted to explore the current knowledge and understanding of right ventricular dysfunction and failure. We advocate an integrated approach to the complete right sided circulation from systemic venous pressures- and compliance through right atrial function, function of the right ventricular free wall and interventricular septum to pulmonary vascular compliance and resistance and lastly the interplay with left ventricular function. The sparsity of consensus and clinical guidelines in right heart pathology makes a physiological understanding of this part of the circulatory system even more important when investigating medications with potential effects on the right ventricle or the pulmonary circulation.

### **7.2 Paper 2**

Cinaciguat and Riociguat represent new drugs that have been developed for their ability to activate or stimulate soluble guanylate cyclase and increase the synthesis of cGMP. Since lack of NO and reduced sensitivity of NO on sGC are common problems in cardiovascular disease these drugs have a multitude of potential therapeutic effects. In study 2 we wanted to study the integrated hemodynamic effects of these two drugs in a closed chest model of healthy juvenile pigs and characterized the interaction with NO. Of special interest was the prospect of a selective pulmonary vascular vasodilation, since the number of systemic drugs that achieve this is sparse.

### **7.3 Paper 3**

Study 3 revealed that Cinaciguat resulted in a profound blockade of NO-modulation and proposed that Riociguat is better suited as a clinical vasodilator.

A potential benefit of stimulating the sGC-cGMP-axis is an oxygen sparing effect in the myocardium. In study 3 we therefore studied the cardiometabolic efficiency of Riociguat in the left ventricle. We also did try to assess the cardiometabolic efficiency in the right ventricle. However, to create a stable in vivo model for cardiometabolic efficiency, particularly oxygen measurements, in the intact right ventricle proved exceedingly difficult. These data were discarded due to their inconsistency and variability. The effects of Riociguat were assessed by applying NO-blockade (L-NAME) in Riociguat pretreated animals. As L-

NAME has a known negative effect on efficiency, these studies were designed to assess whether Riociguat could substitute the NO function during this blockade.

## **7.4 Paper 4**

Study 2 and 3 focused on the heart and the arterial circulation. Increased filling pressure is a common problem in cardiovascular disease. In study 4 we, therefore, wanted to investigate the effects of Riociguat and Cinaciguat on the venous circulation and specifically the hepatic circulation as the liver has the potential to act as a venous reservoir during periods of volume overload. We used a liver outflow occlusion model with flow and pressure monitoring of liver in- and outflow to determine liver compliance and capacitance.

## 8 Results

### 8.1 Paper 1

The paper consists of a discussion of the current concepts of right heart circulation. As stated in numerous papers during the last two decades, the right heart is still “the dark side of the moon” in terms of sound experimental basis for concepts of right heart physiology.

### 8.2 Paper 2

#### 8.2.1 Hemodynamics in a closed chest model

In this study we have characterized the integrated hemodynamic impact of the sGC-stimulator Riociguat and the activator Cinaciguat in different NO-states in healthy juvenile pigs. Most importantly, we observed a more pronounced vasodilatory effect in the systemic than pulmonary circulation for both drugs.

Riociguat reduced the systemic vascular resistance by 40% and induced lower systemic blood pressures. The same dose, with an evident systemic effect, reduced PVR by 20% but did not decrease pulmonary systolic or mean pulmonary blood pressures. CO was slightly increased.

Cinaciguat lowered systemic and pulmonary systolic, diastolic, mean and venous blood pressures. CO was slightly reduced. Also, calculated SVR decreased while PVR remained unchanged

L-NAME resulted in reduced CO, higher systemic and pulmonary blood pressures, and a corresponding calculated increase in SVR and PVR.

Riociguat, given after L-NAME, increased CO, reduced MAP, SVR, MPAP, and PVR demonstrating a NO-independent vasodilatory effect. L-NAME administered after Riociguat in separate experiments decreased CO and increased MAP, SVR, MPAP, and PVR, an indication that Riociguat interacts with NO in an additive manner.

Cinaciguat, given after L-NAME induced both systemic and pulmonary vasodilation. However, L-NAME, given after Cinaciguat, had almost no vascular effect, indicating that the effect of Cinaciguat could not be modulated by altering NO-tone.

Finally, nitroglycerine, given after Riociguat and L-NAME, resulted in unchanged CO, decreased MAP, SVR, systolic and diastolic pulmonary pressures, MPAP, and PVR

confirming that NO retains its dose-dependent effect also after giving Riociguat.

Nitroglycerine given directly after Cinaciguat had almost no vasoactive effect.

Riociguat act integrated with NO in an additive manner while Cinaciguat, in principle, completely blocked the endogenous NO effect on vascular control.

	Test drug alone		LNAME alone, Rio-group	LNAME alone, Cina-group	Test drug after LNAME		LNAME after test drug		Nitroglycerin after test drug and LNAME		Nitroglycerin after LNAME and test drug	
	Rio	Cina	LNAME	LNAME	LNAME	LNAME	Rio	Cina	Rio	Cina	LNAME	LNAME
					+Rio	+Cina	+LNAME	+LNAME	+LNAME	+LNAME	+Rio	+Cina
									+NG	+NG	+NG	+NG
MAP	-	-	++	++	-	-	+++	NS	---	NS	-	-
SVR	-	-	++++	+++	-	---	+++	NS	---	-	NS	NS
MPAP	NS	-	+++	++	-	-	+++	NS	---	NS	-	NS
PVR	-	NS	++++	+++	-	---	+++	-	---	NS	-	NS

Table 2. Data from study 2. MAP is mean arterial pressure in the aorta. Rio is Riociguat, Cina is Cinaciguat, NG is nitroglycerine. MPAP is mean pressure the pulmonary artery, SVR is systemic vascular resistance, PVR is pulmonary vascular resistance. +/- ≤ 25% change, ++/-- = 25 - 50% change, +++/--- = >51% -100 change, ++++/-- -- > 100% change from previous combination of medications.

Neither compound demonstrated pronounced cardiac effects but had unloading effect on both systolic and diastolic function.

The load-related parameters of time-dependent pressure development were slightly reduced for both left and right ventricle. However, calculating the load-independent parameters of PRSW showed that Riociguat in this dose had a neutral effect on cardiac contractility.

Cinaciguat induced a small reduction in the PRSW in the left ventricle.

Both Riociguat and Cinaciguat demonstrated a slower maximum intraventricular pressure fall rate, expressed as dP/dt min in the left ventricle. For the right ventricle, Cinaciguat gave a small decrease in dP/dt min, while Riociguat did not have any effect on this index. Using the Tau-index, both Cinaciguat and Riociguat resulted in significantly faster relaxation of the left ventricle compared to baseline, and both Cinaciguat and Riociguat counteracted the prolonged isovolumic relaxation seen after L-NAME by reducing the Tau index. Both Cinaciguat and Riociguat demonstrated unchanged left ventricular end-diastolic volumes at lower end-diastolic pressures.



Taken together, these data show that the effect on cardiac function for all practical purposes is determined by their vasodilatory and unloading effects.

## **8.3 Paper 3**

### **8.3.1 Hemodynamics in an open chest model**

Infusion of Riociguat gave a modest systemic vasodilatation, including the coronary circulation, as seen by a drop in coronary and systemic vascular resistance of  $36\% \pm 21\%$  ( $p=0,01$ ) and  $26\% \pm 18\%$  ( $p=0,00$ ). No effect was measured in the pulmonary vasculature. L-NAME after Riociguat resulted in both pulmonary and systemic vasoconstriction as seen by a  $2,5 \pm 1,6$  ( $p=0,01$ ) and  $1,5 \pm 0,2$  ( $p=0,00$ ) fold increase in PVR and SVR respectively.

Riociguat did not alter CO or EF. Left ventricular maximum pressure development decreased by  $24\% \pm 12\%$  ( $p=0,00$ ), while no change in this index was seen for the right ventricle. SW was reduced by  $20\% \pm 8\%$  ( $p=0,00$ ) for the left, but not the right ventricle. Left ventricular ESPVR, was reduced by  $14\% \pm 14\%$  ( $p=0,01$ ). Right ventricular ESPVR remained stable. PRSW decreased by  $13\% \pm 7\%$  ( $p=0,01$ ) for the left ventricle, but did not change for the right ventricle. Ventricular dimensions remained unchanged. All results were in line with the hemodynamic results from paper 2.

### **8.3.2 Cardiometabolic efficiency**

Right and left ventriculoarterial coupling index,  $E_{es}/E_a$ ,  $SW_{eff}$ , and the relationship between left ventricular  $MVO_2$  and total mechanical work, PVA were unaffected by Riociguat. L-NAME shifted the  $E_{es}/E_a$  ratio toward reduced  $SW_{eff}$  in both systemic and pulmonary circulation. Importantly, there was no surplus oxygen consumption, measured by the  $MVO_2/PVA$  relationship after L-NAME in Riociguat treated pigs.

## **8.4 Paper 4**

### **8.4.1 Hepatic flows and pressures**

Neither Cinaciguat nor Riociguat did affect the portal or arterial liver blood flows. No difference could be found in portal pressure or liver venous pressures. Cinaciguat, however, resulted in a  $43\%$  ( $\pm 84\%$ ) fall in arterio-venous resistance from baseline, while no such effect was seen for Riociguat. L-NAME caused a decrease in portal and arterial flows through the liver and increased the arterio-venous resistance by  $140\%$  ( $\pm 98\%$ ) but did not affect the porto-

venous resistance. Both Cinaciguat and Riociguat reversed the increased arterio-venous resistance induced by L-NAME. Also, pre-treatment with Cinaciguat but not Riociguat prevented the arteriolar vasoconstriction caused by NO-blockade by L-NAME.

#### **8.4.2 Liver compliance and capacitance**

Neither Riociguat nor Cinaciguat or L-NAME had any influence on hepatic micro sonometric dimensions or liver compliance. The liver's venous capacitance (the unstressed volume or y-intercept of the liver volume-pressure-curve) did not change by Riociguat, Cinaciguat, or L-NAME.

## 9 Discussion

### 9.1 Discussion of the state of the literature

Neither Riociguat nor Cinaciguat seem to have pure pulmonary vasodilatory properties.

Most studies of Riociguat and Cinaciguat using systemic administration (per oral, intraperitoneal, intravenous), and even direct infusion into the pulmonary artery in doses that produce clinically relevant pulmonary vasodilatation, produce potent systemic vasodilatation (tables 1-4).

#### 9.1.1 Animal studies on Riociguat

<i>Species</i>	<i>Investigator/ Study name</i>	<i>Number of animals</i>	<i>Pathology, model</i>	<i>Route of administration</i>	<i>PVR</i>	<i>SVR</i>	<i>CO</i>	<i>Primary aim</i>	<i>Secondary findings</i>
<i>Minipig</i>	Becker, 2013 <sup>140</sup>	30	PAH after one lung ventilation	i.v.	↓	↓	↑	Redistribution of pulmonary blood flow.	
<i>Mice</i>	Rai, 2017 <sup>141</sup>	15	PAH after PAB	p.o	-	-	↑	RV function and remodeling.  Comparison of Sildenafil and Riociguat.	Reduced cardiac fibrosis
<i>Mice</i>	Schermuly 2008 <sup>142</sup>		PAH after hypoxia	p.o	↓	↓		Expression of sGC in humans and animals with PAH	Upregulation of sGC, reversed right heart hypertrophy and lung vascular remodeling
<i>Rats</i>	Schermuly 2008 <sup>142</sup>		PAH after monocrotaline	p.o	↓	↓		Right heart hypertrophy  Lung vascular remodeling  Comparison of Sildenafil and Riociguat.	
<i>Mice, guinea pigs</i>	Weissmann, 2014 <sup>143</sup>	39	PAH after smoke inhalation	p.o				Expression of sGC in humans with PAH and animals with experimental	Upregulation of sGC, reversed right heart hypertrophy and

<i>Species</i>	<i>Investigator/ Study name</i>	<i>Number of animals</i>	<i>Pathology, model</i>	<i>Route of administration</i>	<i>PVR</i>	<i>SVR</i>	<i>CO</i>	<i>Primary aim</i>	<i>Secondary findings</i>
								PAH. Effect of Riociguat on hemodynamics and vascular remodeling.	lung vascular remodeling
<i>Rat</i>	Chamorro, 2018 <sup>144</sup>	41	PAH after bleomycin, hypoxia	i.v.	↓	↓			Inhibition of hypoxic pulmonary vasoconstriction
<i>Rat</i>	Donda <sup>145</sup>		Hyperoxia induced BPD I neonatal rats	intraperitoneal	↓			Pulmonary vascular remodeling, hemodynamics and inflammation.	Decreased pulmonary vascular remodeling. Decreased inflammation. Preserved vascular density
<i>Mice</i>	Pradhan <sup>146</sup>	60	Secondary PAH after TAC. Comparison with Sildenafil	p.o	↓			Hemodynamics, pulmonary vascular remodeling, right heart function.	Reduced vascular remodeling, improved right ventricular function
<i>Pig</i>	Schultz <sup>147</sup>	28	PAH after experimental pulmonary embolism with preserved CO. Comparison with Sildenafil, and iNO	i.v.	↓	↔		Acute hemodynamics	Decreased PVR without decrease in SVR. Increased CO.

Table 3, animal studies on riociguat. PAH is pulmonary arterial hypertension, PAB is pulmonary arterial banding.

## 9.1.2 Animal studies on Cinaciguat

<i>Species</i>	<i>Investigator</i>	<i>Number of animals</i>	<i>Pathology</i>	<i>Route of administration</i>	<i>PVR</i>	<i>SVR</i>	<i>CO</i>	<i>Scope</i>	<i>Other findings</i>
<i>Dog</i>	Boerrigter 2007 <sup>148</sup>	7	Pace induced LVF	i.v	↓	↓		Hemodynamics, renal blood flow, neurohumoral responses.	Increased renal blood flow, preserved GFR
<i>Lamb</i>	Evgenov 2007 <sup>149</sup>	35	Monocrotaline induced PAH. Inhaled Cinaciguat	inhalation	↓	-		cGMP-release, hyper oxidation, interaction with iNO,	Responsiveness to iNO reduced after oxidation while the effect of Cinaciguat increased
<i>Apo-sGC knock-in mice</i>	Thoonen <sup>150</sup>		Hypertension in heme-free sGC knock-in mice	p.o		↓		Platelet function, hemodynamic response to NO and Cinaciguat.	sGC knockout mice lack NO responsiveness but have a stronger Cinaciguat effect. WT mice also have some Cinaciguat effect
<i>PASMC Fetal sheep</i>	Chester 2011 <sup>151</sup>		Hyperoxia, H <sub>2</sub> O <sub>2</sub> , ductus arteriosus ligation,	Pulmonary artery	↓	↓		Pulmonary smooth muscle cell function, sGC levels, interaction with NO and hyper oxidation.	Responsiveness to iNO reduced after oxidation while the effect of Cinaciguat increased
<i>Fetal sheep</i>	Chester 2009 <sup>152</sup>		Normal fetal status, Cinaciguat infused into PA	Pulmonary artery	↓	rm		Hemodynamics, pulmonary smooth muscle cell function, hyper oxidation.	Effect of Cinaciguat increased after oxidative stress
<i>Nitric synthetase knock out mice</i>	Dumitrascu, 2006 <sup>148</sup>		Hypoxia induced PAH Monocrotaline induced PAH	p.o	↓	↓		Hemodynamics, right ventricular hypertrophy, pulmonary	Reduced right ventricular and pulmonary

<i>Species</i>	<i>Investigator</i>	<i>Number of animals</i>	<i>Pathology</i>	<i>Route of administration</i>	<i>PVR</i>	<i>SVR</i>	<i>CO</i>	<i>Scope</i>	<i>Other findings</i>
Rats								vascular remodeling.	artery hypertrophy

Table 4, animal studies on cinaciguat. PAH is pulmonary hypertension, PAB is pulmonary arterial banding, LVF: left ventricular failure

### 9.1.3 Lessons learned from animal studies of Riociguat and Cinaciguat

The only two animal study of these drugs that have shown selectivity for the pulmonary vasculature is Evgenovs study with inhalation of Cinaciguat in awake lambs with monocrotaline induced PAH<sup>149</sup> and Schultz’s study in pigs with experimental allogenic blood cloth pulmonary embolism<sup>147</sup>. In this latter study pulmonary embolism produced a threefold increase in PVR without reducing MAP or CO. Riociguat and iNO lowered PVR without affecting SVR. Sildenafil lowered both PVR and SVR, but with a higher effect on PVR and without affecting MAP. In this study both iNO, Sildenafil and Riociguat have similar vasodilatory effects, meaning that sCG in this model of pulmonary embolism is sensitive to NO and that cGMP is being produced at a level that make PDE inhibition effective. This phenotype may not be universal for other pathologies with increased pulmonary resistance.

### 9.1.4 Human studies on Riociguat

<i>Phase</i>	<i>RCT, study DB, PC</i>	<i>Study name</i>	<i>N of patients</i>	<i>Pathology</i>	<i>PVR</i>	<i>SVR</i>	<i>CO</i>	<i>6MWD</i>	<i>WHO FC</i>	<i>Follow-up time</i>	<i>Adverse effects</i>
II	-	Grimminger 2009 <sup>153</sup>	19	PAH, CTEPH	↓					2 h	Mild in 20%, no serious AEs
II	-	Ghofrani 2010 <sup>60</sup>	75	PAH, CTEPH	↓	↓		↑		12 w	Mild to moderate in 96%, serious in 4%
II	-	Hoepfer 2012 <sup>154</sup>	22	PH-ILD	↓	↓		↑		12 w	104 AEs in 22 patients. Serious in 9%
IIb	+	LEPAH 2013 <sup>155</sup>	201	PH-LVF	↓	↓	↑			16 w	81-91% AEs. Hypotension 9-12%, Dizziness 12-16%, nausea 6-16%

<i>Phase RCT, study DB, PC</i>	<i>Study name</i>	<i>N of patients</i>	<i>Pathology</i>	<i>PVR</i>	<i>SVR</i>	<i>CO</i>	<i>6MWD</i>	<i>WHO FC</i>	<i>Follow-up time</i>	<i>Adverse effects</i>
III	+	CHEST-1 2013 <sup>63</sup>	261	CTEPH	↓		↑	↑	16 w	92% AEs. Hypotension 9%, headache 25%, dizziness 23%
III	+	PATENT-1 2013 <sup>156</sup>	443	Idiopathic, familial, connective tissue disease	↓		↑	↑	30 d	89-92% AEs, Hypotension 10%, Anemia 8%, Headache 32%, Dizziness 24%
IIa	+	DILATE 2014 <sup>157</sup>	39	PH-HFpEF	-	↓	↑		6 h	38-50% AEs, Hypotension 0- 30%, acute renal failure 0-10%
II	+	PATENT PLUS 2015 <sup>158</sup>	18	PAH on sildenafil	-	-	-	-	12 w	100% AEs, 17% hypotension, 17% dizziness, 17% headache
II	-	Ghofrani 2015 <sup>58</sup>	23	PH-COPD	↓	↓	↑		4 h	AEs 40.46%, anemia, dizziness
II	-	Hoepfer 2015 <sup>154</sup>	68	PAH, CTEPH			↑	↑	3 – 87 m	AEs 93%, 37% peripheral oedema
III	+	CHEST-2 2015 <sup>59</sup>	237	CTEPH			↑	↑	0 – 42 m	96% AEs, 7% syncope, 6% hypotension, 19% dizziness
III	+	PATENT-2 2015 <sup>159</sup>	396	PAH			↑	↑	0 - 45 m	97% AEs, 9% hypotension, 7% syncope, 23% dizziness
II	-	RIVER 2018 <sup>160</sup>		PAH, CTEPH					12 m	
II	-	RESPITE 2016 <sup>161</sup>	61	PAH failing on sildenafil	↓	↓	↑	↑	24 w	95% AEs, 16% serious, 16%

Phase RCT, study DB, PC	Study name	N of patients	Pathology	PVR	SVR	CO	6MWD	WHO FC	Follow-up time	Adverse effects
										hypotension, 16 % headache
IIIb	-	CTEPH EAS 2017 <sup>162</sup>	300	CTEPH			↑	↑	12 w	91% AE, 10% hypotension, syncope 6%
II	-	Taran, 2018 <sup>163</sup>	20	IPAH	↓	↓	↑	↑	12 w	Hypotension 10%, tachycardia 10%
II		Ahmadi, 2018 <sup>164</sup>	6	CTEPH					6 m	2 patients with postural dizziness
II		Darocha, 2018 <sup>165</sup>	28	CTEPH, failing on sildenafil	↓	↓	↑	↑	6 m	61% AEs, hypotension 25%, headache 14%

Table 5, human studies on riociguat. PAH: pulmonary hypertension, PAB: Pulmonary arterial banding, LVF: left ventricular failure, COPD: chronic obstructive pulmonary disease, CTEPH: Chronic thromboembolic pulmonary hypertension, IPAH: Idiopathic pulmonary hypertension, 6MWD is the distance walked in 6 minutes.

### 9.1.5 Human studies on Cinaciguat

Phase RCT, study DB, PC	Study name	N of patients	Pathology	PVR	SVR	CO	6MWD	WHO FC	Follow-up time	Adverse effects
IIb	+	COMPOSE, 2012 <sup>166</sup>	76	Acute heart failure	↓	↓	-		48 h	Terminated due to systemic hypotension
I/II	-	Lapp, 2009 <sup>167</sup>	27+33	Acute decompensated heart failure	↓	↓	↑		6 h	Hypotension
IIb	+	Erdmann, 2012 <sup>168</sup>	139	Acute decompensated heart failure	↓	↓	↑		16 – 40 h	Terminated due to hypotension

Table 6, human studies on cinaciguat. PAH: pulmonary hypertension, PAB: Pulmonary arterial banding, LVF: left ventricular failure, COPD: chronic obstructive pulmonary disease, CTEPH: Chronic thromboembolic pulmonary hypertension, IPAH: Idiopathic pulmonary hypertension



### 9.1.6 Lessons learned from human studies of Riociguat and Cinaciguat

Riociguat is mainly investigated in patients with pulmonary hypertension due to chronic thromboembolic pulmonary embolism with insufficient effect of thrombolysis and contraindications to or insufficient effect of surgically removal of emboli <sup>58,59,169,60,62,63,153,160,162,164,165</sup>. Two studies have investigated the effect of Riociguat in pulmonary hypertension secondary to left ventricular failure <sup>155,157</sup>. Follow-up times in Riociguat studies range from 6 hours to 87 months. Cinaciguat on the other hand, is only studied in the setting of acute decompensated left heart failure with no long term follow-up <sup>166-168</sup>.

Human studies, summarized in table 3 and 4, have confirmed the hemodynamic profile of Riociguat and Cinaciguat with no pulmonary selectivity of vasodilatation when the medication is given orally.

All studies measuring 6-minute walk test and WHO function class report improvement in these physical outcome scores. However, the lack of pulmonary vascular selectivity causes a tendency for systemic hypotension, and the frequency of hypotension related symptoms are high for both drugs. For Riociguat the tendency to induce systemic hypotension appears self-limiting after extended use. For Cinaciguat, on the other hand, the hypotensive effects has led to early termination of studies <sup>166,168</sup>.

Riociguat, on the market as Adempas (Bayer AG, Leverkusen, Germany) is currently the only sGC-modulator approved for human use as a pulmonary vasodilator in CTEPH I patients deemed unfit for surgery <sup>170</sup>. There are no ongoing studies on Cinaciguat at the time of this review. Thirteen studies on PAH using Riociguat are currently recruiting patients (Clinicaltrials.gov, accessed 29. Nov 2022).

Of notice, the sGC-stimulator Vericiguat has been tested in two phase II studies in patients with reduced or preserved ejection fraction, The SOCRATES-REDUCED <sup>171</sup> and SOCRATES-PRESERVED <sup>172</sup> studies. In SOCRATES-REDUCED a once daily dose for 12 weeks was well tolerated with no difference in adverse effects compared to placebo (77,2% vs 78,9%). Treatment-emergent hypotension occurred in 15% in the 10 mg Vericiguat group with higher incidence of serious adverse events in the placebo group. However, there was no difference in Pro-BNP (primary endpoint). In SOCRATES-PRESERVED these results was reproduced with no difference in adverse events between placebo and Vericiguat 10 mg (73,1 vs 69,8%) and no change in blood pressure, left atrial volume or Pro-BNP after 12 weeks of

treatment. Vericiguat-patients improved on the Kansas City Cardiomyopathy Questionary Clinical Summary Score. Exploratory echocardiography suggests improved early relaxation ( $e^{-}$ -velocity).

In the phase III VICTORIA trial <sup>173</sup> 5050 patients with congestive heart failure (NYHA II-IV) and EF < 45% were randomized to Vericiguat 10 mg once daily or placebo with 12 months follow-up. This study demonstrated a reduction in the combined outcome of cardiovascular death or hospitalization for heart failure from 38,5 to 35,5% (p=0,019) but no change in cardiovascular or all-cause mortality. Adverse events were not different between groups.

A recent metanalysis, comprising 5604 patients from 6 RCTs comparing Vericiguat or Riociguat to placebo found a reduction in the composite endpoint of cardiovascular mortality or heart failure readmission to hospital. The sGCS-stimulators had no effect on all-cause mortality or cardiovascular mortality. The safety was the same in treatment and placebo groups <sup>174</sup>.

### **9.1.7 Summary of the current literature**

A review of the literature shows that both Riociguat and Cinaciguat are alternative substances to stimulate or activate sGC under conditions with reduced sensitivity for NO in the sGC enzyme. Cinaciguat have an isolated NO-independent effects, while Riociguat-treated animals remain NO-sensitive. None of the drugs have innate selectivity for the pulmonary vasculature and systemic hypotension is a limiting factor for their clinical use. For Riociguat the systemic vasodilatation, at doses with meaningful pulmonary vasodilatation, is manageable but for Cinaciguat systemic hypotension limits its clinical use when given as per oral or intravenous medication.

## **9.2 Discussion of the results from our studies**

### **9.2.1 General hemodynamics**

We have shown in study that both Cinaciguat and Riociguat have pronounced vasodilatory properties in the normal systemic vasculature. However, in healthy juvenile pigs, these compounds have only minor direct effects in the pulmonary circulation. After NO-blockade with L-NAME, a vasodilatory effect in both vasculatures was unmasked. Importantly, no additional vasoactive effect of NO could be observed after Cinaciguat infusion, indicating a functional NO-blocking effect of this compound. In contrast, NO modulation after Riociguat

infusion altered vascular tone in an interactive, qualitative physiological expected manner. The direct cardiac responses of both drugs were dominated by their unloading effects, and only a small possible reduction in load-independent contractility observed from Cinaciguat. The small lusitropic effect for both drugs may also be related to the unloading effect from their vasodilation.

### **9.2.2 Interplay with the NO-system**

The interplay of Riociguat and Cinaciguat with the NO-system in the pulmonary circulation has previously been studied primarily in PAH-models <sup>149,175–179</sup>. These observations are somewhat in contrast with the relative weak pulmonary effects in healthy animals observed in our study. A possible explanation might be a different level of the sGC red-ox forms in pathological and normal pulmonary vessels. Soluble Guanylate Cyclase is upregulated in human idiopathic pulmonary hypertension and animal models of PAH <sup>179</sup>, and the vasodilatory effect of both sGC-stimulators and activators is augmented by oxidation of sGC. It is not known what the proportion of the different oxidation levels of sGC is in intact, healthy animals. The effects of these drugs given intravenously in intact animals and the interactions with NO are consequently unknown. Our study using Cinaciguat indicates that there is a functional oxidized sGC also in the healthy systemic circulation, but the activity seems to be low in the pulmonary vasculature. An alternative explanation for the small effects of these drugs in the pulmonary vasculature is the probable normal level of NO synthetase and a concomitant higher activity in healthy animals compared to reduced levels in pulmonary vascular pathology <sup>180</sup>. This may also explain the conflicting results in our study and Schultz study in pigs with experimental pulmonary embolism where Riociguat had a selective vasodilatory effect <sup>147</sup>.

In a clinical study with Riociguat applied in pulmonary hypertension secondary to diastolic heart failure, but without increased PVR, there was no change in transpulmonary pressure gradient or PVR <sup>157</sup>. The explanation for this might be a lower expression of and lower oxidation levels of sGC in the lungs with no primary pathology, abolishing any pulmonary vascular selectivity when the drug is applied intravenously. Inhalation, in contrast to intravenous administration of sGC-activators and stimulators, has been shown to give selective pulmonary vasodilatation in awake lambs with acutely thromboxane-induced pulmonary hypertension <sup>149</sup>. Still, such an application has not to our knowledge been tested in humans or in healthy animals.

The dynamics between NO, sGC-activators, sGC-stimulators, and sGC have been studied in cell cultures with outcomes indicating that sGC-activators can skew the redox balance between a small pool of oxidized sGC in the direction of increased oxidation, rendering the sGC insensitive to NO<sup>181</sup>. An in-vitro study on healthy porcine coronary arteries and rat thoracic aortas have shown that Cinaciguat has a profound vasodilatory effect even in the absence of vascular pathology<sup>182</sup>. In that study, Cinaciguat exhibited an irreversible effect, and the authors proposed that Cinaciguat shift the red-ox-equilibrium of sGC toward the heme-free species. This, in turn, could explain the observed insensitivity to NO-manipulation after Cinaciguat in our study. The timespan for potential recovery of this effect is unknown.

The prolonged action and loss of NO-system modulation seem to make Cinaciguat a potent but difficult drug to use in clinical practice. There are no ongoing patient studies with Cinaciguat<sup>183</sup>, but there are nine actively recruiting studies on Riociguat in scleroderma, sickle cell disease, PAH, and CTEPH (chronic thromboembolic pulmonary hypertension)<sup>184</sup>. As seen from our research, the sGC activators have profound and partly unphysiological effects demanding considerable preclinical assessments before clinical application. There are some phase I studies ongoing with sGC-activators in patients with chronic kidney failure, pulmonary arterial hypertension, and acquired pulmonary distress syndrome (ARDS)<sup>185</sup>. These studies need to be monitored closely for possible adverse systemic circulatory effects.

### **9.2.3 Cardiac effects of SGC-stimulators and activators**

We did not observe any effect of Riociguat on cardiac contractility evaluated by PRSW, and only a small negative effect of Cinaciguat. Studies on ischemia-reperfusion injuries in the heart have shown cytoprotective properties of both Cinaciguat and Riociguat, but no fundamental change in heart function<sup>186-189</sup>. Such a protective effect can potentially be related to myocardial calcium handling<sup>190,191</sup>. Infusion of NO-donors to the coronary circulation seems to work in a biphasic and concentration-dependent fashion with increased contractility and chronotropy in low normophysiological concentrations and the opposite effect at higher concentrations<sup>3</sup>. Therefore, the effect of exogenous NO through NO-donors may be hard to predict, and since the direct activation or stimulation of sGC additionally bypasses the cGMP-independent effects of NO, they will predictably have a different pharmacological profile compared to endogenous NO-stimulation<sup>3</sup>.

In our study, the most pronounced diastolic effect was a shortened left ventricular relaxation, expressed in the Tau index. The maximum pressure fall rate in the left ventricle also

decreased concomitantly with the Tau index reduction indicating an unloading effect of both Riociguat and Cinaciguat <sup>192</sup>. This effect was also reported in a recent paper using the sGC-stimulator Bay 41-8543 in an experimental rat model of HFpEF (Heart Failure with Preserved Ejection Fraction); Wilck and coworkers observed a normalization of diastolic dysfunction <sup>193</sup>.

#### **9.2.4 Cardiometabolic efficiency**

The main finding in study 2 was an observed neutral effect of Riociguat on myocardial oxygen consumption. There was no shift in the  $MVO_2/PVA$  relationship for Riociguat, indicating that stimulation of sGC did not influence myocardial metabolism in healthy pigs in the dose given in this study. The dose chosen was the highest dose possible to administer while avoiding excessive systemic hypotension. Of notice, the subsequent administration of the NO-blocker L-NAME did not increase the relative oxygen consumption in the myocardium, and this suggests that the expected surplus  $MVO_2$  after using L-NAME <sup>84</sup> was attenuated by this dose of Riociguat.

The impact of NO on contractility and cardiometabolic efficiency has been an area of particular attention. NO and cGMP seem to influence contractile function in a NO and cGMP-concentration dependent bidirectional fashion. In an in-vitro model, the effect of NO on cardiomyocytes was found to be dependent on intact endothelium. Cyclic GMP affected the contractile response of the myocytes via a biphasic inhibition and then stimulation of cGMP dependent cAMP phosphodiesterase inhibitor through modulation of intracellular  $Ca^{2+}$  levels and myofilament  $Ca^{2+}$  sensitivity <sup>3</sup>. In that study, increasing NO and cGMP levels induced first an increase in contractility followed by a fall at high concentrations. In a human study on cardiac failure, on the other hand, blockade of NOS increased inotropic response to  $\beta$ -adrenergic stimulus<sup>194</sup>. The complex interaction between the NO-sGC-cGMP-pathway and contractility makes it challenging to predict the exact optimum dose of NO-donors or sGC-activators or -stimulators when aiming for increased cardiac contractility.

In our study, Riociguat had a predominantly systemic vasodilatory effect. Using the same experimental setup in earlier studies, we have shown that NO-blockade, inotropic drugs and systemic infections have clear metabolic effects in the myocardium evaluated in the framework of an  $MVO_2/PVA$  analysis <sup>195-200</sup>.

There is consistent evidence that blocking enzymes in the NO pathway causes reduced cardiac efficiency by surplus myocardial oxygen consumption <sup>84,201,202</sup>. This is at least partly

caused by vasoconstriction and subsequent disruption of the ventriculo-arterial matching by elevated afterload without a concomitant increase in contractility<sup>84</sup>. The maximum stroke work at a given end-diastolic volume will, of geometrical reasons, occur when  $E_{es}$  equals  $E_{ea}$ . Stroke work efficiency (the fraction of total cardiac work, PVA delivered to the circulation as stroke work), on the other hand, increases as the  $E_{es}/E_{ea}$  ratio increases<sup>203</sup>. At an increased ratio, a lower proportion of oxygen utilization is metabolized as PE, corresponding to the metabolism necessary to preserve the wall tension of the heart at end-systole. This means that a higher proportion of oxygen is used for energy transfer to the aorta, and the oxygen cost of stroke work is, therefore, lower<sup>204</sup>. The correlation between oxygen consumption and ventriculo-arterial matching is well established<sup>205,206</sup>, and holds true also in our study with a linear correlation between measured oxygen consumption and PVA.

In addition, NO has a distinct metabolic effect independent of loading conditions<sup>207</sup>. Various metabolic studies, as reviewed by Chang et al.<sup>208</sup>, have demonstrated that the normal NO-tone in tissues reduces the mitochondrial oxygen consumption by reducing the oxygen interaction with cytochrome c oxidase/complex I. However, there is only one study demonstrating a decreased in non-contractile oxygen utilization combined with an unchanged contractile efficiency ( $MVO_2/PVA$ ) after infusion of the NO-precursor L-arginine. In that study the authors also observed the predicted opposite effect by infusion of a NOS inhibitor<sup>201</sup>. By employing a pig model in our laboratory, we have not been able to reproduce a decrease in basal oxygen requirements in the post ischemic, stunned heart after infusion of L-arginine, even though biochemical assessments demonstrated a substantial turnover of L-arginine to l-citrulline and thus a simultaneous production of NO<sup>209</sup>. Studying experimental cardiogenic shock study in our lab, however, L-NAME was shown to increase the basal oxygen requirements in the heart<sup>84</sup>. The impaired stroke work efficiency induced by L-NAME was not mirrored in the current study since there was no surplus  $MVO_2$  when L-NAME was given after Riociguat. This is in contrast to the effect of L-NAME given alone in other studies, as this compound has been shown to induce increased unloaded oxygen consumption<sup>84,201</sup>.

Our study again showed that Riociguat given to healthy animals has only a minor effect in the pulmonary circulation with no impact on the right ventriculo-pulmonary arterial coupling.

### 9.2.5 Liver circulation and venous hemodynamics

We have used the framework of Smiseth and co-workers<sup>132–135</sup> in study no. 3 with sonometric measurements of the liver calibrated to liver blood inflow during occlusion of the liver veins to evaluate the effects of Riociguat and Cinaciguat. This method has been difficult to operate in various studies, mainly due to a high spatial variability in liver dimension during blood volume change<sup>136</sup>. In our study we calibrated the sonometric dimensions against the integral of flow in the portal vein and hepatic artery after occluding the liver veins, and thus eliminating the uncertainties of a cubic volumetric model. Even so, the changes in liver dimensions using micro sonometry are in the submillimeter range, and using the spleen as marker of venous capacitance and compliance rather than the liver has been shown to increase the accuracy of such calculations<sup>136</sup>. At all registered points the relationship between liver dimensions and increase in liver volume had high linear correlation mainly driven by the change in calculated liver volume.

Cinaciguat, but not Riociguat, reduced the arterio-venous resistance through the liver and both drugs did reverse the increase in arterio-venous resistance seen when pre-treating the animals with the NO-blocker L-NAME. Cinaciguat, but not Riociguat, effectively blocked the effect of subsequent effect of L-NAME on hepatic arterio-venous resistance. None of the drugs altered the porto-venous resistance, but pretreatment with Cinaciguat or Riociguat blocked the vasoconstrictive effect of NO blockade on the portal vein flow. None of the medications changed liver compliance, but Riociguat resulted in a small reduction of liver capacitance.

In our Hexamethonium-treated, healthy pigs the sympathetic tone is expected to be low, and the unstressed liver volume is therefore expected to be at the upper part of the volume curve. The effects of Riociguat and Cinaciguat in a state of sympathetic venoconstriction could predictably be different. Kjekshus et al<sup>132</sup> have investigated the effect of nitroprusside given directly in vena porta in a pig model with no sympathetic blockade but instead using lightly sedated animals with muscular blockade. They observed that nitroprusside in this pharmacological state did increase the unstressed liver volume without changing the compliance. Norepinephrine had the opposite effect. Of notice, the average heart rate in their animal at baseline was  $131 \pm 7$  beats/min with a mean systemic blood pressure of  $110 \pm 5$  mmHg. In comparison, our pigs under continuous sedation had a heart rate of 100 and a mean systemic blood pressure of 79. The small effects of Riociguat and Cinaciguat in our study may reflect that our pigs are already at a low sympathetic level and that the liver already is near its maximum blood volume capacity at baseline. Indeed, systemic administration of L-

NAME in healthy, anesthetized rats has been shown to increase hepatic arterio-venous resistance, but not porto-venous resistance. On the other hand, administration of a NO-donor in the same rats had the opposite effects, pointing to differential regulation of arterio-venous and porto-venous flow in the liver <sup>210</sup>.

Taken together, the results indicate that both the sGC-stimulator and activator can influence the NO-tone of the liver circulation interactive with other pharmacological effects



## **10 Strengths and limitations**

### **10.1 Strengths**

The strength of our studies is that they are made in an animal model well known in our lab, with the exception of the venous hemodynamic model. The instrumentation is refined through numerous earlier experiments and the monitoring is well established. We have chosen a stable model with healthy animals to focus on principal effects of the studied drugs. The use of hexamethonium has likewise made it possible to single out strict effects from the drugs isolated from autonomous reflexes. The design of the studies has enabled us to focus on pure arterial, venous, cardiac and hepatic effects.

### **10.2 Limitations**

Large animal experiments have inherent limitations. Due to animal welfare we strive to keep the number of animals as low as possible and this introduces statistical uncertainty in our analysis. We also have not randomized our experiments, and variation due to subtle changes in instrumentation or animal characteristics cannot be ruled out. Furthermore, interventions were not blinded, and observer-bias is hard to completely rule out.

Since the experiments are acute, we have not explored long term effects of the drugs, or the integration with long term homeostatic mechanisms in the animals. Also, the use of hexamethonium introduces an unphysiological environment regarding the integrated effects of the compounds. The drugs were only given intravenously, and we have not investigated the effects using a different route of administration. The choice to use only liver volume as a marker of venous capacitance and capacity proved to be with little merit, and the venous hemodynamic study would probably have been more robust if measurements of the spleen were included. The lack of pathology in our animals make generalization of our results to disease states invalid, and studies of effects of the drugs in similar models with induced pathology is warranted.



## Conclusions

### 10.3 Paper 1

The understanding of right sided circulation is lagging that of the systemic circulation. Right ventricular circulation must be understood as an integrated unit consisting of systemic veins, right ventricle, interventricular septum and the pulmonary vasculature. Furthermore, pathology in the systemic circulation has great impact on the right sided circulation and must be evaluated as well. No one index is suitable to describe the integrated function of the right sided circulation. A multimodal approach is necessary to evaluate the right sided circulation.

### 10.4 Paper 2

Both Cinaciguat and Riociguat have vasodilatory properties in the healthy systemic circulation but only a weak effect in the pulmonary vasculature. After blocking NO production with L-NAME, both drugs demonstrate vasodilatory effects in both vasculatures. Further, after giving Cinaciguat NO-modulation is without any effect on vascular resistance, indicating a functional block of the active NO sites on all forms of sGC.

### 10.5 Paper 3

Riociguat alone has no effect on myocardial oxygen consumption in the healthy heart. Both ventriculoarterial coupling and basal myocardium oxygen metabolism are unaffected by infusion of  $100 \text{ ug} \cdot \text{kg}^{-1}$  Riociguat. However, the subsequent administration of L-NAME did not increase the relative oxygen consumption in the myocardium, and this suggests that the expected surplus basal  $\text{MVO}_2$  in the heart after blocking the endogenous NO-tone by L-NAME was attenuated by this dose of Riociguat. This oxygen-conserving effect during L-NAME-stimulation indicates that Riociguat can induce “metabolic protection” in stressed myocardium and potentially also in pathological states.

### 10.6 Paper 4

Cinaciguat, but not Riociguat given in the highest tolerable doses to avoid excessive hypotension in healthy juvenile, anesthetized pigs, reduced the arterio-venous resistance through the liver, and reversed the increase in arterio-venous resistance induced by L-NAME. None of the drugs altered the porto-venous resistance, but pre-treatment with Cinaciguat or Riociguat blocked the vasoconstrictive effect of NO-blockade on the portal vein flow. None

of the medications changed liver compliance, but Riociguat resulted in a slight reduction of liver capacitance.

## 11 Future perspectives

Pharmaceutical companies continues to publish patent applications for thousands of substances sharing structural similarities with Riociguat, Cinaciguat and Vericiguat <sup>34</sup>. Differences in pharmacokinetics and administration routes might result in tissue selectivity not seen in the established sGC activators and stimulators. The goal regarding PAH is to identify a compound that exerts a high degree of pulmonary vascular vasodilatation and with a tolerable adverse effects profile. Given the ubiquitous nature of the NO-axis, the principle of sGC activation and stimulation need to be explored for a wide variety of conditions outside cardiovascular disease.



## 12 References

1. Naseem KM. The role of nitric oxide in cardiovascular diseases. *Mol Aspects Med.* 2005;26(1-2 SPEC. ISS.):33-65.
2. Xie YW, Shen W, Zhao G, Xu X, Wolin MS, Hintze TH. Role of endothelium-derived nitric oxide in the modulation of canine myocardial mitochondrial respiration in vitro. Implications for the development of heart failure. *Circ Res.* 1996;79(3):381-387.
3. Mohan P, Brutsaert DL, Paulus WJ, Sys SU. Myocardial Contractile Response to Nitric Oxide and cGMP. *Circulation.* 1996;93(6):1223-1229.
4. Kuriyama K, Ohkuma S. Role of Nitric Oxide in Central Synaptic Transmission: Effects on Neurotransmitter Release. *Jpn J Pharmacol.* 1995;69(1):1-8.
5. Sharma JN, Al-Omran A, Parvathy SS. Role of nitric oxide in inflammatory diseases. *Inflammopharmacology.* 2007;15(6):252-259.
6. Förstermann U, Münzel T. Endothelial Nitric Oxide Synthase in Vascular Disease. *Circulation.* 2006;113(13):1708-1714.
7. Castillo J, Rama R, Dávalos A. Nitric Oxide–Related Brain Damage in Acute Ischemic Stroke. *Stroke.* 2000;31(4):852-857.
8. Förstermann U. Nitric oxide and oxidative stress in vascular disease. *Pflugers Arch Eur J Physiol.* 2010;459(6):923-939.
9. Loscalzo J, Welch G. Nitric oxide and its role in the cardiovascular system. *Prog Cardiovasc Dis.* 1995;38(2):87-104.
10. Li H, Cui H, Kundu TK, Alzawahra W, Zweier JL. Nitric oxide production from nitrite occurs primarily in tissues not in the blood: Critical role of xanthine oxidase and aldehyde oxidase. *J Biol Chem.* 2008;283(26):17855-17863.
11. Beckman JS, Koppenol WH. Nitric oxide, superoxide, and peroxynitrite: the good, the bad, and ugly. *Am J Physiol Physiol.* 1996;271(5):C1424-C1437.
12. Ebong EE, Lopez-Quintero S V., Rizzo V, Spray DC, Tarbell JM. Shear-induced endothelial NOS activation and remodeling via heparan sulfate, glypican-1, and syndecan-1. *Integr Biol (United Kingdom).* 2014;6(3):338-347.
13. Petroff MG, Kim SH, Pepe S, et al. Endogenous nitric oxide mechanisms mediate the

- stretch dependence of Ca<sup>2+</sup> release in cardiomyocytes. *Nat Cell Biol.* 2001;3(10):867-873.
14. Balligand JL. Regulation of cardiac  $\beta$ -adrenergic response by nitric oxide. *Cardiovasc Res.* 1999;43(3):607-620.
  15. Schulz R, Rassaf T, Massion PB, Kelm M, Balligand J-L. Recent advances in the understanding of the role of nitric oxide in cardiovascular homeostasis. *Pharmacol Ther.* 2005;108(3):225-256.
  16. Brealey D, Karyampudi S, Jacques TS, et al. Mitochondrial dysfunction in a long-term rodent model of sepsis and organ failure. *Am J Physiol - Regul Integr Comp Physiol.* 2004;286(3 55-3):491-497.
  17. Chung HT, Pae HO, Choi BM, Billiar TR, Kim YM. Breakthroughs and views: Nitric oxide as a bioregulator of apoptosis. *Biochem Biophys Res Commun.* 2001;282(5):1075-1079.
  18. Busse R, Mülsch A. Calcium-dependent nitric oxide synthesis in endothelial cytosol is mediated by calmodulin. *FEBS Lett.* 1990;265(1-2):133-136.
  19. Stuehr DJ, Cho HJ, Kwon NS, Weise MF, Nathan CF. Purification and characterization of the cytokine-induced macrophage nitric oxide synthase: An FAD- and FMN-containing flavoprotein. *Proc Natl Acad Sci U S A.* 1991;88(17):7773-7777.
  20. Trzeciak S, Cinel I, Dellinger RP, et al. Resuscitating the microcirculation in sepsis: The central role of nitric oxide, emerging concepts for novel therapies, and challenges for clinical trials. *Acad Emerg Med.* 2008;15(5):399-413.
  21. Kao CC, Bandi V, Guntupalli KK, Wu M, Castillo L, Jahoor F. Arginine, citrulline and nitric oxide metabolism in sepsis. *Clin Sci.* 2009;117(1):23-30.
  22. Bryk J, Ochoa JB, Correia MIT, Munera-Seeley V, Popovic PJ. Effect of Citrulline and Glutamine on Nitric Oxide Production in RAW 264.7 Cells in an Arginine-Depleted Environment. *J Parenter Enter Nutr.* 2008;32(4):377-383.
  23. Enkhbaatar P, Connelly R, Wang J, et al. Inhibition of neuronal nitric oxide synthase in ovine model of acute lung injury\*. *Crit Care Med.* 2009;37(1):208-214.
  24. Kone BC, Kuncewicz T, Zhang W, Yu ZY. Protein interactions with nitric oxide synthases: Controlling the right time, the right place, and the right amount of nitric



- oxide. *Am J Physiol - Ren Physiol*. 2003;285(2 54-2):178-190.
25. Farah C, Michel LYM, Balligand J-L. Nitric oxide signalling in cardiovascular health and disease. *Nat Rev Cardiol*. 2018;15(5):292-316.
  26. Dasgupta a, Bowman L, D'Arsigny C, Archer S. Soluble Guanylate Cyclase: A New Therapeutic Target for Pulmonary Arterial Hypertension and Chronic Thromboembolic Pulmonary Hypertension. *Clin Pharmacol Ther*. 2015;97(1):88-102.
  27. Wink DA, Mitchell JB. Chemical biology of nitric oxide: Insights into regulatory, cytotoxic, and cytoprotective mechanisms of nitric oxide. *Free Radic Biol Med*. 1998;25(4-5):434-456.
  28. Surks HK, Mochizuki N, Kasai Y, et al. Regulation of myosin phosphatase by a specific interaction with cGMP- dependent protein kinase Ia. *Science (80- )*. 1999;286(5444):1583-1587.
  29. Lee SJ, Stull JT. Calmodulin-dependent regulation of inducible and neuronal nitric-oxide synthase. *J Biol Chem*. 1998;273(42):27430-27437.
  30. Gebhart V, Reiß K, Kollau A, Mayer B, Gorren ACF. Site and mechanism of uncoupling of nitric-oxide synthase: Uncoupling by monomerization and other misconceptions. *Nitric Oxide - Biol Chem*. 2019;89(April):14-21.
  31. Luo S, Lei H, Qin H, Xia Y. Molecular Mechanisms of Endothelial NO Synthase Uncoupling. *Curr Pharm Des*. 2014;20(22):3548-3553.
  32. Bhorade S, Christenson J, O'Connor M, Lavoie A, Pohlman A, Hall JB. Response to inhaled nitric oxide in patients with acute right heart syndrome. *Am J Respir Crit Care Med*. 1999;159(2):571-579.
  33. Sandner P, Stasch JP. Discovery and development of sGC stimulators for the treatment of pulmonary hypertension and rare diseases. *Nitric Oxide*. 2018;77(May):88-95.
  34. Sandner P, Vakalopoulos A, Hahn MG, Stasch JP, Follmann M. Soluble guanylate cyclase stimulators and their potential use: a patent review. *Expert Opin Ther Pat*. 2021;31(3):203-222.
  35. Evgenov O V., Pacher P, Schmidt PM, Haskó G, Schmidt HHHW, Stasch J-P. NO-independent stimulators and activators of soluble guanylate cyclase: discovery and therapeutic potential. *Nat Rev Drug Discov*. 2006;5(9):755-768.

36. Ghio S, Gavazzi A, Campana C, et al. Independent and additive prognostic value of right ventricular systolic function and pulmonary artery pressure in patients with chronic heart failure. *J Am Coll Cardiol.* 2001;37(1):183-188.
37. Simonneau G, Montani D, Celermajer DS, et al. Haemodynamic definitions and updated clinical classification of pulmonary hypertension. *Eur Respir J.* 2019;53(1).
38. Kapur NK, Esposito ML, Bader Y, et al. Mechanical Circulatory Support Devices for Acute Right Ventricular Failure. *Circulation.* 2017;136(3):314-326.
39. Mehta SR, Eikelboom JW, Natarajan MK, et al. Impact of right ventricular involvement on mortality and morbidity in patients with inferior myocardial infarction. *J Am Coll Cardiol.* 2001;37(1):37-43.
40. Frea S, Pidello S, Bovolo V, et al. Prognostic incremental role of right ventricular function in acute decompensation of advanced chronic heart failure. *Eur J Heart Fail.* 2016;18(5):564-572.
41. Iglesias-Garriz I, Olalla-Gómez C, Garrote C, et al. Contribution of right ventricular dysfunction to heart failure mortality: A meta-analysis. *Rev Cardiovasc Med.* 2012;13(2-3):62-69.
42. Gorter TM, Hoendermis ES, van Veldhuisen DJ, et al. Right ventricular dysfunction in heart failure with preserved ejection fraction: a systematic review and meta-analysis. *Eur J Heart Fail.* 2016;18(12):1472-1487.
43. Caforio ALP, Calabrese F, Angelini A, et al. A prospective study of biopsy-proven myocarditis: Prognostic relevance of clinical and aetiopathogenetic features at diagnosis. *Eur Heart J.* 2007;28(11):1326-1333.
44. DANG N, TOPKARA V, MERCANDO M, et al. Right Heart Failure After Left Ventricular Assist Device Implantation in Patients With Chronic Congestive Heart Failure. *J Hear Lung Transplant.* 2006;25(1):1-6.
45. Bozbaş H, Karaçağlar E, Ozkan M, et al. The Prevalence and Course of Pulmonary Hypertension and Right Ventricular Dysfunction in Patients Undergoing Orthotopic Heart Transplantation. *Transplant Proc.* 2013;45(10):3538-3541.
46. Vlahakes GJ. Right ventricular failure following cardiac surgery. *Coron Artery Dis.* 2005;16(1):27-30.

47. Maslow AD, Regan MM, Panzica P, Heindel S, Mashikian J, Comunale ME. Precardiopulmonary bypass right ventricular function is associated with poor outcome after coronary artery bypass grafting in patients with severe left ventricular systolic dysfunction. *Anesth Analg.* 2002;95(6):1507-1518.
48. Harjola VP, Mebazaa A, Čelutkienė J, et al. Contemporary management of acute right ventricular failure: A statement from the Heart Failure Association and the Working Group on Pulmonary Circulation and Right Ventricular Function of the European Society of Cardiology. *Eur J Heart Fail.* 2016;18(3):226-241.
49. TAQUINI AC, FERMOSO JD, ARAMENDIA P. Behavior of the right ventricle following acute constriction of the pulmonary artery. *Circ Res.* 1960;8:315-318.
50. Grignola JC, Ginés F, Guzzo D. Comparison of the Tei index with invasive measurements of right ventricular function. *Int J Cardiol.* 2006;113(1):25-33.
51. Grignola JC, Domingo E. Acute Right Ventricular Dysfunction in Intensive Care Unit. *Biomed Res Int.* 2017;2017(Figure 1).
52. Konstam MA, Kiernan MS, Bernstein D, et al. *Evaluation and Management of Right-Sided Heart Failure: A Scientific Statement From the American Heart Association.* Vol 137.; 2018.
53. Fischer LG, Van Aken H, Bürkle H. Management of pulmonary hypertension: Physiological and pharmacological considerations for anesthesiologists. *Anesth Analg.* 2003;96(6):1603-1616.
54. Pozzi M, Metge A, Martelin A, et al. Efficacy and safety of extracorporeal membrane oxygenation for high-risk pulmonary embolism: A systematic review and meta-analysis. *Vasc Med (United Kingdom).* 2020;25(5):460-467.
55. Kim NH, Delcroix M, Jais X, et al. Chronic thromboembolic pulmonary hypertension. *Eur Respir J.* 2019;53(1).
56. Delcroix M, Lang I, Pepke-Zaba J, et al. Long-Term Outcome of Patients with Chronic Thromboembolic Pulmonary Hypertension : Results from an International Prospective Registry. *Circulation.* 2016;133(9):859-871.
57. Nižňanský M, Ambrož D, Prskavec T, Jansa P, Lindner J. Surgical treatment of chronic thromboembolic pulmonary hypertension. *Vnitr Lek.* 2019;65(5):353-358.

58. Ghofrani HA, Staehler G, Grünig E, et al. Acute Effects of Riociguat in Borderline or Manifest Pulmonary Hypertension Associated with Chronic Obstructive Pulmonary Disease. *Pulm Circ.* 2015;5(2):296-304.
59. Simonneau G, D'Armini AM, Ghofrani H-A, et al. Riociguat for the treatment of chronic thromboembolic pulmonary hypertension: a long-term extension study (CHEST-2). *Eur Respir J.* 2015;45(5):1293-1302.
60. Ghofrani H a., Hoeper MM, Halank M, et al. Riociguat for chronic thromboembolic pulmonary hypertension and pulmonary arterial hypertension: A phase II study. *Eur Respir J.* 2010;36(4):792-799.
61. Kim NH, D'Armini AM, Grimminger F, et al. Haemodynamic effects of riociguat in inoperable/recurrent chronic thromboembolic pulmonary hypertension. *Heart.* 2017;103(8):599-606.
62. Marra AM, Egenlauf B, Ehlken N, et al. Change of right heart size and function by long-term therapy with riociguat in patients with pulmonary arterial hypertension and chronic thromboembolic pulmonary hypertension. *Int J Cardiol.* 2015;195:19-26.
63. Ghofrani HA, D'Armini AM, Grimminger F, et al. Riociguat for the treatment of chronic thromboembolic pulmonary hypertension. *N Engl J Med.* 2013;369(4):319-329.
64. *NRiociguat (Adempas): Management of Inoperable Chronic Thromboembolic Pulmonary Hypertension.* Ottawa: Canadian Agency for Drugs and Technologies in Health; 2015.
65. Van Aelst LNL, Arrigo M, Placido R, et al. Acutely decompensated heart failure with preserved and reduced ejection fraction present with comparable haemodynamic congestion. *Eur J Heart Fail.* 2018;20(4):738-747.
66. Mullens W, Damman K, Harjola VP, et al. The use of diuretics in heart failure with congestion — a position statement from the Heart Failure Association of the European Society of Cardiology. *Eur J Heart Fail.* 2019;21(2):137-155.
67. Molloy WD, Lee KY, Girling L, Schick U, Prewitt RM. Treatment of shock in a canine model of pulmonary embolism. *Am Rev Respir Dis.* 1984;130(5):870-874.
68. Ghignone M, Girling L, Prewitt RM. Volume expansion versus norepinephrine in treatment of a low cardiac output complicating an acute increase in right ventricular

- afterload in dogs. *Anesthesiology*. 1984;60(2):132-135.
69. Schneider a J, Teule GJ, Groeneveld a B, Nauta J, Heidendal G a, Thijs LG. Biventricular performance during volume loading in patients with early septic shock, with emphasis on the right ventricle: a combined hemodynamic and radionuclide study. *Am Heart J*. 1988;116(1 Pt 1):103-112.
  70. Tello K, Dalmer A, Axmann J, et al. Reserve of Right Ventricular-Arterial Coupling in the Setting of Chronic Overload. *Circ Heart Fail*. 2019;12(1):e005512.
  71. Ikonomidis I, Aboyans V, Blacher J, et al. The role of ventricular–arterial coupling in cardiac disease and heart failure: assessment, clinical implications and therapeutic interventions. A consensus document of the European Society of Cardiology Working Group on Aorta & Peripheral Vascular Diseases. *Eur J Heart Fail*. 2019;21(4):402-424.
  72. Kerbaul F, Rondelet B, Demester J-P, et al. Effects of levosimendan versus dobutamine on pressure load-induced right ventricular failure\*. *Crit Care Med*. 2006;34(11):2814-2819.
  73. Yenerçağ M, Arslan U, Dereli S, Çoksevim M, Doğduş M, Kaya A. Effects of angiotensin receptor neprilysin inhibition on pulmonary arterial stiffness in heart failure with reduced ejection fraction. *Int J Cardiovasc Imaging*. 2021;37(1):165-173.
  74. Elmi-Sarabi M, Deschamps A, Delisle S, et al. Aerosolized Vasodilators for the Treatment of Pulmonary Hypertension in Cardiac Surgical Patients. *Anesth Analg*. 2017;125(2):393-402.
  75. Bocchi EA, Bacal F, Auler JC, de Carvalho Carmone MJ, Bellotti G, Pileggi F. Inhaled nitric oxide leading to pulmonary edema in stable severe heart failure. *Am J Cardiol*. 1994;74(1):70-72.
  76. Lundgren J, Rådegran G. Pathophysiology and potential treatments of pulmonary hypertension due to systolic left heart failure. *Acta Physiol*. 2014;211(2):314-333.
  77. Chen SH, Chen LK, Teng TH, Chou WH. Comparison of inhaled nitric oxide with aerosolized prostacyclin or analogues for the postoperative management of pulmonary hypertension: a systematic review and meta-analysis. *Ann Med*. 2020;52(3-4):120-130.
  78. Price LC, Wort SJ, Finney SJ, Marino PS, Brett SJ. Pulmonary vascular and right ventricular dysfunction in adult critical care: current and emerging options for management: a systematic literature review. *Crit Care*. 2010.

79. Kaestner M, Schranz D, Warnecke G, Apitz C, Hansmann G, Miera O. Pulmonary hypertension in the intensive care unit. Expert consensus statement on the diagnosis and treatment of paediatric pulmonary hypertension. The European Paediatric Pulmonary Vascular Disease Network, endorsed by ISHLT and DGPK. *Heart*. 2016;102:ii57-ii66.
80. Olsson KM, Halank M, Egenlauf B, et al. Decompensated right heart failure, intensive care and perioperative management in patients with pulmonary hypertension: Updated recommendations from the Cologne Consensus Conference 2018. *Int J Cardiol*. 2018;272:46-52.
81. Brown G, Humpl T. Approach to pulmonary vascular disease in the ICU. *Curr Opin Pediatr*. 2018;30(3):326-331.
82. Víteček J, Lojek A, Valacchi G, Kubala L. Arginine-based inhibitors of nitric oxide synthase: Therapeutic potential and challenges. *Mediators Inflamm*. 2012;2012.
83. Rees DD, Palmer RMJ, Schulz R, Hodson HF, Moncada S. Characterization of three inhibitors of endothelial nitric oxide synthase in vitro and in vivo. *Br J Pharmacol*. 1990;101(3):746–752.
84. Nordhaug D, Steensrud T, Aghajani E, Korvald C, Myrmet T. Nitric oxide synthase inhibition impairs myocardial efficiency and ventriculo-arterial matching in acute ischemic heart failure. *Eur J Heart Fail*. 2004;6(6):705-713.
85. Klabunde R. Autonomic Ganglia. *Cardiovascular Pharmacology Concepts*. Available at: [https://www.cvpharmacology.com/autonomic\\_ganglia](https://www.cvpharmacology.com/autonomic_ganglia).
86. Large WA, Sim JA. A comparison between mechanisms of action of different nicotinic blocking agents on rat submandibular ganglia. *Br J Pharmacol*. 1986;89(3):583-592.
87. Zhao G, Walsh E, Shryock JC, et al. Antiadrenergic and Hemodynamic Effects of Ranolazine in Conscious Dogs. *J Cardiovasc Pharmacol*. 2011;57(6):639-647.
88. Mueck W, Frey R. Population pharmacokinetics and pharmacodynamics of cinaciguat, a soluble guanylate cyclase activator, in patients with acute decompensated heart failure. *Clin Pharmacokinet*. 2010;49(2):119-129.
89. Becker C, Frey R, Hesse C, Unger S, Reber M, Mueck W. Absorption behavior of riociguat: bioavailability, food effects, and dose-proportionality. *BMC Pharmacol Toxicol*. 2013;14(Suppl 1):P7.

90. Zhao X, Wang Z, Wang Y, et al. Pharmacokinetics of the Soluble Guanylate Cyclase Stimulator Riociguat in Healthy Young Chinese Male Non-Smokers and Smokers: Results of a Randomized, Double-Blind, Placebo-Controlled Study. *Clin Pharmacokinet.* 2015.
91. Champion HC, Michelakis ED, Hassoun PM. Comprehensive invasive and noninvasive approach to the right ventricle-pulmonary circulation unit state of the art and clinical and research implications. *Circulation.* 2009;120(11):992-1007.
92. Karunanithi MK, Michniewicz J, Copeland SE, Feneley MP. Right ventricular preload recruitable stroke work, end-systolic pressure- volume, and dP/dt(max)-end-diastolic volume relations compared as indexes of right ventricular contractile performance in conscious dogs. *Circ Res.* 1992;70(6):1169-1179.
93. Little WC, Freeman GL, O'Rourke RA. Simultaneous determination of left ventricular end-systolic pressure-volume and pressure-dimension relationships in closed-chest dogs. *Circulation.* 1985;71(6):1301-1308.
94. Little WC, Cheng CP, Mumma M, Igarashi Y, Vinten-Johansen J, Johnston WE. Comparison of measures of left ventricular contractile performance derived from pressure-volume loops in conscious dogs. *Circulation.* 1989;80(5):1378-1387.
95. Burkhoff D, Mirsky I, Suga H. Assessment of systolic and diastolic ventricular properties via pressure-volume analysis: a guide for clinical, translational, and basic researchers. *Am J Physiol Heart Circ Physiol.* 2005;289(2):H501-12.
96. Aghajani E, Muller S, Kjørstad KE, et al. THE PRESSURE-VOLUME LOOP REVISITED. *Shock.* 2006;25(4):370-376.
97. Ogilvie LM, Edgett BA, Huber JS, et al. Hemodynamic assessment of diastolic function for experimental models. *Am J Physiol Circ Physiol.* 2020;318(5):H1139-H1158.
98. Daggett M, Daggett M. Hemodynamic dP / dt determinants of maximum negative and periods of diastole. 2020;227(3).
99. Matsubara H, Takaki M, Yasuhara S, Araki J, Suga H. Logistic Time Constant of Isovolumic Relaxation Pressure–Time Curve in the Canine Left Ventricle. *Circulation.* 1995;92(8):2318-2326.
100. Senzaki H, Kass DA. Analysis of isovolumic relaxation in failing hearts by

- monoexponential time constants overestimates lusitropic change and load dependence mechanisms and advantages of alternative logistic fit. *Circ Hear Fail*. 2010;3(2):268-276.
101. Anavekar NS, Gerson D, Skali H, Kwong RY, Yucel EK, Solomon SD. Two-dimensional assessment of right ventricular function: an echocardiographic-MRI correlative study. *Echocardiography*. 2007;24(5):452-456.
  102. Brown SB, Raina A, Katz D, Szerlip M, Wiegers SE, Forfia PR. Longitudinal shortening accounts for the majority of right ventricular contraction and improves after pulmonary vasodilator therapy in normal subjects and patients with pulmonary arterial hypertension. *Chest*. 2011;140(1):27-33.
  103. Kapa S, Elias R, Connolly HJ, Syed IS, Asirvatham SJ. Utility of transthoracic echocardiography to estimate severity of right ventricular dysfunction: an MRI comparison study. *Int J Cardiovasc Imaging*. 2012;28(2):251-261.
  104. Lindqvist P, Calcuttea A, Henein M. Echocardiography in the assessment of right heart function. *Eur J Echocardiogr*. 2008;9(2):225-234.
  105. van der Zwaan HB, Geleijnse ML, McGhie JS, et al. Right ventricular quantification in clinical practice: two-dimensional vs. three-dimensional echocardiography compared with cardiac magnetic resonance imaging. *Eur J Echocardiogr*. 2011;12(9):656-664.
  106. Leary PJ, Kurtz CE, Hough CL, Waiss M-P, Ralph DD, Sheehan FH. Three-dimensional analysis of right ventricular shape and function in pulmonary hypertension. *Pulm Circ*. 2012;2(1):34-40.
  107. Calcuttea A, Chung R, Lindqvist P, Hodson M, Henein MY. Differential right ventricular regional function and the effect of pulmonary hypertension: three-dimensional echo study. *Heart*. 2011;97(12):1004-1011.
  108. Lang RM, Badano LP, Tsang W, et al. EAE/ASE recommendations for image acquisition and display using three-dimensional echocardiography. *J Am Soc Echocardiogr*. 2012;25(1):3-46.
  109. Atsumi A, Ishizu T, Kameda Y, et al. Application of 3-Dimensional Speckle Tracking Imaging to the Assessment of Right Ventricular Regional Deformation. *Circ J*. 2013;77(July):1760-1768.
  110. Zimmer H-G. Who Discovered the Frank-Starling Mechanism? *Physiology*.



- 2002;17(5):181-184.
111. Baan J, van der Velde ET, de Bruin HG, et al. Continuous measurement of left ventricular volume in animals and humans by conductance catheter. *Circulation*. 1984;70(5):812-823.
  112. Dickstein ML, Yano O, Spotnitz HM, Burkhoff D. Assessment of right ventricular contractile state with the conductance catheter technique in the pig. *Cardiovasc Res*. 1995;29(6):820-826.
  113. Nicolosi AC, Hettrick DA, Warltier DC. Assessment of right ventricular function in swine using sonomicrometry and conductance. *Ann Thorac Surg*. 1996;61(5):1381-1387; discussion 1387-8.
  114. Applegate RJ, Cheng CP, Little WC. Simultaneous conductance catheter and dimension assessment of left ventricle volume in the intact animal. *Circulation*. 1990;81(2):638-648.
  115. Stamato TM, Szwarc RS, Benson LN. Measurement of right ventricular volume by conductance catheter in closed-chest pigs. *Am J Physiol*. 1995;269(3 Pt 2):H869-76.
  116. White P a, Chaturvedi RR, Bishop a J, Brookes CI, Oldershaw PJ, Redington a N. Does parallel conductance vary during systole in the human right ventricle? *Cardiovasc Res*. 1996;32(5):901-908.
  117. Wei AE, Maslov MY, Pezone MJ, Edelman ER, Lovich MA. Use of Pressure-volume Conductance Catheters in Real-time Cardiovascular Experimentation. *Hear Lung Circ*. 2014;23(11):1059-1069.
  118. Feneley MP, Elbeery JR, Gaynor JW, Gall S a., Davis JW, Rankin JS. Ellipsoidal shell subtraction model of right ventricular volume. Comparison with regional free wall dimensions as indexes of right ventricular function. *Circ Res*. 1990;67(6):1427-1436.
  119. Erb TO, Craig DM, Gaskin PM, Cheifetz IM, Resai Bengur A, Sanders SP. Preload recruitable stroke work relationship in the right ventricle: simultaneous assessment using conductance catheter and sonomicrometry. *Crit Care Med*. 2002;30(11):2535-2541.
  120. Pugsley J, Lerner AB. Cardiac output monitoring: Is there a gold standard and how do the newer technologies compare? *Semin Cardiothorac Vasc Anesth*. 2010;14(4):274-282.

121. Pironet A, Dauby PC, Chase JG, et al. A comparison between four techniques to measure cardiac output. *Proc Annu Int Conf IEEE Eng Med Biol Soc EMBS*. 2016;2016-Octob:2717-2720.
122. Cholley B, Gall A Le. Ventriculo-arterial coupling: the comeback? *J Thorac Dis*. 2016;8(9):2287.
123. How O-J, Aasum E, Larsen TS. Work-independent assessment of efficiency in ex vivo working rodent hearts within the PVA–MVO<sub>2</sub> framework. *Acta Physiol*. 2007;190(2):171-175.
124. Suga H. Total mechanical energy of a ventricle model and cardiac oxygen consumption. *Am J Physiol*. 1979;236(3).
125. Suga H. Ventricular energetics. *Physiol Rev*. 1990;70(2):247-277.
126. Pang CC. *Autonomic Control of the Venous System in Health and Disease: Effects of Drugs*. Vol 90.; 2001.
127. Rothe CF. Reflex control of veins and vascular capacitance. *Physiol Rev*. 1983;63(4):1281-1342.
128. Greenway C V., Lutt WW. Blood volume, the venous system, preload, and cardiac output. *Can J Physiol Pharmacol*. 1986;64(4):383-387.
129. Greenway C V., Lister GE. Capacitance effects and blood reservoir function in the splanchnic vascular bed during non-hypotensive haemorrhage and blood volume expansion in anaesthetized cats. *J Physiol*. 1974;237(2):279-294.
130. Noble BJ, Drinkhill MJ, Myers DS, Hainsworth R. Reflex control of splanchnic blood volume in anaesthetized dogs. *J Physiol*. 1998;513(1):263-272.
131. Rothe CF. Mean circulatory filling pressure: Its meaning and measurement. *J Appl Physiol*. 1993;74(2):499-509.
132. Kjekshus H, Risoe C, Scholz T, Smiseth OA. Regulation of Hepatic Vascular Volume : Contributions From Active and Passive Mechanisms During Catecholamine and Sodium Nitroprusside Infusion. *Circulation*. 1997;96(12):4415-4423.
133. Risøe C, Hall C, Smiseth OA. Splanchnic vascular capacitance and positive end-expiratory pressure in dogs. *J Appl Physiol*. 1991;70(2):818-824.
134. Smith ER, Smiseth O a, Kingma I, Manyari D, Belenkie I, Tyberg J V. Mechanism of

- action of nitrates. Role of changes in venous capacitance and in the left ventricular diastolic pressure-volume relation. *Am J Med.* 1984;76(6A):14-21.
135. Kjekshus H, Risoe C, Scholz T, Smiseth O a. Methods for assessing hepatic distending pressure and changes in hepatic capacitance in pigs. *Am J Physiol Heart Circ Physiol.* 2000;279(4):H1796-803.
  136. Greenway C V, Rothe CF. Ultrasonic crystal measurement of blood volume changes in liver and spleen. *Am J Physiol.* 1992;262(5 Pt 1):G934-9.
  137. Wang and L. A. Goonewardene Z. The use of MIXED models in the analysis of animal experiments with repeated measures data. *Can J Anim Sci.* 2004;84(1):1-11.
  138. West BT. Analyzing longitudinal data with the linear mixed models procedure in SPSS. *Eval Heal Prof.* 2009;32(3):207-228.
  139. Oskolkov N. How linear Mixed Model Works. Available at: <https://towardsdatascience.com/how-linear-mixed-model-works-350950a82911>. Date accessed: October 20, 2021.
  140. Becker EM, Stasch JP, Bechem M, et al. Effects of Different Pulmonary Vasodilators on Arterial Saturation in a Model of Pulmonary Hypertension. *PLoS One.* 2013;8(8):2-9.
  141. Rai N, Veeroju S, Schymura Y, et al. Effect of Riociguat and Sildenafil on Right Heart Remodeling and Function in Pressure Overload Induced Model of Pulmonary Arterial Banding. *Biomed Res Int.* 2018;2018:1-9.
  142. Schermuly RT, Stasch J-P, Pullamsetti SS, et al. Expression and function of soluble guanylate cyclase in pulmonary arterial hypertension. *Eur Respir J Off J Eur Soc Clin Respir Physiol.* 2008;32(4):881-891.
  143. Weissmann N, Lobo B, Pichl A, et al. Stimulation of soluble guanylate cyclase prevents cigarette smoke-induced pulmonary hypertension and emphysema. *Am J Respir Crit Care Med.* 2014;189(11):1359-1373.
  144. Chamorro V, Morales-Cano D, Milara J, et al. Riociguat versus sildenafil on hypoxic pulmonary vasoconstriction and ventilation/perfusion matching. *PLoS One.* 2018;13(1):e0191239.
  145. Donda K, Zambrano R, Moon Y, et al. Riociguat prevents hyperoxia-induced lung

- injury and pulmonary hypertension in neonatal rats without effects on long bone growth. *PLoS One*. 2018;13(7):1-20.
146. Pradhan K, Sydykov A, Tian X, et al. Soluble guanylate cyclase stimulator riociguat and phosphodiesterase 5 inhibitor sildenafil ameliorate pulmonary hypertension due to left heart disease in mice. *Int J Cardiol*. 2016;216:85-91.
  147. Schultz J, Andersen A, Gade IL, Kjaergaard B, Nielsen-Kudsk JE. Riociguat, sildenafil and inhaled nitric oxide reduces pulmonary vascular resistance and improves right ventricular function in a porcine model of acute pulmonary embolism. *Eur Hear J Acute Cardiovasc Care*. 2020;9(4):293-301.
  148. Boerrigter G, Costello-Boerrigter LC, Cataliotti A, Lapp H, Stasch JP, Burnett JC. Targeting heme-oxidized soluble guanylate cyclase in experimental heart failure. *Hypertension*. 2007;49(5):1128-1133.
  149. Evgenov O V., Kohane DS, Bloch KD, et al. Inhaled agonists of soluble guanylate cyclase induce selective pulmonary vasodilation. *Am J Respir Crit Care Med*. 2007;176(11):1138-1145.
  150. Thoonen R, Cauwels A, Decaluwe K, et al. Cardiovascular and pharmacological implications of haem-deficient NO-unresponsive soluble guanylate cyclase knock-in mice. *Nat Commun*. 2015;6:8482.
  151. Chester M, Seedorf G, Tourneux P, et al. Cinaciguat, a soluble guanylate cyclase activator, augments cGMP after oxidative stress and causes pulmonary vasodilation in neonatal pulmonary hypertension. *Am J Physiol Lung Cell Mol Physiol*. 2011;301(5):L755-64.
  152. Chester M, Tourneux P, Seedorf G, Grover TR, Gien J, Abman SH. Cinaciguat, a soluble guanylate cyclase activator, causes potent and sustained pulmonary vasodilation in the ovine fetus. *Am J Physiol Lung Cell Mol Physiol*. 2009;297(2):L318-25.
  153. Grimminger F, Weimann G, Frey R, et al. First acute haemodynamic study of soluble guanylate cyclase stimulator riociguat in pulmonary hypertension. *Eur Respir J*. 2009;33(4):785-792.
  154. Hoepfer MM, Halank M, Wilkens H, et al. Riociguat for interstitial lung disease and pulmonary hypertension: a pilot trial. *Eur Respir J*. 2013;41(4):853-860.

155. Bonderman D, Ghio S, Felix SB, et al. Riociguat for patients with pulmonary hypertension caused by systolic left ventricular dysfunction: A phase IIb double-blind, randomized, placebo-controlled, dose-ranging hemodynamic study. *Circulation*. 2013;128(5):502-511.
156. Ghofrani HA, Galiè N, Grimminger F, et al. Riociguat for the treatment of pulmonary arterial hypertension. *N Engl J Med*. 2013;369(4):330-340.
157. Bonderman D, Pretsch I, Steringer-Mascherbauer R, et al. Acute Hemodynamic Effects of Riociguat in Patients With Pulmonary Hypertension Associated With Diastolic Heart Failure (DILATE-1). *CHEST J*. 2014;146(5):1274.
158. Galiè N, Müller K, Scalise AV, Grünig E. PATENT PLUS: A blinded, randomised and extension study of riociguat plus sildenafil in pulmonary arterial hypertension. *Eur Respir J*. 2015;45(5):1314-1322.
159. Rubin LJ, Galiè N, Grimminger F, et al. Riociguat for the treatment of pulmonary arterial hypertension: A long-term extension study (patent-2). *Eur Respir J*. 2015;45(5):1303-1313.
160. Marra AM, Halank M, Benjamin N, et al. Right ventricular size and function under riociguat in pulmonary arterial hypertension and chronic thromboembolic pulmonary hypertension (the RIVER study) 11 Medical and Health Sciences 1102 Cardiorespiratory Medicine and Haematology. *Respir Res*. 2018;19(1):1-11.
161. Hoepfer MM, Simonneau G, Corris PA, et al. RESPITE: Switching to riociguat in pulmonary arterial hypertension patients with inadequate response to phosphodiesterase-5 inhibitors. *Eur Respir J*. 2017;50(3).
162. McLaughlin V V., Jansa P, Nielsen-Kudsk JE, et al. Riociguat in patients with chronic thromboembolic pulmonary hypertension: Results from an early access study. *BMC Pulm Med*. 2017;17(1):1-9.
163. Taran IN, Belevskaya AA, Saidova MA, Martynyuk T V., Chazova IE. Initial Riociguat Monotherapy and Transition from Sildenafil to Riociguat in Patients with Idiopathic Pulmonary Arterial Hypertension: Influence on Right Heart Remodeling and Right Ventricular–Pulmonary Arterial Coupling. *Lung*. 2018;196(6):745-753.
164. Ahmadi A, Thornhill RE, Pena E, et al. Effects of Riociguat on Right Ventricular Remodelling in Chronic Thromboembolic Pulmonary Hypertension Patients: A

- Prospective Study. *Can J Cardiol.* 2018;34(9):1137-1144.
165. Darocha S, Banaszkiwicz M, Pietrasik A, et al. Sequential treatment with sildenafil and riociguat in patients with persistent or inoperable chronic thromboembolic pulmonary hypertension improves functional class and pulmonary hemodynamics. *Int J Cardiol.* 2018;269:283-288.
  166. Gheorghide M, Greene SJ, Filippatos G, et al. Cinaciguat, a soluble guanylate cyclase activator: Results from the randomized, controlled, phase IIb COMPOSE programme in acute heart failure syndromes. *Eur J Heart Fail.* 2012;14(9):1056-1066.
  167. Lapp H, Mitrovic V, Franz N, et al. Cinaciguat (BAY 58-2667) improves cardiopulmonary hemodynamics in patients with acute decompensated heart failure. *Circulation.* 2009;119(21):2781-2788.
  168. Erdmann E, Semigran MJ, Nieminen MS, et al. Cinaciguat, a soluble guanylate cyclase activator, unloads the heart but also causes hypotension in acute decompensated heart failure. *Eur Heart J.* 2013;34(1):57-67.
  169. Hoepfer M, Ghofrani H-A, Halank M, et al. Riociguat for pulmonary arterial hypertension (PAH) and chronic thromboembolic pulmonary hypertension (CTEPH): Final data from a phase II long-term extension (LTE) study. In: *4.3 Pulmonary Circulation and Pulmonary Vascular Disease*. European Respiratory Society; 2015:PA4560.
  170. Khaybullina D, Patel A, Zerilli T. Riociguat (adempas): a novel agent for the treatment of pulmonary arterial hypertension and chronic thromboembolic pulmonary hypertension. *P T.* 2014;39(11):749-758.
  171. Gheorghide M, Greene SJ, Butler J, et al. Effect of vericiguat, a soluble guanylate cyclase stimulator, on natriuretic peptide levels in patients with worsening chronic heart failure and reduced ejection fraction the socrates-reduced randomized trial. *JAMA - J Am Med Assoc.* 2015;314(21):2251-2262.
  172. Pieske B, Maggioni AP, Lam CSP, et al. Vericiguat in patients with worsening chronic heart failure and preserved ejection fraction: Results of the SOLuble guanylate Cyclase stimulator in heArT failurE patientS with PRESERVED EF (SOCRATES-PRESERVED) study. *Eur Heart J.* 2017;38(15):1119-1127.
  173. Armstrong PW, Pieske B, Anstrom KJ, et al. Vericiguat in Patients with Heart Failure

- and Reduced Ejection Fraction. *N Engl J Med.* 2020;382(20):1883-1893.
174. Ullah W, Mukhtar M, Al-Mukhtar A, et al. Safety and efficacy of soluble guanylate cyclase stimulators in patients with heart failure: A systematic review and meta-analysis. *World J Cardiol.* 2020;12(10):501-512.
  175. Stasch J-P, Pacher P, Evgenov O V. Soluble guanylate cyclase as an emerging therapeutic target in cardiopulmonary disease. *Circulation.* 2011;123(20):2263-2273.
  176. Deruelle P, Grover TR, Abman SH. Pulmonary vascular effects of nitric oxide-cGMP augmentation in a model of chronic pulmonary hypertension in fetal and neonatal sheep. 2005;1088:798-806.
  177. Dumitrascu R, Weissmann N, Ghofrani HA, et al. Activation of soluble guanylate cyclase reverses experimental pulmonary hypertension and vascular remodeling. *Circulation.* 2006;113(2):286-295.
  178. Deruelle P, Grover TR, Storme L, Abman SH. Effects of BAY 41-2272, a soluble guanylate cyclase activator, on pulmonary vascular reactivity in the ovine fetus. *Am J Physiol Lung Cell Mol Physiol.* 2005;288(4):L727-33.
  179. Evgenov O V., Ichinose F, Evgenov N V., et al. Soluble guanylate cyclase activator reverses acute pulmonary hypertension and augments the pulmonary vasodilator response to inhaled nitric oxide in awake lambs. *Circulation.* 2004;110(15):2253-2259.
  180. Giaid A, Saleh D. Reduced Expression of Endothelial Nitric Oxide Synthase in the Lungs of Patients with Pulmonary Hypertension. *N Engl J Med.* 1995;333(4):214-221.
  181. Ghosh A, Stasch JP, Papapetropoulos A, Stuehr DJ. Nitric oxide and heat shock protein 90 activate soluble guanylate cyclase by driving rapid change in its subunit interactions and heme content. *J Biol Chem.* 2014;289(22):15259-15271.
  182. Kollau A, Opelt M, Wölkart G, et al. Irreversible Activation and Stabilization of Soluble Guanylate Cyclase by the Protoporphyrin IX Mimetic Cinaciguat. *Mol Pharmacol.* 2018;93(2):73-78.
  183. Actively recruiting human studies on Cinaciguat. Available at: [https://clinicaltrials.gov/ct2/results?term=riociguat&recrs=a&age\\_v=&gndr=&type=&rslt=&Search=Apply](https://clinicaltrials.gov/ct2/results?term=riociguat&recrs=a&age_v=&gndr=&type=&rslt=&Search=Apply). Date accessed: April 20, 2020.
  184. Actively recruiting human studies on Riociguat. Available at:

[https://clinicaltrials.gov/ct2/results?term=riociguat&recrs=a&age\\_v=&gndr=&type=&rslt=&Search=Apply](https://clinicaltrials.gov/ct2/results?term=riociguat&recrs=a&age_v=&gndr=&type=&rslt=&Search=Apply). Date accessed: April 20, 2020.

185. Sandner P, Zimmer DP, Milne GT, Follmann M, Hobbs A, Stasch J-P. Soluble Guanylate Cyclase Stimulators and Activators. In: *Handbook of Experimental Pharmacology*. Berlin, Heidelberg: Springer; 2018:355-394.
186. Radovits T, Korkmaz S, Miesel-Gröschel C, et al. Pre-conditioning with the soluble guanylate cyclase activator Cinaciguat reduces ischaemia-reperfusion injury after cardiopulmonary bypass. *Eur J Cardio-thoracic Surg*. 2011;39(2):248-255.
187. Frankenreiter S, Bednarczyk P, Kniess A, et al. cGMP-Elevating Compounds and Ischemic Conditioning Provide Cardioprotection Against Ischemia and Reperfusion Injury via Cardiomyocyte-Specific BK Channels. *Circulation*. 2017;136(24):2337-2355.
188. Reinke Y, Gross S, Eckerle LG, et al. The soluble guanylate cyclase stimulator riociguat and the soluble guanylate cyclase activator cinaciguat exert no direct effects on contractility and relaxation of cardiac myocytes from normal rats. *Eur J Pharmacol*. 2015;767:1-9.
189. Methner C, Buonincontri G, Hu C-H, et al. Riociguat Reduces Infarct Size and Post-Infarct Heart Failure in Mouse Hearts: Insights from MRI/PET Imaging. Salloum FN, ed. *PLoS One*. 2013;8(12):e83910.
190. Simon JN, Duglan D, Casadei B, Carnicer R. Nitric oxide synthase regulation of cardiac excitation-contraction coupling in health and disease. *J Mol Cell Cardiol*. 2014;73:80-91.
191. Paulus WJ, Bronzwaer JG. Myocardial contractile effects of nitric oxide. *Hear Fail*. 2002;7(4):371-383.
192. Raff GL, Glantz SA. Volume loading slows left ventricular isovolumic relaxation rate. Evidence of load-dependent relaxation in the intact dog heart. *Circ Res*. 1981;48(6):813-824.
193. Wilck N, Markó L, Balogh A, et al. Nitric oxide-sensitive guanylyl cyclase stimulation improves experimental heart failure with preserved ejection fraction. *JCI insight*. 2018;3(4):15-17.
194. Hare JM, Givertz MM, Creager MA, Colucci WS. Increased sensitivity to nitric oxide



- synthase inhibition in patients with heart failure: Potentiation of  $\beta$ -adrenergic inotropic responsiveness. *Circulation*. 1998;97(2):161-166.
195. Korvald C, Elvenes OP, Ytrebø LM, Sørli DG, Myrmel T. Oxygen-wasting effect of inotropy in the “virtual work model”. *Am J Physiol*. 1999;276(4 Pt 2):H1339-45.
  196. Nordhaug D, Steensrud T, Korvald C, Aghajani E, Myrmel T. Preserved myocardial energetics in acute ischemic left ventricular failure -- studies in an experimental pig model. *Eur J Cardiothorac Surg*. 2002;22(1):135-142.
  197. Elvenes OP, Korvald C, Ytrebø LM, Irtun Ø, Myrmel T, Larsen TS. Myocardial Metabolism and Efficiency After Warm Continuous Blood Cardioplegia. 2000;4975(00).
  198. Aghajani E, Nordhaug D, Korvald C, et al. Mechanoenergetic inefficiency in the septic left ventricle is due to enhanced oxygen requirements for excitation-contraction coupling. *Cardiovasc Res*. 2004;63(2):256-263.
  199. Aghajani E, Korvald C, Nordhaug D, Revhaug A, Myrmel T. Increased oxygen cost of contractility in the endotoxemic porcine left ventricle. *Scand Cardiovasc J*. 2004;38(3):187-192.
  200. How O, Aasum E, Kunnathu S, Severson DL, Myhre ESP, Larsen TS. Influence of substrate supply on cardiac efficiency, as measured by pressure-volume analysis in ex vivo mouse hearts. *Am J Physiol Heart Circ Physiol*. 2005;288(6):H2979-85.
  201. Suto N, Mikuniya A, Okubo T, Hanada H, Shinozaki N, Okumura K. Nitric oxide modulates cardiac contractility and oxygen consumption without changing contractile efficiency. *Am J Physiol Circ Physiol*. 1998;275(1):H41-H49.
  202. Chen Y, Traverse JH, Du R, Hou M, Bache RJ. Nitric oxide modulates myocardial oxygen consumption in the failing heart. *Circulation*. 2002;106(2):273-279.
  203. Burkhoff D, Sagawa K. Ventricular efficiency predicted by an analytical model. *Am J Physiol Integr Comp Physiol*. 1986;250(6):R1021-R1027.
  204. De Tombe PP, Jones S, Burkhoff D, Hunter WC, Kass DA. Ventricular stroke work and efficiency both remain nearly optimal despite altered vascular loading. *Am J Physiol Circ Physiol*. 2017;264(6):H1817-H1824.
  205. Hayashida K, Sunagawa K, Noma M, Sugimachi M, Ando H, Nakamura M.

- Mechanical matching of the left ventricle with the arterial system in exercising dogs. *Circ Res.* 1992;71(3):481-489.
206. Nozawa T, Yasumura Y, Futaki S, et al. Relation between oxygen consumption and pressure-volume area of in situ dog heart. *Am J Physiol Circ Physiol.* 1987;253(1):H31-H40.
207. Recchia FA, McConnell PI, Loke KE, Xu X, Ochoa M, Hintze TH. Nitric oxide controls cardiac substrate utilization in the conscious dog. *Cardiovasc Res.* 1999;44(2):325-332.
208. Chang C-F, Diers AR, Hogg N. Cancer cell metabolism and the modulating effects of nitric oxide. *Free Radic Biol Med.* 2015;79:324-336.
209. Andersen IA, Igumnova E, Kildal AB, Myrmel T. Reassessment of a suggested pharmacological approach to heart failure: L-arginine is only a marginal NO donor in pigs. *J Cardiovasc Pharmacol.* 2012;60(3):262-268.
210. Pannen BHJ, Bauer M. Differential regulation of hepatic arterial and portal venous vascular resistance by nitric oxide and carbon monoxide in rats. *Life Sci.* 1998;62(22):2025-2033.

## 13 Papers



## 13.1 Paper 1





## Propulsion of blood through the right heart circulatory system

Torvind Næsheim, Ole-Jakob How & Truls Myrmel

To cite this article: Torvind Næsheim, Ole-Jakob How & Truls Myrmel (2018) Propulsion of blood through the right heart circulatory system, Scandinavian Cardiovascular Journal, 52:1, 4-12, DOI: [10.1080/14017431.2017.1409909](https://doi.org/10.1080/14017431.2017.1409909)

To link to this article: <https://doi.org/10.1080/14017431.2017.1409909>



Published online: 30 Nov 2017.



Submit your article to this journal [↗](#)



Article views: 279



View related articles [↗](#)



View Crossmark data [↗](#)

## 13.2 Paper 2





# Hemodynamic Effects of a Soluble Guanylate Cyclase Stimulator, Riociguat, and an Activator, Cinaciguat, During NO-Modulation in Healthy Pigs

Journal of Cardiovascular  
Pharmacology and Therapeutics  
2021, Vol. 26(1) 75-87  
© The Author(s) 2020



Article reuse guidelines:  
sagepub.com/journals-permissions  
DOI: 10.1177/1074248420940897  
journals.sagepub.com/home/cpt



Torvind Næsheim, MD<sup>1,2</sup> , Ole-Jakob How, PhD<sup>3</sup>, and Truls Myrmed, MD, PhD<sup>1,4</sup>

## Abstract

Cardiovascular diseases are often characterized by dysfunctional endothelium. To compensate for the related lack of nitric oxide (NO), a class of soluble guanylate cyclase (sGC) stimulators and activators have been developed with the purpose of acting downstream of NO in the NO-sGC-cGMP cascade. These drugs have been discovered using photoaffinity labeling of sGC and high-throughput screening of a vast number of chemical compounds. Therefore, an understanding of the integrated physiological effects of these drugs in vivo is necessary on the path to clinical application. We have characterized the integrated hemodynamic impact of the sGC stimulator riociguat and the activator cinaciguat in different NO-states in healthy juvenile pigs ( $n = 30$ ). We assessed the vascular effects in both systemic and pulmonary circulation, the contractile effects in the right and left ventricles, and the effects on diastolic cardiac functions. Nitric oxide-tone in these pigs were set by using the NO-blocker L-NAME and by infusion of nitroglycerine. The studies show a more pronounced vasodilatory effect in the systemic than pulmonary circulation for both drugs. Riociguat acts integrated with NO in an additive manner, while cinaciguat, in principle, completely blocks the endogenous NO effect on vascular control. Neither compound demonstrated pronounced cardiac effects but had unloading effect on both systolic and diastolic function. Thus, riociguat can potentially act in various disease states as a mean to increase NO-tone if systemic vasodilation can be balanced. Cinaciguat is a complicated drug to apply clinically due to its almost complete lack of integration in the NO-tone and balance.

## Keywords

nitric oxide signaling, sGC-activator, sGC-stimulator, pulmonary hypertension, vasodilator

## Introduction

Cardiovascular diseases are often characterized by reduced production and sensitivity to nitric oxide (NO) in vascular tissue, and dynamic production and effect of this compound is a marker of a healthy vasculature. Nitric oxide is produced from an NO-synthase action on the amino acid arginine and acts downstream by stimulating soluble guanylate cyclase (sGC) in various cells, in particular, vascular smooth muscle cells.<sup>1</sup> Guanylate cyclase, in turn, catalyzes the conversion of GTP to cGMP, an intracellular messenger acting through protein kinase G (PKG) and thus elicits a multitude of physiological responses including smooth muscle relaxation. The sensitivity of sGC to NO depends on the red-ox-state of sGC. In the physiologically reduced state, the NO-sensitivity is normal. In the oxidized heme-free state, NO cannot stimulate sGC.<sup>2</sup>

To circumvent the need for physiological NO production and a normal NO-affinity in the reduced sGC, a group of substances acting directly as pharmacological stimulators<sup>3</sup> or activators<sup>4</sup> of soluble guanylate cyclase has been developed. One of these compounds, the NO-stimulator riociguat (Adempas), is

currently applied clinically in pulmonary hypertension.<sup>5</sup> Although hemodynamically reasonable, the use of these compounds in clinical trials of heart failure has been hampered by extensive systemic hypotensive effects of both stimulators<sup>6</sup> and particularly activators.<sup>7-9</sup> However, the recently published VICTORIA study found a clinical benefit for the sGC

<sup>1</sup> Department of Clinical Medicine, Cardiovascular Research Groups, Faculty of Health Sciences, UiT The Arctic University of Norway, Tromsø, Norway

<sup>2</sup> Department of Anaesthesiology, University Hospital of North Norway, Tromsø, Norway

<sup>3</sup> Department of Medical Biology, Cardiovascular Research Groups, Faculty of Health Sciences, UiT The Arctic University of Norway, Tromsø, Norway

<sup>4</sup> Department of Cardiothoracic and Vascular Surgery, Heart and Lung Clinic, University Hospital of North Norway, Tromsø, Norway

**Manuscript submitted:** April 22, 2020; **accepted:** June 12, 2020.

## Corresponding Author:

Truls Myrmed, Department of Clinical Medicine, UiT The Arctic University of Norway, 9037 Tromsø, Norway.  
Email: truls.myrmed@uit.no

stimulator vericiguat in patients with heart failure with reduced ejection fraction already on established guideline heart failure therapy.<sup>10</sup>

In theory, the sGC stimulators act directly on sGC and in concert with NO. On the other hand, sGC activators exert its activity independent of NO and has been found to bind primarily to “de-hemmed” sGC in its oxidized forms. As stated, oxidized sGC is found predominantly in pathological tissues.<sup>2,5,11,12</sup>

There are many unknowns of the physiological effects and pharmacological applications of these compounds. From their biochemical profile, the activators should have minimal effects in normal vasculature. However, this has not been extensively addressed in intact, healthy animals. Furthermore, discrimination of relative effects in the pulmonary and systemic circulation have received little attention and will be valuable knowledge for their pharmacological application in various clinical settings. Finally, the extent to which the 2 different principal compounds interact with the NO-tone *in vivo* needs further clarification.

In this study, we have compared the circulatory effects of the sGC-stimulator riociguat, BAY 63-2521 (Bayer AG) and the activator cinaciguat, BAY 58-2667 (Bayer AG) in healthy, juvenile pigs. The study aimed to explore the relative systemic and pulmonary vascular effects of these 2 pharmacological compounds. Both drugs were applied in animals with normal, NO blocked, or NO-stimulated endothelial function. We also assessed whether the activator cinaciguat would, in fact, have effects in these healthy young animals with the presumed intact reduced form of sGC. Finally, the study aimed specifically to clarify how both drugs act on cardiac function.

## Material and Methods

### Experimental Animals

Thirty castrated male domestic pigs weighing  $30 \pm 5$  kg were adapted to the Animal Department for 5 to 7 days. They were fasted overnight before experiments with free access to water. The experimental protocol was approved by the local steering committee of the National Animal Research Authority located at the Faculty of Health Sciences, UIT, The Arctic University of Norway. The FDF reference is 2012/55972.

### Surgical Preparation and Instrumentation

The pigs were premedicated with an intramuscular injection of 20 mg·kg<sup>-1</sup> ketamine (Pfizer AS) and 1 mg of atropine (Nycomed Pharma). Anesthesia was induced by intravenous injection of 10 mg·kg<sup>-1</sup> pentobarbital sodium (Abbott) and 0.01 mg·kg<sup>-1</sup> fentanyl (Hameln Pharmaceuticals). The animals were normo-ventilated after tracheostomy. Fraction of inspired oxygen (FiO<sub>2</sub>) was chosen to maintain partial pressure of oxygen in the blood of  $100 \pm 2$  mm Hg. FiO<sub>2</sub> ranged from 0.20 to 0.30. Normo-ventilation was defined as an arterial PaCO<sub>2</sub> of  $40 \pm 2$  mm Hg. A central venous catheter was placed through the left internal jugular vein. Anesthesia was maintained

throughout the experiment by a normative continuous infusion of 4 mg·kg<sup>-1</sup> h<sup>-1</sup> pentobarbital sodium, 0.02 mg·kg<sup>-1</sup> h<sup>-1</sup> fentanyl, and 0.3 mg·kg<sup>-1</sup> h<sup>-1</sup> midazolam (B. Braun). Anesthesia was titrated to avoid stress reactions during interventions. The circulating volume was maintained by a 10 to 20 mL·kg<sup>-1</sup> h<sup>-1</sup> continuous infusion of 0.9% NaCl supplemented with 1.25 g·L<sup>-1</sup> glucose.

The animals received 2500 IU of heparin and 5 mg·kg<sup>-1</sup> amiodarone (Sanofi-Synthelabo) to avoid blood clotting of catheters and to prevent cardiac arrhythmias. Hexamethonium chloride, trimethyl-[6-(trimethylazaniumyl)hexyl]azanium (Sigma-Aldrich) 15 mg·kg<sup>-1</sup> was administered to avoid autonomic reflexes and single out vascular effects during interventions and measurements.<sup>13</sup>

A 7F manometer pressure-volume catheter (Millar MPVS Ultra) was inserted through an introducer sheath via the carotid artery into the left ventricle as proposed by Baan et al.<sup>14</sup> The correct position was verified using 2-dimensional (2D) echocardiography and analysis of each volume segment of the catheter. The volume of the conductance catheter was calibrated at each point of the experiment by 2D echocardiography and stroke volume estimation by thermodilution. A 5F Swan-Ganz catheter (Edwards Lifescience Corp.) was advanced into the normal position in a pulmonary artery. A second balloon catheter was floated from the superior caval vein into the right ventricle for pressure measurements. Central venous pressure was measured in the right atrium. The systemic arterial pressure was assessed from a vascular catheter in the abdominal aorta. An 8F 50 mL IABP-balloon catheter (Maquet Cardiovascular) was introduced into the inferior caval vein and positioned just below the right atrium for intermittent preload reduction.

### Experimental Drugs

Riociguat and cinaciguat were obtained from Chemoki Synthesi-Tech as a dry powder. The drugs were solubilized as described in the study by Becker et al<sup>15</sup>: pH neutral solutions were prepared with dimethyl sulfoxide ([DMSO] Sigma-Aldrich) and a 1:1 solution of Transcutol, diethylene glycol ethyl ether (Sigma-Aldrich), and Cremophor, macrogolglycerol ricinoleate (Sigma-Aldrich). We used 5% Transcutol and 5% Cremophor solutions, and the ratio between DMSO, Transcutol, and Cremophor was 0.05:2.5:2.5. This solution was then further diluted with 0.9 mg·mL<sup>-1</sup> NaCl to a final concentration of test drug of 0.01 to 0.1 mg·mL<sup>-1</sup> of riociguat or cinaciguat, depending on the dose to be given. The maximum DMSO concentration was 0.02%. L-NAME, N(G)-nitro-L-arginine methyl ester (Sigma-Aldrich), was used as an NO synthase inhibitor<sup>16</sup> and nitroglycerine ([NG] Takeda AS) as NO-donor.

### Experimental Protocol

Four and 3 pigs were used in a dose-response study for riociguat and cinaciguat, respectively (Table 1).

**Table 1.** Dose-Response Data for Riociguat and Cinaciguat.<sup>a</sup>

Riociguat, n = 4							
Dose in $\mu\text{g}\cdot\text{kg}^{-1}$	Before vehicle	Baseline	10	20	50	100	
MAP, mm Hg	89 ± 22	88 ± 21	87 ± 22	66 ± 11 <sup>b</sup>	56 ± 13 <sup>b</sup>	50 ± 9 <sup>b</sup>	
MPAP, mm Hg	24 ± 3	25 ± 3	22 ± 2	23 ± 5	25 ± 7	25 ± 8	
SVR, dynes $\text{s}^{-1}\text{cm}^{-5}$	1228 ± 171	1066 ± 248	957 ± 204	760 ± 180 <sup>b</sup>	568 ± 124 <sup>b</sup>	497 ± 161 <sup>b</sup>	
PVR, dynes $\text{s}^{-1}\text{cm}^{-5}$	205 ± 100	166 ± 109	146 ± 87	162 ± 76	179 ± 76	167 ± 65	
Cinaciguat, n = 3							
Dose in $\mu\text{g}\cdot\text{kg}^{-1}\cdot\text{min}^{-1}$	Before vehicle	Baseline	0.01	0.05	0.1	0.50	1.00
MAP, mm Hg	99 ± 20	96 ± 21	94 ± 22,	93 ± 18	84 ± 14	74 ± 12 <sup>b</sup>	63 ± 6 <sup>b</sup>
MPAP, mm Hg	20 ± 2	20 ± 2	20 ± 3	20 ± 3	20 ± 4	18 ± 2	18 ± 2
SVR, dynes $\text{s}^{-1}\text{cm}^{-5}$	1668 ± 164	1630 ± 199	1675 ± 347	1726 ± 287	1396 ± 152	1179 ± 251 <sup>b</sup>	925 ± 232 <sup>b</sup>
PVR, dynes $\text{s}^{-1}\text{cm}^{-5}$	146 ± 34	148 ± 38	184 ± 72	170 ± 62	176 ± 116	130 ± 43	134 ± 8

Abbreviations: MAP, mean systemic arterial pressure; MPAP, mean pulmonary arterial pressure; PVR, pulmonary vascular resistance; SVR, systemic vascular resistance.

<sup>a</sup>Values are mean ± SD. Mixed models statistics with pig identity as random effect was used. Significance levels are given between doses of test drug and before vehicle and between doses of test drug and baseline.

<sup>b</sup> $P < .05$ .

The following experiments were conducted using a repeated measurements design. After instrumentation, the pigs were allowed to rest for 30 minutes before baseline measurements.

Cinaciguat  $1\ \mu\text{g}\cdot\text{kg}^{-1}\text{min}^{-1}$  was given as a continuous infusion and riociguat  $100\ \mu\text{g}$  as a bolus, L-NAME  $15\ \text{mg}\cdot\text{kg}^{-1}$ , and NG  $5\ \mu\text{g}\cdot\text{kg}^{-1}\text{min}^{-1}$  was then given in alternating sequences in 4 different groups, each with 5 to 6 pigs (Figure 1). Administration form and timing of measurements were based on human pharmacokinetic studies.<sup>17,18</sup> Equilibration after 30 minutes was observed between each measurement. The vehicle was given before baseline. Hemodynamic measurements were sampled at steady state with the ventilator in expiratory pause. Following hemodynamic measurements, the IABP-balloon in the inferior vena cava was inflated during data sampling to acquire pressure-volume data at different states of left ventricular (LV) work.<sup>19</sup>

### Registration of Data and Analysis

Data were sampled, digitized, and analyzed using ADI Lab-Chart Pro software v 8.1.8. Cardiac output (CO) was obtained from thermodilution with the hardware Vigilance (Medtronic). Transthoracic echocardiography (Philips iE33) was done at all time points to measure end-diastolic and end-systolic diameters. End-diastolic volume (Ved) was calculated by Teicholts formula from echocardiographic end-diastolic diameter. End-systolic volume was calculated as the difference between end-diastolic volume and the stroke volume derived from the Swan-Ganz catheter. End-diastolic and systolic volumes were used to calibrate the conductance catheter at each time point. The time constant of relaxation was calculated with Weiss' method from the exponential curve fitting of the LV pressure curve after  $dP/dt$  min (most negative pressure development during isovolumetric relaxation of the left

ventricle). The Tau end point was set to 3 mm Hg above left ventricular end-diastolic pressure (LVEDP). Left ventricular stroke work (LVSW) and right ventricular stroke work (RVSW) were calculated as the respective areas of the pressure-volume relationship of the left and right ventricles, and preload recruitable stroke work (PRSW) were calculated from data derived from deloading of the heart as described by Burkoff et al.<sup>19</sup>

### Statistical Analysis

All data in the main protocol have been tested to have normal or normality like distribution. The data are expressed as mean and SD in tables and figures. A linear mixed model<sup>20</sup> with pig identity as subject (random effect, including intercept) and drug or drugs combinations as fixed effects was used to compare physiological values. The best covariance structure was found to be autoregressive, and a comparison of means was made by least significant difference. Restricted maximum likelihood ratio was used for model fitting.  $P$  values  $< .05$  were regarded as statistically significant. All statistical analyses were conducted in SPSS 25.0.

### Results

Based on the dose-response studies, we chose the tested dose of riociguat and cinaciguat at  $100\ \mu\text{g}\cdot\text{kg}^{-1}$  and  $1\ \mu\text{g}\cdot\text{kg}^{-1}\cdot\text{min}^{-1}$ , respectively. At these doses, the pigs showed a marked, but tolerable systemic vasodilatation, and remained hemodynamic stable with mean systemic arterial pressure (MAP) above 50 mm-Hg (Table 1).

Basic hemodynamic data for all experimental animals are shown in Figures 2 and 3 (riociguat experiments) and Figures 4 and 5 (cinaciguat experiments). Also shown in these figures are

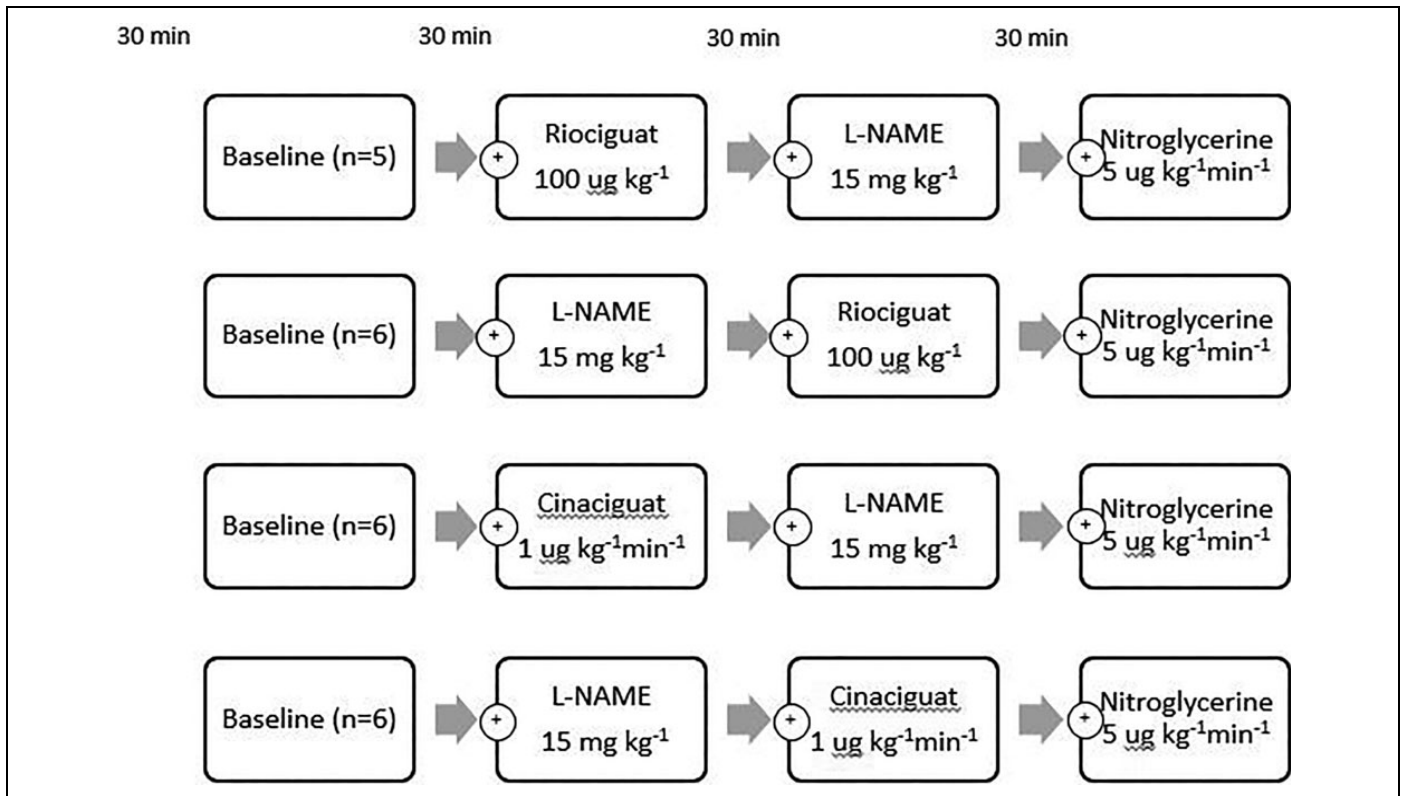


**Figure 1.** Outline of the 4 experimental groups. Following instrumentation and baseline recordings, NO modulation was induced by alternating administration of cinaciguat (Cina)  $1 \mu\text{g kg}^{-1} \text{min}^{-1}$  or riociguat (Rio)  $100 \mu\text{g kg}^{-1}$  combined with L-NAME  $15 \text{ mg kg}^{-1}$ . At the end of all protocols remaining inducible NO response was assessed by NG  $5 \mu\text{g kg}^{-1} \text{min}^{-1}$  infusion. L-NAME indicates N(G)-nitro-L-arginine methyl ester; NG, nitroglycerine; NO, nitric oxide.

the data after infusion of L-NAME and NG. The interactive effects of riociguat or cinaciguat with NO-modulation are summarized schematically in Table 2.

### Interactive Effects of Riociguat and NO on Vascular Tone

Compared to vehicle, riociguat reduced the systemic vascular resistance by 40% and induced lower systemic blood pressures. The same dose, with an evident systemic effect, reduced pulmonary vascular resistance by 20% but did not decrease pulmonary systolic or mean pulmonary blood pressures. Cardiac output was slightly increased.

L-NAME resulted in reduced CO, higher systemic and pulmonary blood pressures, and a corresponding calculated increase in systemic vascular resistance (SVR) and pulmonary vascular resistance (PVR), all compatible with its known NO blocking effect. Riociguat, given after L-NAME, increased CO, reduced MAP, SVR, mean pulmonary arterial pressure (MPAP), and PVR demonstrating an NO-independent vasodilatory effect. L-NAME administered after riociguat in separate experiments decreased CO and increased MAP, SVR, MPAP, and PVR, an indication that riociguat interacts with NO in an additive manner.

Finally, nitroglycerine, given after riociguat and L-NAME, resulted in unchanged CO, decreased MAP, SVR, systolic and

diastolic pulmonary pressures, MPAP, and PVR confirming that NO retains its dose-dependent effect also after giving riociguat.

### Interactive Effects of Cinaciguat and NO on Vascular Tone

Introduced in untreated animals, cinaciguat lowered systemic and pulmonary systolic, diastolic, mean, and venous blood pressures. Cardiac output was slightly reduced. Also, calculated SVR decreased, while PVR remained unchanged. Thus, cinaciguat, as riociguat, shows no selective pulmonary vascular dilatory effect.

Cinaciguat given after the NO-blocker L-NAME induced both systemic and pulmonary vasodilation. However, L-NAME, given after cinaciguat, had almost no vascular effect, indicating that the effect of cinaciguat could not be modulated by altering NO-tone. This was confirmed by giving nitroglycerine directly after cinaciguat, as this had almost no vasoactive effect, as shown in Table 2 and Figures 4 and 5.

### The Effects of Riociguat and Cinaciguat on Cardiac Function

The effects of riociguat and cinaciguat on integrated cardiac function were tested in load-dependent and independent calculations summarized in Figure 2 and 4 and Table 2. The

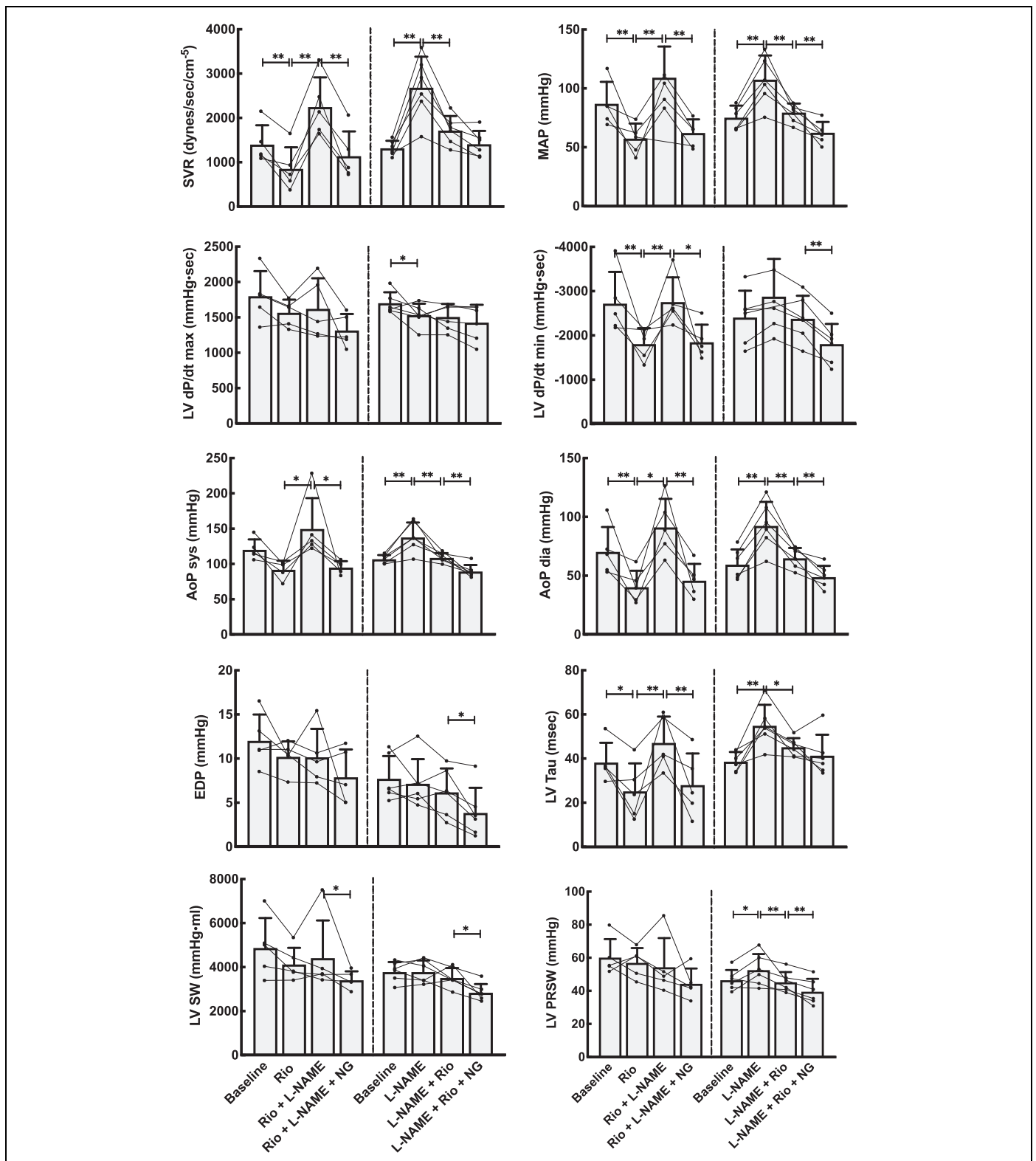


**Figure 2.** Hemodynamic effects on the systemic circulation by NO modulation using the stimulator riociguat (Rio). Left panels stacked bars show data from the group that received Rio as the first drug, whereas right panels are from the group with primary NO-blockade using L-NAME. Both groups received the NO donor NG as the last drug. Line plots represent the individual animals, while bars are mean values for each combination of medications. Error bars are SD of the mean values at each point. AoPdia indicates diastolic pressure in the aorta; AoPsyst, systolic pressure in the aorta; EDP, end-diastolic pressure; LV dP/dt max and min, maximal left ventricular pressure rises and decline; LV PRSW, preload recruitable stroke work; LV SW, left ventricular stroke work; LV Tau, ventricular relaxation constant; MAP, mean arterial pressure in the aorta; NG, nitroglycerine; SVR, systemic vascular resistance. Linear mixed model statistics. \* $P < .05$ , \*\* $P < .01$ .

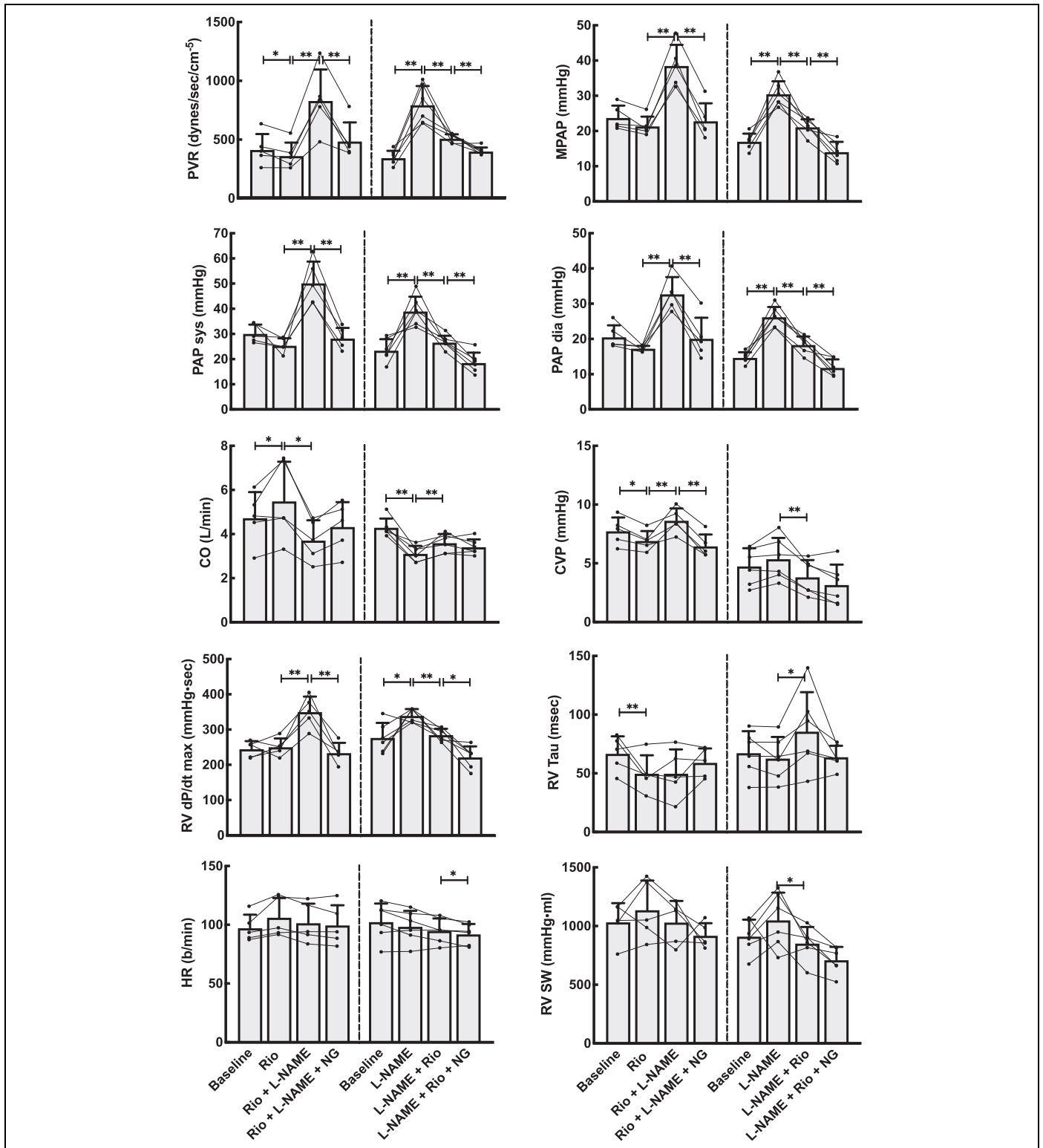


**Figure 3.** Hemodynamic effects on the pulmonary circulation by NO modulation using the stimulator riociguat (Rio). Left panels show data from the group that received Rio as the first drug, whereas the right panels are from the group where the NO system was first blocked using L-NAME. Both groups received the NO donor NG as the last drug. Line plots represent the individual animals, while bars are mean values for each combination of medications. Error bars are SD of the mean values at each point. CO indicates cardiac output by thermodilution; PVR, pulmonary vascular resistance; PAP sys, PAP dia and MPAP, systolic, diastolic and mean pulmonary artery pressure; RV dP/dt max, maximal right ventricular pressure development; RV Tau, right ventricular relaxation; HR, heart rate; RV SW, right ventricular stroke work. Linear mixed model statistics. \* $P < .05$ , \*\* $P < .01$ .

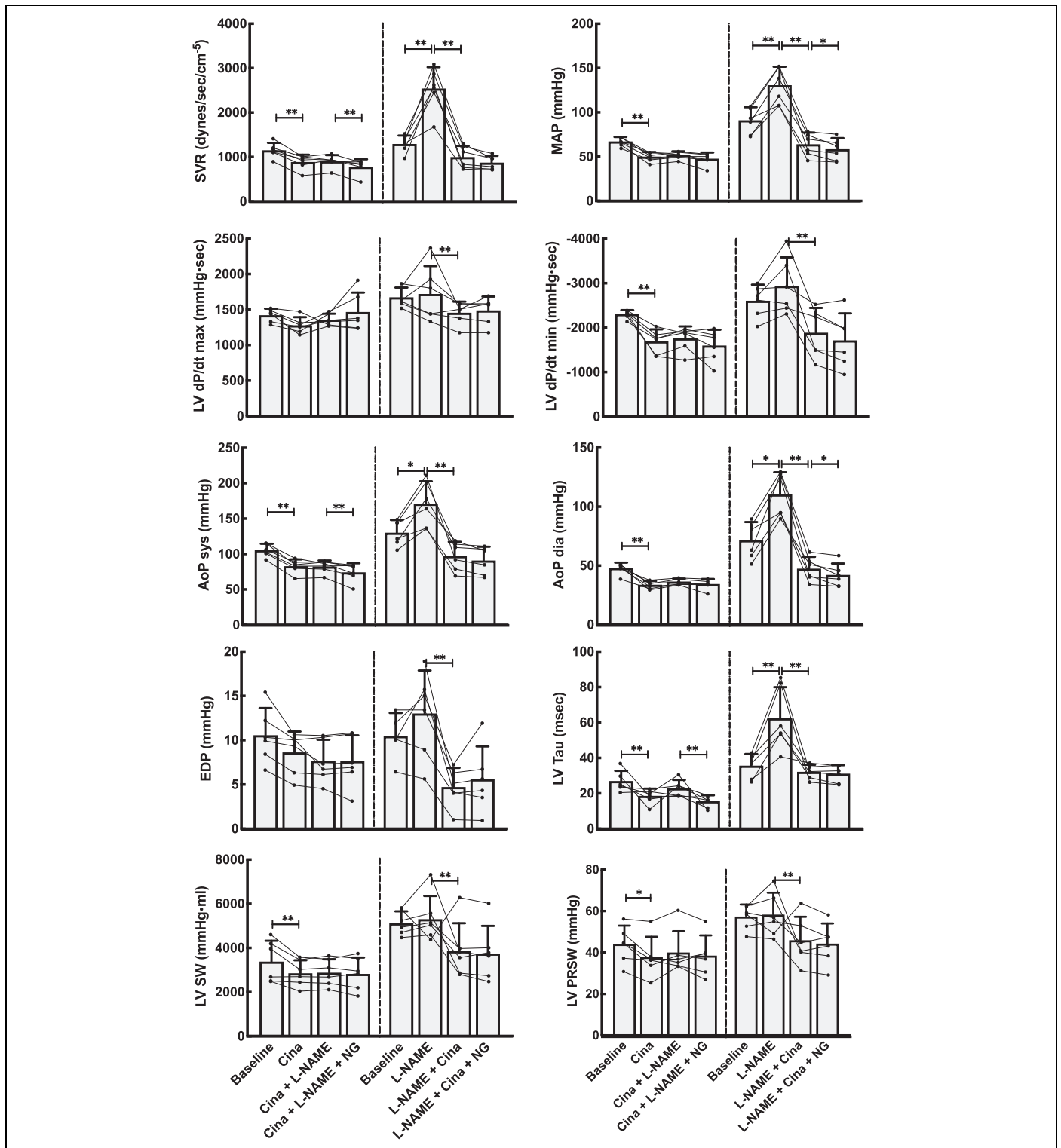


**Figure 4.** Hemodynamic effects on the systemic circulation by NO modulation using the activator cinaciguat (Cina). Left panels show data from the group that received Cina as the first drug. The right panels show data when the NO system was first blocked using L-NAME. Both groups received the NO donor NG as the last drug. Line plots represent the individual animals, while bars are mean values for each combination of medications. Error bars are SD of the mean values at each point. AoP sys, AoP dia, and MAP, systolic, diastolic, and mean aortic pressure; EDP, end-diastolic pressure; NG, nitroglycerine; LV dP/dt max and min, maximal left ventricular pressure development and reduction; LV PRSW, left ventricular preload recruitable stroke work; LV SW, left ventricular stroke work; LV Tau, ventricular relaxation constant; SVR, systemic vascular resistance. Linear mixed model statistics. \* $P < .05$ , \*\* $P < .01$ .



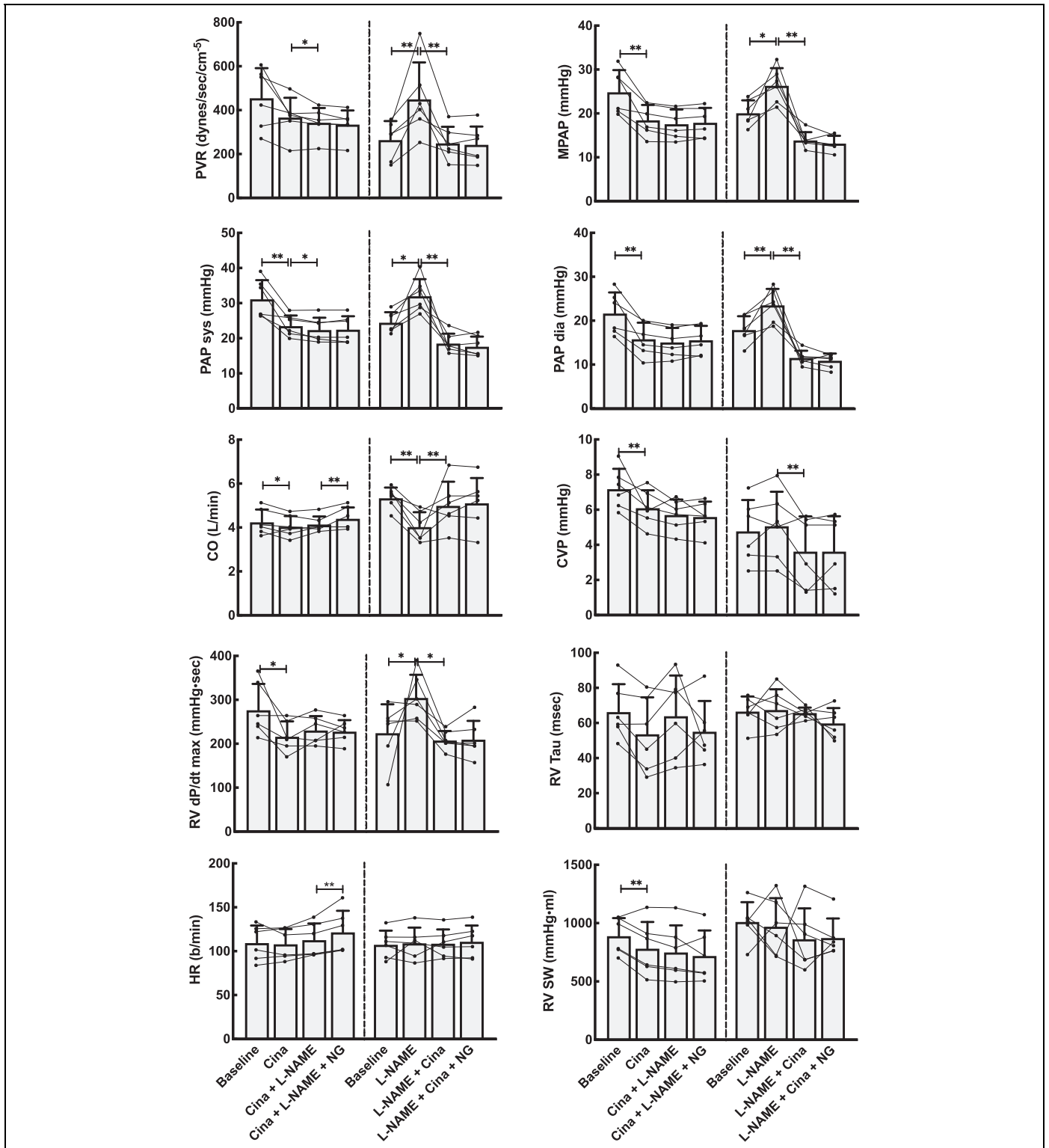


**Figure 5.** Hemodynamic effects on the pulmonary circulation by NO modulation using the activator cinaciguat (Cina). Left panels show data from the group that received Cina as the first drug, whereas the right panels are from the group where the NO system was first blocked using L-NAME. Both groups received the NO donor NG as the last drug. Line plots represent the individual animals, while bars are mean values for each combination of medications. Error bars are SD of the mean values at each point. CO indicates cardiac output by thermodilution; HR, heart rate; NG, nitroglycerine; PAP sys, PAP dia, and MPAP, systolic, diastolic, and mean pulmonary artery pressure; PVR, pulmonary vascular resistance; RV dP/dt max, maximal right ventricular pressure development; RV SW, right ventricular stroke work; RV Tau, right ventricular relaxation. Linear mixed model statistics. \* $P < .05$ , \*\* $P < .01$ .

**Table 2.** Semi-Quantitative Interactive Effects of Riociguat and Cinaciguat Using NO-Modulation.

	Test drug alone		L-NAME alone, Rio-group	L-NAME alone, Cina-group	Test drug after L-NAME		L-NAME after test drug		Nitroglycerin after test drug and L-NAME		Nitroglycerin after L-NAME and test drug	
	Rio	Cina	L-NAME	L-NAME	L-NAME + Rio	L-NAME + Cina	Rio + L-NAME	Cina + L-NAME	Rio + L-NAME + NG	Cina + L-NAME + NG	Rio + NG	L-NAME + Cina + NG
	CO	+	-	-	-	+	+	-	NS	NS	+	NS
LVEDP	NS	NS	NS	NS	NS	----	NS	NS	NS	NS	----	NS
MAP	-	-	++	++	-	-	+++	NS	----	NS	-	-
SVR	-	-	++++	++++	-	----	+++	NS	----	-	NS	NS
LVEF	+	NS	-	-	++	++	-	NS	+	NS	NS	NS
LVSWS	NS	-	NS	NS	NS	-	NS	NS	-	NS	-	NS
LV dP/dt max	NS	-	-	NS	NS	-	NS	NS	NS	NS	NS	NS
LV dP/dt min	++	++	NS	NS	NS	++	----	NS	++	NS	++	NS
LV Tau	-	-	++	+++	-	----	+++	+	----	-	NS	NS
LVPRSW	NS	-	+	NS	-	-	NS	NS	NS	NS	-	NS
RAP	-	-	NS	NS	-	-	+	NS	NS	NS	NS	NS
MPAP	NS	-	+++	++	-	-	+++	NS	----	NS	-	NS
PVR	-	NS	++++	+++	-	----	+++	-	----	NS	-	NS
RV dP/dt max	NS	-	+	++	-	-	++	NS	-	NS	-	NS
RV dP/dt min	NS	+	----	----	++	++	----	NS	+++	NS	++	NS
RV Tau	-	NS	NS	NS	++	NS	NS	NS	NS	NS	NS	NS

Abbreviations: AoPdia, diastolic pressure in the aorta; AoPsyst, systolic pressure in the aorta; CO, cardiac output; Cina, cinaciguat; Es, the end-systolic pressure-volume relationship; LV dP/dt max, maximum rate of developed left ventricular pressure during systole; LV dP/min, maximum rate of pressure decay in the left ventricle during diastole; LVEDV, end-diastolic volume in the left ventricle; LVEF, left ventricular ejection fraction; LVESV, end-systolic volume in the left ventricle; LVP developed pressure, pressure difference between maximum and end-diastolic pressure in the left ventricle; LVPed, end-diastolic pressure left ventricle; LVPmax, maximum intraventricular pressure in the left ventricle; LVPRSW, preload recruitable stroke work in the left ventricle; LVSWS, left ventricular stroke work; MAP, mean arterial pressure in the aorta; MPAP, mean pulmonary arterial pressure, NG, nitroglycerine; PAPdia, diastolic pressure in the pulmonary artery; PAPsys, systolic pressure in the pulmonary artery; PVR, pulmonary vascular resistance; RAPmean, mean right atrial pressure; Rio, riociguat; RV dP/dt max, maximum rise in right ventricular pressure during systole; RV dP/dt min, maximum pressure decay in the right ventricle during diastole; RVPmax, maximum pressure in the right ventricle; RVPmin, minimum pressure in the right ventricle; RVP developed pressure, the difference between RVPmax and RVPmin; SVR, system vascular resistance. +/- ≤ 25% change, ++/-- = 25% to 50% change, +++/---- = >51% to 100% change, ++++/----- > 100% change from previous combination of medications

load-related parameters of time-dependent pressure development were slightly reduced for both left and right ventricle. However, calculating the load-independent parameters of pre-load recruitable stroke work showed that riociguat in this dose had a neutral effect on cardiac contractility. Cinaciguat induced a small reduction also on the load-independent PRSW in the left ventricle.

Both riociguat and cinaciguat demonstrated a slower maximum intraventricular pressure fall rate, expressed as dP/dt min in the left ventricle. For the right ventricle, cinaciguat gave a small decrease in the absolute value of dP/dt min, while riociguat did not have any effect on this index. Using the Tau-index to curve fit the pressure decay during diastole, both cinaciguat and riociguat resulted in significantly faster relaxation of the left ventricle compared to baseline, and both cinaciguat and riociguat counteracted the effect on isovolumic relaxation seen after L-NAME by again reducing the Tau index. Both cinaciguat and riociguat demonstrated unchanged LV end-diastolic volumes at lower end-diastolic pressures.

## Discussion

We have shown that both cinaciguat and riociguat have pronounced vasodilatory properties in the normal systemic vasculature. However, in these healthy juvenile pigs, these compounds have only minor direct effects in the pulmonary circulation. After NO-blockade with L-NAME, a vasodilatory effect in both vasculatures was unmasked. Importantly, no vasoactive effect of NO could be observed after cinaciguat infusion, indicating a functional NO-blocking effect of this compound. In contrast, NO modulation after riociguat infusion altered vascular tone in an interactive, qualitative physiological expected manner. The direct cardiac responses of both drugs were dominated by their unloading effects, and only a small possible reduction in load-independent contractility observed from cinaciguat. The small lusitropic effect for both drugs may also be related to the unloading effect from their vasodilation.

The interplay of riociguat and cinaciguat with the NO-system in the pulmonary circulation has previously been

studied primarily in pulmonary arterial hypertension (PAH) models.<sup>21-26</sup> These observations are somewhat in contrast with the relative weak pulmonary effects in healthy animals observed in our study. A possible explanation might be a different level of the sGC redox-forms in pathological and normal pulmonary vessels. Soluble guanylate cyclase is upregulated in human idiopathic pulmonary hypertension and animal models of PAH,<sup>25</sup> and the vasodilatory effect of both sGC stimulators and activators is augmented by the oxidation of sGC. It is not known what the proportion of the different oxidation levels of sGC is in intact, healthy animals. The effects of these drugs given intravenously in intact animals and the interactions with NO are consequently unknown. Our study using cinaciguat indicates that there is a functionally oxidized sGC also in the healthy systemic circulation, but the activity seems to be low in the pulmonary vasculature. An alternative explanation for the small effects of these drugs in the pulmonary vasculature is the probable normal level of nitric oxide synthase and a concomitant higher activity in healthy animals compared to reduced levels in pulmonary vascular pathology.<sup>27</sup>

In a clinical study with riociguat applied in pulmonary hypertension secondary to diastolic heart failure, but without increased PVR, there was no change in transpulmonary pressure gradient or pulmonary vascular resistance.<sup>28</sup> The explanation for this might be a lower expression of and lower oxidation levels of sGC in the lungs with no primary pathology, abolishing any pulmonary vascular selectivity when the drug is applied intravenously. Inhalation, in contrast to intravenous administration of sGC-activators and stimulators, has been shown to give selective pulmonary vasodilatation in awake lambs with acutely thromboxane-induced pulmonary hypertension.<sup>26</sup> Still, such an application has not to our knowledge been tested in humans or healthy animals.

The dynamics between NO, sGC activators, sGC stimulators, and sGC have been studied in cell cultures with outcomes indicating that sGC activators can skew the redox balance between a small pool of oxidized sGC in the direction of increased oxidation, rendering the sGC insensitive to NO.<sup>29</sup> An *in vitro* study on healthy porcine coronary arteries and rat thoracic aortas have shown that cinaciguat has a profound vasodilatory effect even in the absence of vascular pathology.<sup>30</sup> In that study, cinaciguat exhibited an irreversible effect, and the authors proposed that cinaciguat shift the red-ox-equilibrium of sGC toward the heme-free species. This, in turn, could explain the observed insensitivity to NO-manipulation after cinaciguat in our study. The time span for potential recovery of this effect is unknown.

A phase II study on cinaciguat in acutely decompensated heart failure was stopped prematurely due to the observation that 71% of patients experiencing adverse events, mostly hypotension. The prolonged action and loss of NO-system modulation seem to make cinaciguat a potent but difficult drug to master in clinical practice. There are no ongoing patient studies with cinaciguat,<sup>31</sup> but there are 9 actively recruiting studies on riociguat in scleroderma, sickle cell disease, PAH, and chronic thromboembolic pulmonary hypertension.<sup>32</sup> As seen from our

research, the sGC activators have profound and partly unphysiological effects demanding considerable preclinical assessments before clinical application. There are some phase I studies ongoing with sGC activators in patients with chronic kidney failure, PAH, and acquired pulmonary distress syndrome.<sup>33</sup> These studies need to be monitored closely for possible adverse circulatory effects.

We did not observe any effect of riociguat on cardiac contractility evaluated by preload recruitable stroke work and only a small negative effect of cinaciguat. Studies on ischemia-reperfusion injuries in the heart have shown cytoprotective properties of both cinaciguat and riociguat but no fundamental change in heart function.<sup>11,34-36</sup> Such a protective effect can potentially be related to myocardial calcium handling.<sup>37,38</sup> Infusion of NO donors to the coronary circulation seems to work in a biphasic and concentration-dependent fashion with increased contractility and chronotropy in low normophysiological concentrations and the opposite effect at higher concentrations.<sup>39</sup> Therefore, the effect of exogenous NO through NO donors might be hard to predict, and since the direct activation or stimulation of sGC additionally bypasses the cGMP-independent effects of NO, they will predictably have a different pharmacological profile compared to endogenous NO stimulation.<sup>39</sup>

In our study, the most pronounced diastolic effect was a shortened LV relaxation, expressed in the Tau index. The maximum pressure fall rate in the left ventricle also decreased concomitantly with the Tau index reduction indicating an unloading effect of both riociguat and cinaciguat.<sup>40</sup> In a recent paper using the sGC stimulator Bay 41-8543 in an experimental rat model of HEFPEF (Heart Failure with Preserved Ejection Fraction), Wilck and coworkers observed a normalization of diastolic dysfunction.<sup>41</sup> Of particular clinical interest, the phase 3 study of Vericiguat in HEFPEF still awaits conclusion.<sup>42</sup>

## Methodological Aspects

The pigs were sedated throughout the experiments with no concomitant use of muscle relaxant. Midazolam has a negative inotrope and chronotrope effect in high but not in clinically relevant anesthetic doses.<sup>43</sup> Pentobarbital have negative chronotropic and inotropic effects in anesthetic doses and results in reduced blood pressure, stroke volume, and central venous pressure.<sup>44</sup> Furthermore, pentothal has direct effects on vascular smooth vasculature.<sup>45</sup> The addition of Fentanyl induces no major hemodynamic effects but attenuate pain-mediated stress responses.<sup>46</sup> All these effects influence critical target values in hemodynamic experiments. The goal of the anesthesia protocol was to create a stable hemodynamic environment for the course of the experiment to be able to compare the different stages of the experiment against each other. This protocol has proven to give good stability in prolonged hemodynamic experiments in our lab.<sup>47</sup> Along the same line of reasoning, hexamethonium attenuates sympathetic activation during interventions and isolates the drug effects at each stage of the experiment. As a

trade-off, however, hexamethonium blocks a normal heart-rate response to hypotension.

The dose target for both riociguat and cinaciguat was chosen to keep MAP above 50 mm Hg. We chose a high dose with clear hemodynamic effects in order to induce clear discernable effects of these drugs without the need for excessive amounts of animals to be used in the protocols. In the main study, MAP after cinaciguat infusion was  $50 \pm 5$  mm Hg and in the riociguat group  $57 \pm 13$  ( $P = 0.25$ ). There was no significant difference in SVR, PVR, or MPAP after giving riociguat or cinaciguat. The perfusion pressure in the cinaciguat group is closer to the limit of autoregulation of coronary perfusion pressure<sup>48</sup> than in the riociguat group and may have attenuated cardiac performance predominantly in the cinaciguat group.

We used PRSW as a contractility index. End-systolic pressure–volume relationship and maximum dP/dt are alternative indexes, but PRSW have been shown to be more load-independent and more reproducible than these alternative indexes.<sup>49,50</sup>

## Conclusion

In summary, both cinaciguat and riociguat have vasodilatory properties in the healthy systemic circulation but only a weak effect in the pulmonary vasculature. After blocking NO production with L-NAME, both drugs demonstrate vasodilatory effects in both vasculatures. Furthermore, after giving cinaciguat NO modulation is without any effect on vascular resistance, indicating a functional block of the active NO sites on all forms of sGC. The pharmacological profile of this sGC-activator is, therefore, indiscriminative and, as such, is a difficult drug to handle in a clinical setting. Soluble GC activators seem to have a long way to potential clinical applications.

## Author Contributions

Torvind Næsheim contributed in drafting protocol, sourcing medications, setting up the lab, instrumentation, data collection, analysis, and authoring; Ole-Jakob How contributed in idea, analysis and authoring; and Truls Myrmed helped in idea, drafting protocol, instrumentation, data collection, analysis, and authoring.


## Declaration of Conflicting Interests

The author(s) declared no potential conflicts of interest with respect to the research, authorship, and/or publication of this article.

## Funding

The author(s) disclosed receipt of the following financial support for the research, authorship, and/or publication of this article: The study is funded by UiT, The Arctic University of Norway, Tromsø, Norway.

## ORCID iD

Torvind Næsheim  <https://orcid.org/0000-0002-6294-3667>

## References

1. Farah C, Michel LYM, Balligand JL. Nitric oxide signalling in cardiovascular health and disease. *Nat Rev Cardiol.* 2018;15(5):292-316.
2. Chester M, Seedorf G, Tourneux P, et al. Cinaciguat, a soluble guanylate cyclase activator, augments cGMP after oxidative stress and causes pulmonary vasodilation in neonatal pulmonary hypertension. *Am J Physiol – Lung Cell Mol Physiol.* 2011;301(5):L755-L764.
3. Mittendorf J, Weigand S, Alonso-Alija C, et al. Discovery of riociguat (BAY 63-2521): A potent, oral stimulator of soluble guanylate cyclase for the treatment of pulmonary hypertension. *Chem Med Chem.* 2009;4(5):853-865.
4. Stasch J-P, Schmidt P, Alonso-Alija C, et al. NO- and haem-independent activation of soluble guanylyl cyclase: molecular basis and cardiovascular implications of a new pharmacological principle. *Br J Pharmacol.* 2002;136(5):773-783.
5. Dasgupta A, Bowman L, D’Arsigny C, Archer S. Soluble guanylate cyclase: a new therapeutic target for pulmonary arterial hypertension and chronic thromboembolic pulmonary hypertension. *Clin Pharmacol Ther.* 2015;97(1):88-102.
6. Bonderman D, Ghio S, Felix SB, et al. Riociguat for patients with pulmonary hypertension caused by systolic left ventricular dysfunction: a phase IIb double-blind, randomized, placebo-controlled, dose-ranging hemodynamic study. *Circulation.* 2013;128:502-511.
7. Gheorghiadu M, Greene SJ, Filippatos G, et al. Cinaciguat, a soluble guanylate cyclase activator: results from the randomized, controlled, phase IIb COMPOSE programme in acute heart failure syndromes. *Eur J Heart Fail.* 2012;14(9):1056-1066.
8. Lapp H, Mitrovic V, Franz N, et al. Cinaciguat (BAY 58-2667) improves cardiopulmonary hemodynamics in patients with acute decompensated heart failure. *Circulation.* 2009;119(21):2781-2788.
9. Erdmann E, Semigran MJ, Nieminen MS, et al. Cinaciguat, a soluble guanylate cyclase activator, unloads the heart but also causes hypotension in acute decompensated heart failure. *Eur Heart J.* 2013;34(1):57-67.
10. Armstrong PW, Pieske B, Anstrom KJ, et al. Vericiguat in Patients with Heart Failure and Reduced Ejection Fraction. *N Engl J Med.* 2020;382:1883-1893.
11. Radovits T, Korkmaz S, Miesel-Gröschel C, et al. Preconditioning with the soluble guanylate cyclase activator Cinaciguat reduces ischaemia-reperfusion injury after cardiopulmonary bypass. *Eur J Cardio-thoracic Surg.* 2011;39(2):248-255.
12. Schermuly RT, Stasch J-P, Pullamsetti SS, et al. Expression and function of soluble guanylate cyclase in pulmonary arterial hypertension. *Eur Respir J Off J Eur Soc Clin Respir Physiol.* 2008;32(4):881-891.
13. Douglas WW. The effect of a ganglion-blocking drug, hexamethonium, on the response of the cat’s carotid body to various stimuli. *J Physiol.* 1952;118(3):373-383.
14. Baan J, van der Velde ET, de Bruin HG, et al. Continuous measurement of left ventricular volume in animals and humans by conductance catheter. *Circulation.* 1984;70(5):812-823.
15. Becker EM, Stasch JP, Bechem M, et al. Effects of different pulmonary vasodilators on arterial saturation in a model of pulmonary hypertension. *PLoS One.* 2013;8(8):2-9.

16. Rees DD, Palmer RMJ, Schulz R, Hodson HF, Moncada S. Characterization of three inhibitors of endothelial nitric oxide synthase in vitro and in vivo. *Br J Pharmacol*. 1990;101(3):746-752.
17. Zhao X, Wang Z, Wang Y, et al. Pharmacokinetics of the soluble guanylate cyclase stimulator riociguat in healthy young Chinese male non-smokers and smokers: results of a randomized, double-blind, placebo-controlled study. *Clin Pharmacokinet*. 2016;55(5):615-624.
18. Mueck W, Frey R. Population pharmacokinetics and pharmacodynamics of cinaciguat, a soluble guanylate cyclase activator, in patients with acute decompensated heart failure. *Clin Pharmacokinet*. 2010;49(2):119-129.
19. Burkhoff D, Mirsky I, Suga H. Assessment of systolic and diastolic ventricular properties via pressure-volume analysis: a guide for clinical, translational, and basic researchers. *Am J Physiol Heart Circ Physiol*. 2005;289(2):H501-H512.
20. Wang LA, Goonewardene Z. The use of MIXED models in the analysis of animal experiments with repeated measures data. *Can J Anim Sci*. 2004;84(1):1-11.
21. Stasch J-P, Pacher P, Evgenov OV. Soluble guanylate cyclase as an emerging therapeutic target in cardiopulmonary disease. *Circulation*. 2011;123(20):2263-2273.
22. Deruelle P, Grover TR, Abman SH. Pulmonary vascular effects of nitric oxide-cGMP augmentation in a model of chronic pulmonary hypertension in fetal and neonatal sheep. 2005;1088(1):798-806.
23. Dumitrascu R, Weissmann N, Ghofrani HA, et al. Activation of soluble guanylate cyclase reverses experimental pulmonary hypertension and vascular remodeling. *Circulation*. 2006;113(2):286-295.
24. Deruelle P, Grover TR, Storme L, Abman SH. Effects of BAY 41-2272, a soluble guanylate cyclase activator, on pulmonary vascular reactivity in the ovine fetus. *Am J Physiol Lung Cell Mol Physiol*. 2005;288(4):L727-L733.
25. Evgenov O V., Ichinose F, Evgenov NV, et al. Soluble guanylate cyclase activator reverses acute pulmonary hypertension and augments the pulmonary vasodilator response to inhaled nitric oxide in awake lambs. *Circulation*. 2004;110(15):2253-2259.
26. Evgenov O V., Kohane DS, Bloch KD, et al. Inhaled agonists of soluble guanylate cyclase induce selective pulmonary vasodilation. *Am J Respir Crit Care Med*. 2007;176(11):1138-1145.
27. Giaid A, Saleh D. Reduced expression of endothelial nitric oxide synthase in the lungs of patients with pulmonary hypertension. *N Engl J Med*. 1995;333(4):214-221.
28. Bonderman D, Pretsch I, Steringer-Mascherbauer R, et al. Acute hemodynamic effects of riociguat in patients with pulmonary hypertension associated with diastolic heart failure (DILATE-1). *Chest J*. 2014;146(5):1274.
29. Ghosh A, Stasch JP, Papapetropoulos A, Stuehr DJ. Nitric oxide and heat shock protein 90 activate soluble guanylate cyclase by driving rapid change in its subunit interactions and heme content. *J Biol Chem*. 2014;289(22):15259-15271.
30. Kollau A, Opelt M, Wölkart G, et al. Irreversible activation and stabilization of soluble guanylate cyclase by the protoporphyrin IX mimetic Cinaciguat. *Mol Pharmacol*. 2018;93(2):73-78.
31. Actively recruiting human studies on Cinaciguat. 2020. [https://clinicaltrials.gov/ct2/results?term=riociguat&recrs=a&age\\_v=&gndr=&type=&rslt=&Search=Apply](https://clinicaltrials.gov/ct2/results?term=riociguat&recrs=a&age_v=&gndr=&type=&rslt=&Search=Apply)
32. Actively recruiting human studies on Riociguat. 2020. Accessed 2020. [https://clinicaltrials.gov/ct2/results?term=riociguat&recrs=a&age\\_v=&gndr=&type=&rslt=&Search=Apply](https://clinicaltrials.gov/ct2/results?term=riociguat&recrs=a&age_v=&gndr=&type=&rslt=&Search=Apply)
33. Sandner P, Zimmer DP, Milne GT, Follmann M, Hobbs A, Stasch JP. Soluble guanylate cyclase stimulators and activators. *Handbook of Experimental Pharmacology*. Springer; 2018.
34. Frankenreiter S, Bednarczyk P, Kniess A, et al. cGMP-elevating compounds and ischemic conditioning provide cardioprotection against ischemia and reperfusion injury via cardiomyocyte-specific BK channels. *Circulation*. 2017;136(24):2337-2355.
35. Reinke Y, Gross S, Eckerle LG, et al. The soluble guanylate cyclase stimulator riociguat and the soluble guanylate cyclase activator cinaciguat exert no direct effects on contractility and relaxation of cardiac myocytes from normal rats. *Eur J Pharmacol*. 2015;767:1-9.
36. Methner C, Buonincontri G, Hu C-H, et al. Riociguat reduces infarct size and post-infarct heart failure in mouse hearts: insights from MRI/PET imaging. *Salloum FN, ed. PLoS One*. 2013;8(12):e83910.
37. Simon JN, Duglan D, Casadei B, Carnicer R. Nitric oxide synthase regulation of cardiac excitation-contraction coupling in health and disease. *J Mol Cell Cardiol*. 2014;73:80-91.
38. Paulus WJ, Bronzwaer JG. Myocardial contractile effects of nitric oxide. *Hear Fail*. 2002;7(4):371-383.
39. Mohan P, Brutsaert DL, Paulus WJ, Sys SU. Myocardial contractile response to nitric oxide and cGMP. *Circulation*. 1996;93(6):1223-1229.
40. Raff GL, Glantz SA. Volume loading slows left ventricular isovolumic relaxation rate. Evidence of load-dependent relaxation in the intact dog heart. *Circ Res*. 1981;48(6):813-824.
41. Wilck N, Markó L, Balogh A, et al. Nitric oxide-sensitive guanylyl cyclase stimulation improves experimental heart failure with preserved ejection fraction. *JCI insight*. 2018;3(4):15-17.
42. Butler J, Lam CSP, Anstrom KJ, et al. Rationale and design of the VITALITY-HFpEF trial. *Circ Hear Fail*. 2019;12(5):e005998.
43. Smith AC, Zellner JL, Spinale FG, Swindle MM. Sedative and cardiovascular effects of midazolam in swine. *Lab Anim Sci*. 1991;41(2):157-161.
44. Parker JL, Adams HR. The influence of chemical restraining agents on cardiovascular function: a review. *Lab Anim Sci*. 1978;28(5):575-583.
45. McHale NG, Thornbury KD. The effect of anesthetics on lymphatic contractility. *Microvasc Res*. 1989;37(1):70-76.
46. Brown JN, Thorne PR, Nuttall AL. Blood pressure and other physiological responses in awake and anesthetized guinea pigs. *Lab Anim Sci*. 1989;39(2):142-148.
47. Stenberg TA, Kildal AB, Sanden E, et al. The acute phase of experimental cardiogenic shock is counteracted by microcirculatory and mitochondrial adaptations. *PLoS One*. 2014;9(9):e15.
48. Schulz R, Guth BD, Heusch G. No effect of coronary perfusion on regional myocardial function within the autoregulatory range in pigs: evidence against the Gregg phenomenon. *Circulation*. 1991;83(4):1390-1403.

49. Feneley MP, Skelton TN, Kisslo KB, Davis JW, Bashore TM, Rankin JS. Comparison of preload recruitable stroke work, end-systolic pressure-volume and  $dP/dt_{max}$ -end-diastolic volume relations as indexes of left ventricular contractile performance in patients undergoing routine cardiac catheterization. *J Am Coll Cardiol.* 1992;19(7):1522-1530.
50. Karunanithi MK, Michniewicz J, Copeland SE, Feneley MP. Right ventricular preload recruitable stroke work, end-systolic pressure- volume, and  $dP/dt_{max}$ -end-diastolic volume relations compared as indexes of right ventricular contractile performance in conscious dogs. *Circ Res.* 1992; 70(6):1169-1179.



## 13.1 Paper 3





# The effect of Riociguat on cardiovascular function and efficiency in healthy, juvenile pigs

Torvind Næsheim<sup>1,2</sup>  | Ole-Jakob How<sup>3</sup>  | Truls Myrmel<sup>1,4</sup> 

<sup>1</sup>Cardiovascular Research Group, Department of Clinical Medicine, UiT, The Arctic University of Norway, Tromsø, Norway

<sup>2</sup>Department of Anesthesiology, University Hospital North Norway, Tromsø, Norway

<sup>3</sup>Department of Medical Biology, Faculty of Health Sciences, UiT, The Arctic University of Norway, Tromsø, Norway

<sup>4</sup>Department of Cardiothoracic and Vascular Surgery, University Hospital North Norway, Tromsø, Norway

## Correspondence

Truls Myrmel, Department of Clinical Medicine, UiT, The Arctic University of Norway, 9037 Tromsø, Norway.  
Email: truls.myrmel@uit.no

## Funding information

The study is funded by UiT, The Arctic University of Norway, Tromsø, Norway.

## Abstract

**Introduction:** Riociguat is a soluble guanylate cyclase stimulator approved for the treatment of pulmonary hypertension. Its effect on cardiometabolic efficiency is unknown. A potential cardiac energy sparing effect of this drug could imply a positive prognostic effect, particularly in patients with right heart failure from pulmonary hypertension.

**Method:** We infused Riociguat in six healthy juvenile pigs and measured the integrated cardiovascular effect and myocardial oxygen consumption. To assess the interplay with NO-blockade on cardiac function and efficiency we also administered the NO-blocker L-NAME to the animals after Riociguat.

**Results and Discussion:** Infusion of 100 µg/kg Riociguat gave modest systemic vasodilatation seen as a drop in coronary and systemic vascular resistance of 36% and 26%, respectively. Right and left ventriculoarterial coupling index (Ees/Ea), stroke work efficiency (SWeff), and the relationship between left ventricular myocardial oxygen consumption (MVO<sub>2</sub>) and total mechanical work (pressure–volume area; PVA) were unaffected by Riociguat. In contrast, systemic and pulmonary vasoconstriction induced by L-NAME (15 mg/kg) shifted the Ees/Ea ratio toward reduced SWeff in both systemic and pulmonary circulation. However, there was no surplus oxygen consumption, that was measured by the MVO<sub>2</sub>/PVA relationship after L-NAME in Riociguat-treated pigs. This suggests that Riociguat can reduce the NO-related cardiometabolic inefficiency previously observed by blocking the NO pathway.

## 1 | INTRODUCTION

Myocardial oxygen consumption (MVO<sub>2</sub>) is influenced by substrate metabolism, heart rate, wall tension and contractility (Braunwald, 1969). Under normal physiological conditions, these parameters are determined by the hormonal state of the individual. Importantly, adrenergic hormones and drugs increase contractility and relative oxygen consumption (Müller, How, & Jakobsen, 2010; Vasu et al., 1978). Previous studies in large animal models indicate that an elevated NO-tone will

improve myocardial efficiency, i.e., reduces MVO<sub>2</sub> related to mechanical work (Suto et al., 1998). Riociguat, a soluble guanylate cyclase (sGC) stimulator, exhibits a vasodilatory and NO-like effect by direct stimulation of the sGC enzyme, thus circumventing the need for NO stimulation and compensating for decreased NO sensitivity in vascular pathology. Riociguat could therefore have a favorable energetic profile equal to direct NO effects in the myocardium. This would be particularly beneficial in patients with pulmonary hypertension and right heart failure treated with Riociguat (Adempas®). To assess

This is an open access article under the terms of the Creative Commons Attribution License, which permits use, distribution and reproduction in any medium, provided the original work is properly cited.

© 2020 The Authors. Physiological Reports published by Wiley Periodicals LLC on behalf of The Physiological Society and the American Physiological Society

this possibility, we used a well-established metabolic and energetic effect model (Korvald, Elvenes, & Myrnel, 2017) to determine the myocardial oxygen consumption and function during Riociguat infusion in healthy pigs. Studies have shown that there is a basal oxygen-sparing level of NO in the myocardium (Loke, McConnell, & Tuzman, 1999; Recchia et al., 1999), and blocking this NO-tone by infusion of L-NAME has been shown to induce surplus  $MVO_2$  (Nordhaug, Steensrud, Aghajani, Korvald, & Myrnel, 2004). We hypothesized that Riociguat added to normal hearts would reduce  $MVO_2$  relative to mechanical work in the left ventricle and that the NO-blocker L-NAME would reverse this oxygen-sparing effect.

## 2 | METHODS

### 2.1 | Animals

Six castrated male domestic pigs weighing  $30 \pm 5$  kg were adapted to the animal department for 5–7 days. The pigs were fasted overnight before experiments, with free access to water. The experimental protocol was approved by the Norwegian Animal Research Authority according to the FDF reference; 2012/55972.

### 2.2 | Surgical preparation

The pigs were premedicated with an intramuscular injection of 20 mg/kg ketamine (Pfizer AS, Oslo, Norway) and 1 mg of atropine (Nycomed Pharma, Oslo, Norway). Anesthesia was induced by intravenous injection of 10 mg/kg pentobarbital sodium (Abbott, Stockholm, Sweden) and 0.01 mg/kg fentanyl (Hameln Pharmaceuticals, Hameln, Germany). The animals were ventilated after intubation. Normal ventilation was defined as an  $PaCO_2$  of  $40 \pm 2$  mmHg. A central venous catheter was placed through the left internal jugular vein and anesthesia was maintained throughout the experiment by a continuous infusion of  $4 \text{ mg}\cdot\text{kg}^{-1}\cdot\text{hr}^{-1}$  pentobarbitone sodium,  $0.02 \text{ mg}\cdot\text{kg}^{-1}\cdot\text{hr}^{-1}$  fentanyl, and  $0.3 \text{ mg}\cdot\text{kg}^{-1}\cdot\text{hr}^{-1}$  midazolam (B. Braun, Melsungen, Germany). The circulating volume was maintained by a  $20 \text{ ml}\cdot\text{kg}^{-1}\cdot\text{hr}^{-1}$  continuous infusion of 0.9% NaCl supplemented with  $1.25 \text{ g}\cdot\text{L}^{-1}$  glucose. Following sternotomy, the pericardium was removed, and the coronary arteries and pulmonary trunk were dissected free from connective tissue. The hemiazygos vein was then ligated.

### 2.3 | Instrumentation

A 7-Fr pressure catheter (Millar MPVS Ultra, Houston, TX, USA) was inserted through an introducer sheath via

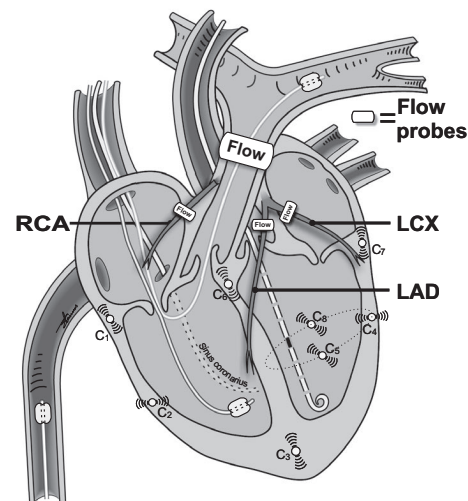


**FIGURE 1** Schematic drawing of the sonometric crystal positions used for assessing right and left ventricular volumes (see equation 1 and 2). The placements of the crystals are in the subendocardial position. Crystal no. 8 is placed in the posterior wall of the left ventricle adjacent to crystal no. 5 in the anterior wall. “Flow” indicates time transit flow probes, RCA is the right coronary artery, LCX is the left circumflex coronary artery, LAD is the left anterior descending artery, C1 to C8 are sonometric crystals placed in the subendocardium. Balloon catheters are drawn in the right ventricle and pulmonary artery

the carotid artery into the left ventricle. A 5 Fr Swan-Ganz catheter (Edwards Lifescience Corp. Irvine, USA) was advanced into the pulmonary artery. A 5 fr balloon catheter was floated from the superior caval vein into the right ventricle for pressure measurements. Central venous pressure was measured in the right atrium. The systemic arterial pressure was assessed from a vascular catheter in the abdominal aorta. An 8 Fr balloon catheter was introduced into the inferior caval vein and positioned just below the right atrium for intermittent preload reduction. A 4 Fr catheter with side holes was placed in the coronary sinus for the collection of coronary venous blood. Transit time flow probes (Transonic Systems Inc, Ithaca, NY, USA) were placed around the pulmonary trunk and the three coronary arteries. Eight sonometric crystals (Sonometrics Corporation, Ontario, Canada) were implanted subendocardially, as described in Figure 1. At the end of the experiment, the heart was stopped by injection of 20 mmol KCl (1 mmol/ml). The heart was then excised, and through a balloon catheter in the left main coronary artery, Evans Blue (Sigma-Aldrich, Saint-Louis, Missouri, USA) was injected, and the stained and unstained heart muscle was weighed.

### 2.4 | Experimental protocol and drugs

The Riociguat dose was based on a dose-response study in four animals (Næsheim, How, & Myrnel, 2020), targeting

a mean systemic blood pressure at 50 mmHg. In this study, the experiments were conducted using a repeated measures design. The ganglion blocker Hexamethonium chloride (Sigma-Aldrich Missouri, USA) 15 mg/kg was given to avoid autonomous reflexes during interventions and measurements (Douglas, 1952). Heparin, 2,500 IU, was given intravenously after instrumentation to prevent clotting of catheters. Following surgery, the pigs were allowed to rest for 30 min before baseline measurements.

Riociguat (100 µg/kg) was then given as an intravenous bolus, and the second recording was carried out after another 30 min. Finally, L-NAME (15 mg/kg) was given, also as a bolus. The dose of L-NAME was based on an earlier dose-response study in our lab (Nordhaug et al., 2004). The last recording was carried out after the hemodynamic parameters had stabilized after approximately 15 min. At each time point, a full set of cardiac function parameters and vascular measurements were recorded. Assessment of cardiometabolic efficiency was done according to an established protocol (Korvald et al., 2017) with some modification particularly related to measurements of cardiac volumes by sonometric crystals (Feneley et al., 1990). A downloading protocol was carried out after every drug intervention: By stepwise inflating the balloon catheter in the caval vein, stroke work, coronary flow, and arterial-to-coronary venous oxygen difference was recorded at 6–8 different preloads.

Riociguat was obtained from Chemoki Synthesi-TECH, Jiangsu, China, as a dry powder. pH neutral solutions were prepared with DMSO (dimethyl sulfoxide) and a 1:1 solution of Transcutol, Diethylene glycol ethyl ether (Sigma-Aldrich, Missouri, USA) and Cremophor, macrogolglycerol ricinolate (Sigma-Aldrich Missouri, USA). We used 5% Transcutol and Chremophore solutions, and the volume ratio between DMSO, Transcutol, and Chremophore was 0.05:2.5:2.5. This solution was then further diluted with 0.9 mg·ml<sup>-1</sup> NaCl to a final concentration of test drug of 0.01 to 0.1 mg·mL<sup>-1</sup> depending on the dose to be given. The maximum DMSO concentration was 0.02%. L-NAME, N-omega-nitro-L-arginine methyl ester, 15 mg/kg, was used as a nitric oxide synthetase inhibitor (Rees, Palmer, Schulz, Hodson, & Moncada, 1990).

## 2.5 | Registration of data and analysis

Data were sampled, digitized and analyzed (using ADI MPVS Ultra and Powerlab hardware and LabChart Pro software v 8.1.8, Dunedin, New Zealand). Cardiac dimension data, obtained by the sonometric crystals (Figure 1), were calibrated to cardiac volumes at baseline with the use of intrathoracic Echocardiography (Philips IE33, Philips Healthcare). Echocardiography was also used to confirm the sphericity of the left ventricle at all time points. For all the

following recordings, cardiac volumes were calculated from the sonometric data using the following formulas:

The volume of the left ventricle was calculated by the bi-plane area-length formula as:

$$V_{lv} = \frac{\pi}{6} D_{5-8}^2 \cdot D_{7-3}$$

The volume of the right ventricle was estimated by a simplified shell subtraction model as:

$$V_{rv} = \frac{\pi}{6} D_{6-3} (D_{4-2}^2 - D_{5-8}^2)$$

$D_{n-n}$  indicates the cardiac dimensions between selected crystals, as shown in Figure 1. This ignores the volume of the intraventricular septum, and will therefore predictably overestimate right ventricular volumes. For assessment of end-systolic elastance (Ees, maximal ventricular tension as an index of contractility) and  $V_0$  (unstressed ventricular volume), an abrupt reduction in preload was carried out by rapid inflation of the balloon catheter situated in the caval vein. Example loops from the left and right ventricle are presented in Figure 4.  $V_0$  was calculated at baseline for each pig and used as a constant for the remainder of the experiment. Arterial elastance, Ea, in both ventricles was calculated as.

$$Ea = ESP/SV$$

ESP is the end-systolic pressure, and SV is the stroke volume (Morimont, Lambermont, & Ghuysen, 2008).

Stroke work efficiency, the ratio of total ventricular mechanical work delivered to the circulation, was calculated by stroke work (SW)/ pressure–volume area (PVA) (Vanderpool et al., 2015). Stroke work was calculated as:

$$SW = (P_{max} - EDP) \times SV$$

$P_{max}$  is the maximum pressure in the ventricle (mmHg), EDP is the end-diastolic pressure in the ventricle (mmHg), and SV is the stroke volume (ml). Pressure–volume area (PVA) was calculated as SW + potential energy (PE):

$$PE = (ESP \times (ESV - V_0)) / 2 - (EDP \times (EDV - V_0)) / 4$$

ESV is the end-systolic volume (ml), EDV is the end-diastolic volume (ml), and  $V_0$  is the x-axis intercept of the regression line of the end-systolic pressure–volume relation at baseline.

Left ventricular mechanoenergetic efficiency was assessed by the linear regression of PVA and myocardial oxygen consumption ( $MVO_2$ ) at various workloads, where  $MVO_2$  was calculated as:

$$MVO_2 = (Hb \times \text{avd}O_2 \times LVCBF \times 1.39) / (HR \times 20.2)$$

Hb is hemoglobin concentration (g/dl), avdO<sub>2</sub> is the difference in arterial and great cardiac vein oxygen saturation (%), LVCBF is the left ventricular coronary blood flow (ml/min) or blood flow through the circumflex and left anterior descending arteries divided by left ventricular weight (LVW in gram (g), as described (Aghajani et al., 2004; Yao, Xue, Yu, Ni, & Chen, 2018)). HR is heart rate (beats per minute), 1.39 is a constant (ml O<sub>2</sub>/g Hb), and 20.2 is a factor for J/mL O<sub>2</sub> to convert MVO<sub>2</sub> to mechanical energy equivalents. In the MVO<sub>2</sub>/PVA framework the y-axis intercept represents myocardial oxygen cost for excitation–contraction coupling and basal metabolism, while 1/slope represents cardiac efficiency of contractile work (Myrmel & Korvald, 2000).

## 2.6 | Statistical analysis

Calculations and statistical analyses were performed using a spreadsheet (Microsoft Excel 365, Microsoft, USA) and a statistical package (IBM SPSS Statistics for Windows, IBM Corp, Version 25.0. Armonk, NY). Values are presented as the mean ± standard deviation. Mixed model analysis with pig identity as random effect, with allowance for variation in both intercept and slopes between pigs, was performed on the graph in Figures 2 and 3. Pairwise comparisons with least significant difference were evaluated between time points. The autoregressive covariance structure was modeled to give the best fit of data. Mixed model linear regression with pig identity as random effect was used on cardiac energetics data. For these calculations, MVO<sub>2</sub> and the product of MVO<sub>2</sub> and the dummy variable for medication were used as fixed effects (linear regression Figure 7). *p*-values \*\*<.01 \* <.05 were regarded as statistically significant.

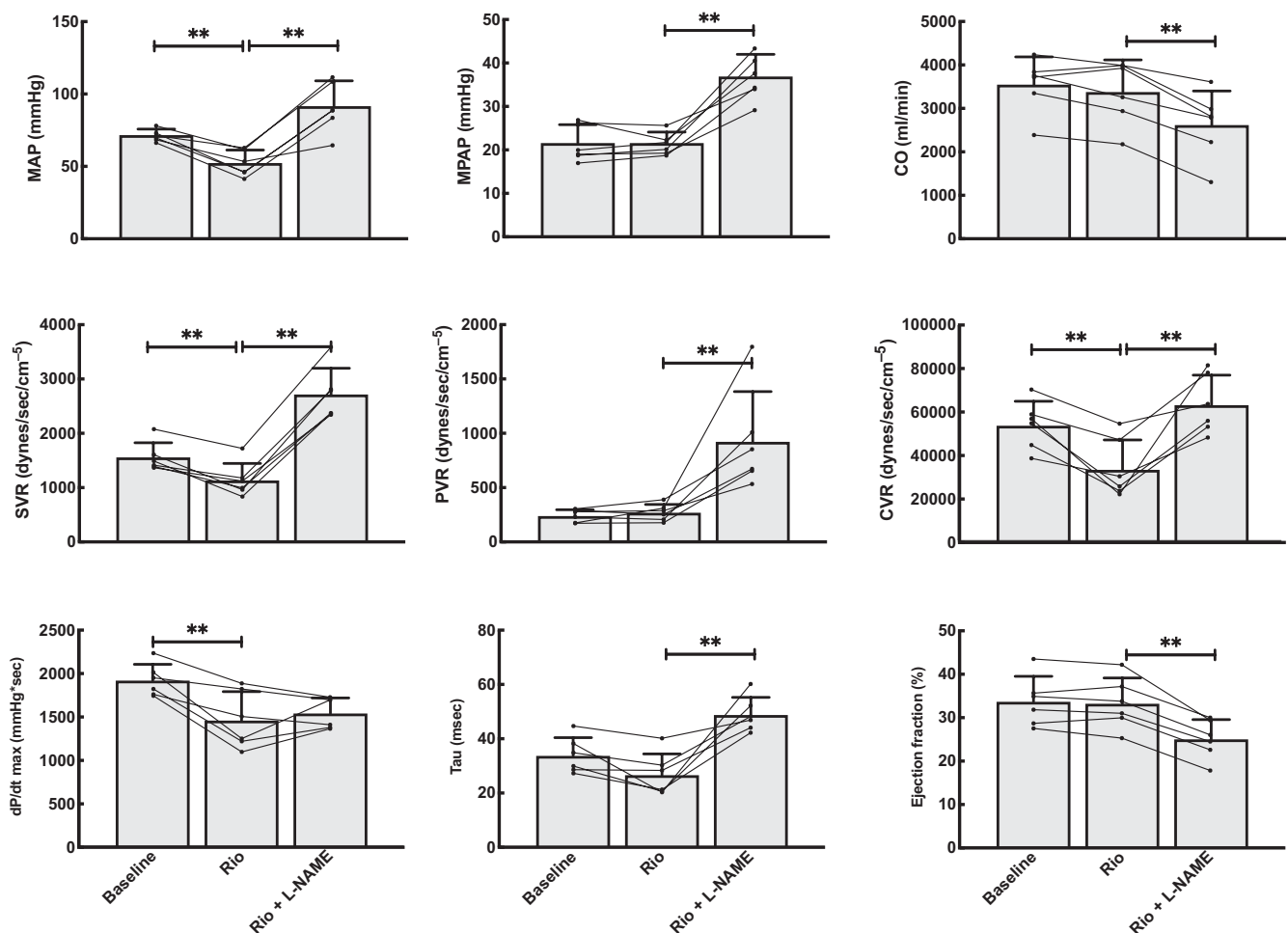
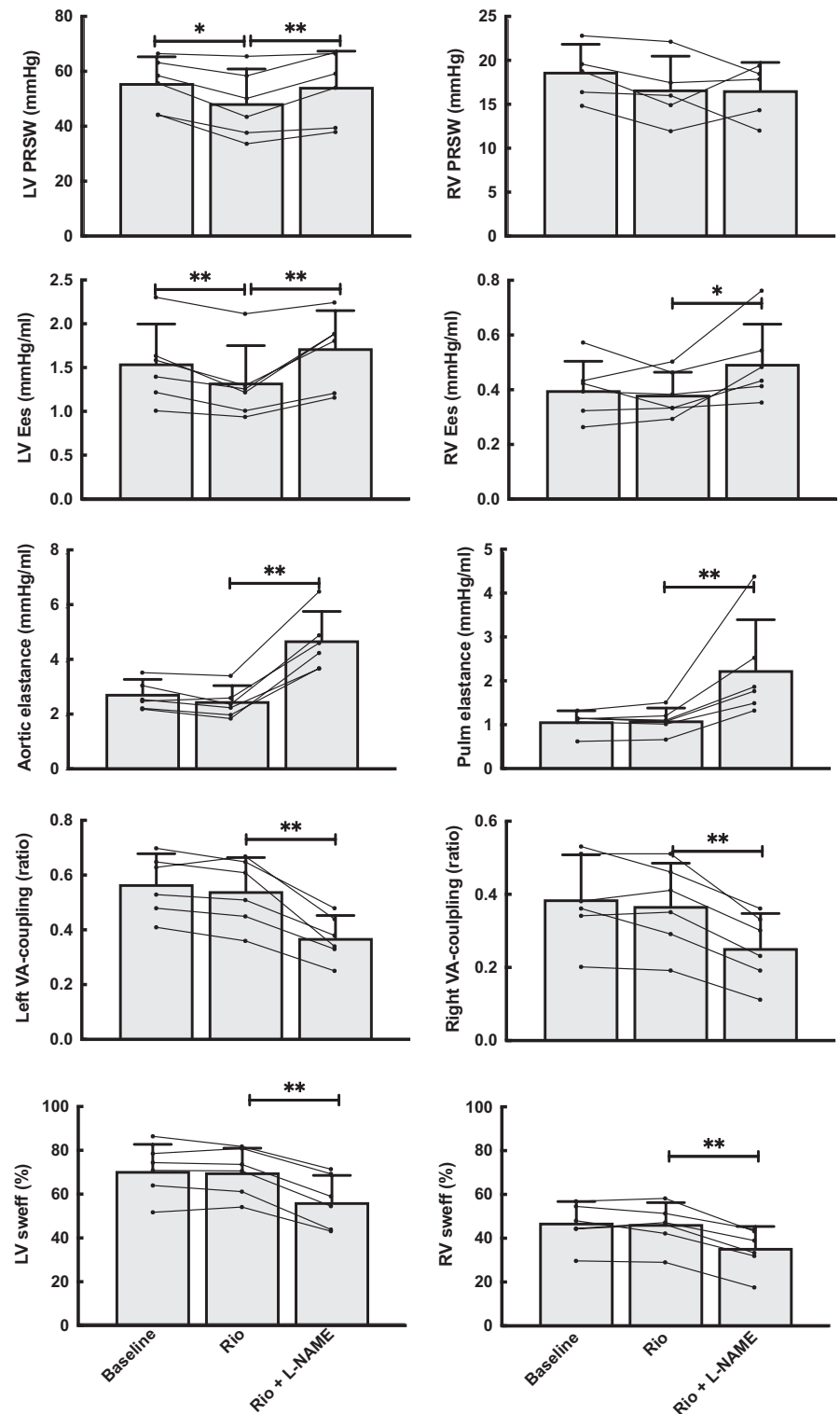


**FIGURE 2** General hemodynamic measurements at baseline (Baseline), after a bolus of 100 µg/kg Riociguat (Rio) and finally after adding 15 mg/kg L-NAME. MAP is the mean systemic arterial pressure, MPAP is the mean pulmonary arterial pressure, CO is the cardiac output. SVR, PVR, and CVR are the systemic, pulmonary and coronary arterial resistances. dP/dT<sub>max</sub> is the maximum slope of left ventricular pressure development. Tau is the time constant of isovolumetric relaxation. EF is the left ventricular ejection fraction. *N* = 6, \*\* denotes *p* < .01 compared to the previous phase of the experiment

**FIGURE 3** Ventriculoarterial coupling (VA coupling) and stroke work efficiency (SWeff) in both the left (LV) and right (RV) ventricles after subsequent boluses of Riociguat and L-NAME (see Figure 2). Left column displays data from the systemic circulation and right column from the pulmonary vasculature. VA coupling was calculated as the ratio of ventricular end-systolic and arterial elastance ( $E_{es}/E_a$ ). SWeff is the portion of total ventricular mechanical work (pressure–volume area, PVA) measured as external pressure and volume work (SW).  $N = 6$ , \*  $p < .05$ , \*\*  $p < .01$  compared to the previous measuring point in the experiment



### 3 | RESULTS

#### 3.1 | Dose-response-study

Increasing doses of Riociguat up to 100  $\mu\text{g}/\text{kg}$  induced progressive systemic vasodilatation and hypotension. No significant

effects were seen in the pulmonary vasculature. At the maximum dose tested the mean systemic pressure reached the predefined threshold of 50 mmHg (manuscript in press). Heart rates in the control state during Riociguat infusion and after L-NAME bolus were  $112 \pm 9 \text{ min}^{-1}$ ,  $111 \pm 14 \text{ min}^{-1}$  and  $111 \pm 11 \text{ min}^{-1}$  respectively, with no significant difference (Table 1).



### 3.2 | Effects on vascular tone

A bolus of 100 µg/kg Riociguat gave modest systemic vasodilatation, including the coronary circulation, as seen by a drop in coronary and systemic vascular resistance of  $36\% \pm 21\%$  ( $p = .01$ ) and  $26\% \pm 18\%$  ( $p = .00$ ), respectively (Figure 2). No significant effect was seen in the pulmonary vasculature.

A bolus of the NOS inhibitor L-NAME (15 mg/kg) after Riociguat resulted in both pulmonary and systemic vasoconstriction as seen by a  $2.5 \pm 1.6$  ( $p = .01$ ) and  $1.5 \pm 0.2$  ( $p = .00$ ) fold increase in PVR and SVR, respectively.

### 3.3 | Cardiac effects

The bolus of Riociguat did not alter cardiac output or ejection fraction (Figure 2). Left ventricular maximum pressure development (LV dp/dt) decreased by  $24\% \pm 12\%$  ( $p = .00$ ), while no change in this index was seen for the right ventricle. Stroke work was reduced by  $20\% \pm 8\%$  ( $p = .00$ ) for the left, but not the right ventricle. Left ventricular end-systolic pressure–volume relation, i.e., elastance (LV  $E_{es}$ ), was reduced by  $14\% \pm 14\%$  ( $p = .01$ ). Right ventricular elastance (RV  $E_{es}$ ), remained stable. Preload recruitable stroke work (PRSW) decreased by  $13\% \pm 7\%$  ( $p = .01$ ) for the left ventricle but did not change for the right ventricle. The diastolic relaxation index, Tau, was unaltered for the left ventricle. Ventricular dimensions remained unchanged.

L-NAME decreased cardiac output by  $23\% \pm 7\%$  ( $p = .00$ ) and left ventricular ejection fraction (EF) decreased from  $33\% \pm 5\%$  to  $25\% \pm 4\%$  ( $p = .00$ ). Heart rate was unchanged. Reduction in EF was accompanied by an increase in end-systolic volumes for both ventricles;  $11\% \pm 8\%$  ( $p = .010$ ) for the left ventricle and  $12\% \pm 10\%$  ( $p = .04$ ) for the right ventricle. Left ventricular elastance increased by  $29\% \pm 23\%$  ( $p = .01$ ) and right ventricular elastance increased by  $18\% \pm 10\%$  ( $p = .02$ ) (Figures 5 and 6). Left ventricular PRSW increased by  $12\% \pm 8\%$  ( $p = .00$ ), while no effect was found on right ventricular PRSW.

### 3.4 | Effects on ventriculoarterial coupling

Riociguat did not impact the relationship between contractility and afterload demonstrated by an unchanged ventriculoarterial coupling and stroke work efficiency for both the systemic and pulmonary circulation. L-NAME, on the other hand, elevated afterload proportionately more than contractility, causing an offset in the Ees/Ea relationship for both ventricles. This resulted in impaired stroke work efficiency in both left and right ventricle by  $19\% \pm 5\%$  ( $p = .00$ ) and  $25\% \pm 10\%$  ( $p = .00$ ) (Figures 3, 5 and 6).

Figure 4 shows an example of pressure–volume relations during preload reductions in one pig at baseline, and Figures 5 and 6 the detailed effects of Riociguat and L-NAME on the time-varying interaction of the two ventricles with their afterloads (ventriculoarterial coupling). These compilations demonstrate that Riociguat mainly acts by reducing the afterload on the left ventricle giving reduced stroke work due to lesser pressure work but no altered ventricular volumes. L-NAME increases the arterial elastance, reduces the volume-related stroke work with an increased end-systolic volume (reduced ejection fraction) with a resulting reduced cardiac output.

### 3.5 | Effects on mechanoenergetic efficiency

The mechanoenergetic efficiency of the left ventricle was unaffected by Riociguat, displayed by unaltered  $MVO_2/PVA$  relationship with regard to both slope and intercept. Blocking NO by applying a subsequent L-NAME bolus did not impact the relative oxygen consumption in Riociguat-treated hearts (Figure 7).

## 4 | DISCUSSION

The main finding in this study was an observed neutral effect of Riociguat on myocardial oxygen consumption. There was no shift in the  $MVO_2/PVA$  relationship for Riociguat,

**TABLE 1** Dose-response study of Riociguat

Riociguat, $n = 4$					
	Vehicle	10 µg/kg	20 µg/kg	50 µg/kg	100 µg/kg
MAP, mmHg	88 ± 21	87 ± 22	66 ± 11 <sup>#</sup>	56 ± 13 <sup>#</sup>	50 ± 9 <sup>#</sup>
MPAP, mmHg	25 ± 23	22 ± 2	23 ± 5	25 ± 7	25 ± 8
SVR, dynes/s/cm <sup>-5</sup>	1,066 ± 248	957 ± 204	760 ± 180 <sup>#</sup>	568 ± 124 <sup>#</sup>	497 ± 161 <sup>#</sup>
PVR, dynes/s/cm <sup>-5</sup>	166 ± 109	146 ± 87	162 ± 76	179 ± 76	167 ± 65

Note: Dose-response data for Riociguat submitted in other publication. MAP, Mean systemic arterial pressure; MPAP, Mean pulmonary arterial pressure; SVR, Systemic vascular resistance; PVR, Pulmonary vascular resistance. Values are mean ± standard deviation. Significance levels between doses of test drug against baseline.

<sup>#</sup>= $p < 0.05$  (mixed model statistics with pig identity as random effect).

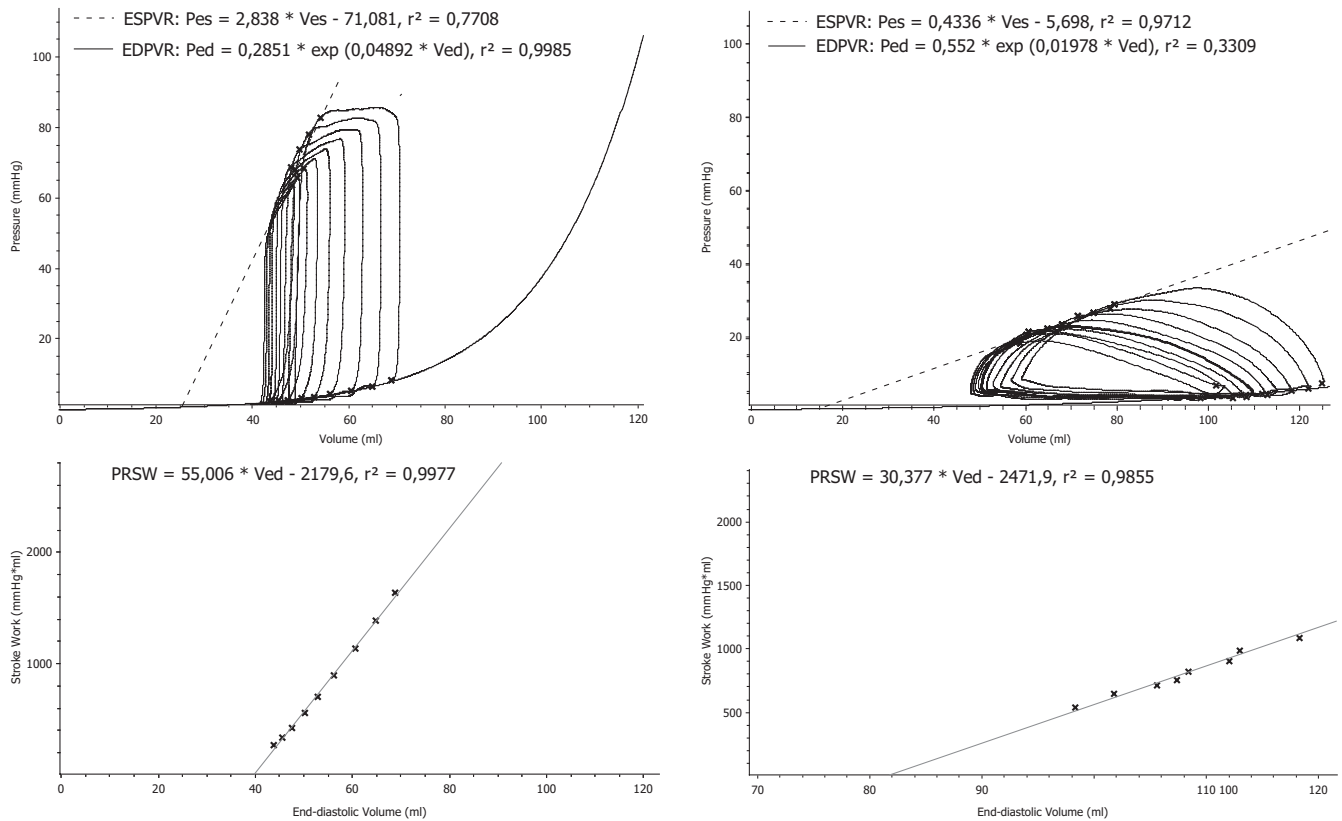


**FIGURE 4** Screenshot of actual recordings from one pig. Pressure–volume loops and calculated preload recruitable stroke work (PRSW) during reduction in preload by inflation of the Fogarty balloon catheter in the inferior caval vein. Left panels are from the left ventricle. Right panels are from the right ventricle. Top panels are the pressure–volume loops with linear curve fitting to the maximum pressure/volume relationship (ESPVR) and curvilinear curve fitting of the end-diastolic pressure/volume relationship (EDPVR). The lower panels show the preload recruitable stroke work for the left and right ventricles, respectively

indicating that stimulation of sGC did not influence myocardial metabolism in healthy pigs in the dose given in this study. The dose chosen was the highest dose possible to administer while avoiding excessive hypotension. Of notice, the subsequent administration of the NO-blocker L-NAME did not increase the relative oxygen consumption in the myocardium, and this suggests that the expected surplus  $MVO_2$  after using L-NAME (Nordhaug et al., 2004) was attenuated by this dose of Riociguat.

The indication for using Riociguat is idiopathic pulmonary artery hypertension (PAH) and chronic thromboembolic pulmonary hypertension (CTEPH), two out of five categories of pulmonary hypertension (PH), according to the World Health Organization (Farber, Miller, & Poms, 2015). Inadequate NO-mediated vasodilation is believed to have an essential role in the pathogenesis of PAH. Thus, stimulating the NO-sGC-cGMP-PKG pathway is a seemingly attractive treatment target (Ghofrani, Humbert, & Langleben, 2017). Indeed, inhibition of the cGMP degradation by the PDE5 inhibitor Sildenafil has improved outcomes for patients with PAH (Galiè et al., 2005). However, PAH is associated with reduced NO availability and reduced sensitivity of the sGC as caused by oxidative

stress that may restrict the effectiveness of PDE5 inhibitors (Hoepfer, Simonneau, & Corris, 2017; Lang, Kojonazarov, & Tian, 2012). Riociguat works through the same pathway; by stimulating sGC partly independent of available NO and with higher potency than NO when sGC has undergone oxidation in pathological tissues (Thoonen et al., 2015). While efforts have been taken to investigate the vascular effects of Riociguat in the diseased state with particular emphasis on PAH, little attention has been on the physiological effects of the drug on the heart in general and the right ventricle in particular. This is relevant since PAH is the leading cause of right heart failure, and heart failure determines the prognosis in PAH (Kylhammar, Kjellström, & Hjalmarsson, 2018; Vonk-Noordegraaf et al., 2013).

The impact of NO on contractility and cardiometabolic efficiency has been an area of particular attention. NO and cGMP seem to influence contractile function in a concentration-dependent bidirectional fashion. In an in vitro model, the effect of NO on cardiomyocytes was found to be dependent on intact endothelium. In this study, cyclic GMP affected the contractile response of the myocytes via a biphasic inhibition and then stimulation of cGMP-dependent cAMP phosphodiesterase inhibitor through modulation of intracellular



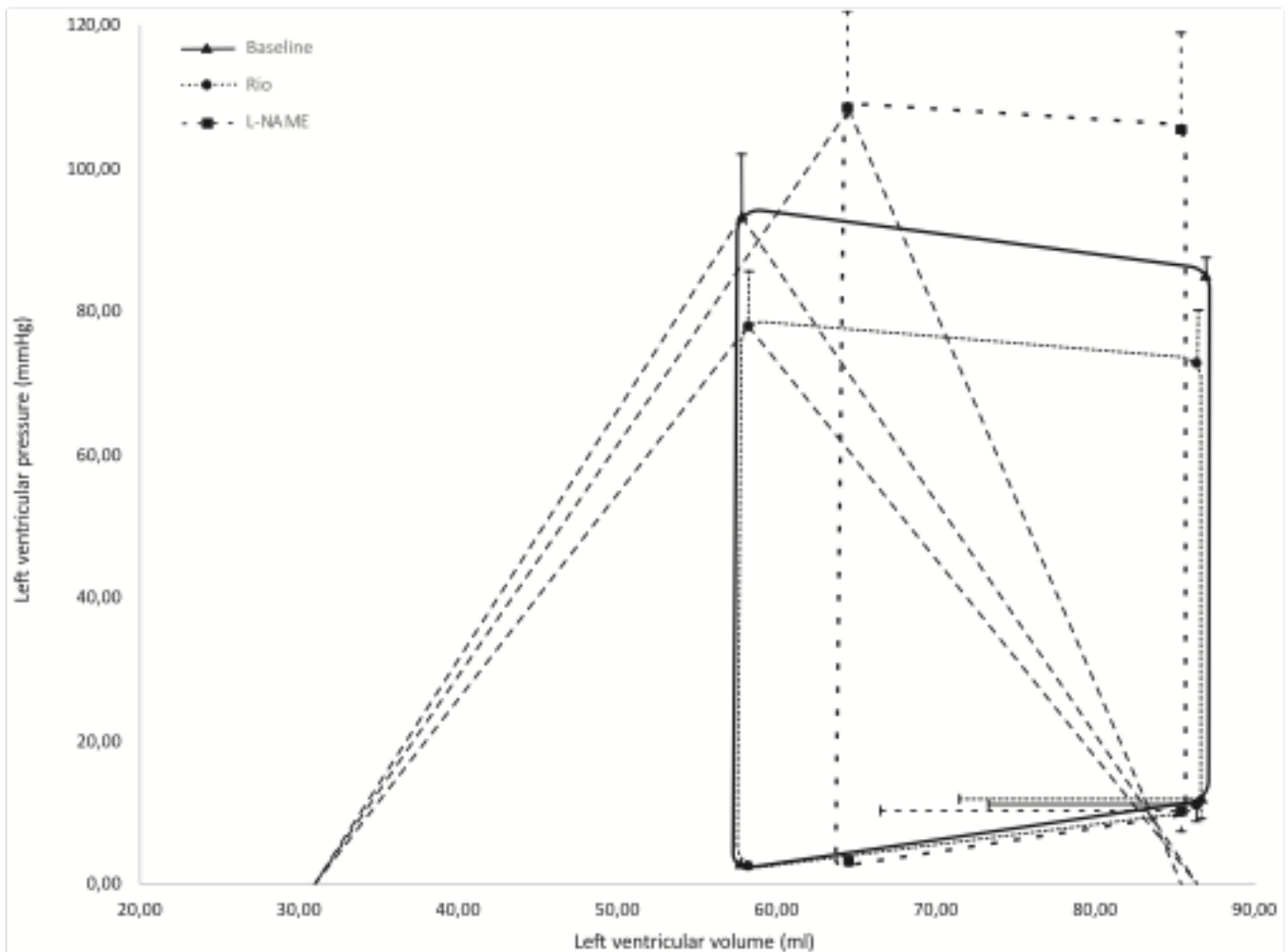


**FIGURE 5** Ventriculoarterial coupling, left ventricle. Schematic pressure–volume curves for the left ventricle based on the average values of the end diastolic pressure–volume relationship (EDPVR), the pressure–volume relationship after isovolumetric contraction, the end systolic pressure–volume relationship, and the pressure–volume relationship at the start of diastole. Curves are fitted through these four points. Also shown is the average volume at the x-axis intercept of the ESPVR line at baseline,  $V_0$ . Left ventricular elastance is the slope of the ESPVR line ( $E_{es}$ ). The slope from the end systolic pressure–volume point to the X-axis intercept of the end-diastolic volume is the aortic elastance ( $E_a$ ). Error bars are standard deviation for pressures and volumes.  $N = 6$

$Ca^{2+}$  levels and myofilament  $Ca^{2+}$  sensitivity. Increasing NO and cGMP levels first induced an increase in contractility followed by a fall at high concentrations (Mohan, Brutsaert, Paulus, & Sys, 1996). In a human study on cardiac failure, on the other hand, blockade of NO synthetase increased inotropic response to  $\beta$ -adrenergic stimulus (Hare, Givertz, Creager, & Colucci, 1998). The complex interaction between the NO-sGC-cGMP-pathway and contractility makes it challenging to predict the exact optimum dose of NO-donors or sGC activators or stimulators when aiming for therapeutically altered contractility.

In our study using sympathetically blocked healthy animals, Riociguat had a predominantly systemic vasodilatory effect. The concomitantly observed hemodynamic effects of the drug can, for a large part, be a consequence of this unloading affect. The effects on contractile function (elastance and PRSW), ventriculoarterial matching ( $E_{es}/E_a$  ratio) and

left ventricular pump efficiency (SW efficiency) were overall minor. The model is therefore well designed to pick up relatively minor direct metabolic or oxygen-consuming effects of test-drugs. Using the same experimental setup, in earlier studies, we have shown that NO-blockade, inotropic drugs and systemic infections have clear metabolic effects in the myocardium evaluated in the frame of an  $MVO_2/PVA$  analysis (Aghajani, Korvald, Nordhaug, Revhaug, & Myrmel, 2004; Aghajani, Nordhaug, et al., 2004; Elvenes et al., 2000; How et al., 2005; Korvald, Elvenes, Ytrebø, Sørli, & Myrmel, 1999; Nordhaug, Steensrud, Korvald, Aghajani, & Myrmel, 2002).

There is consistent evidence that blocking enzymes in the NO pathway causes reduced cardiac efficiency by surplus myocardial oxygen consumption (Chen, Traverse, Du, Hou, & Bache, 2002; Nordhaug et al., 2004; Suto et al., 1998). This is at least partly caused by vasoconstriction and

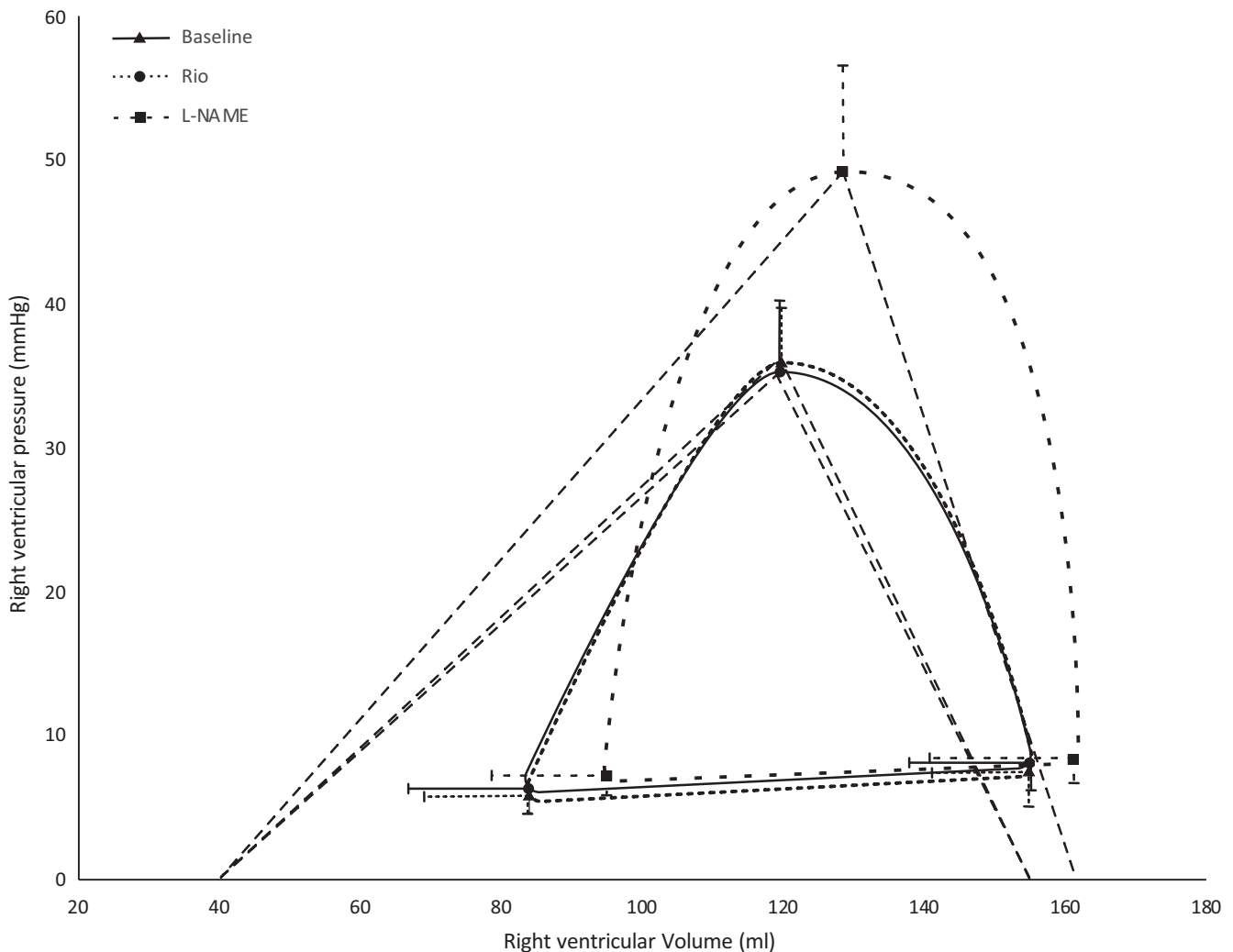


**FIGURE 6** Ventriculoarterial coupling, right ventricle. Schematic pressure–volume curves for the right ventricle based on the average values of the end diastolic pressure–volume relationship (EDPVR), the maximum systolic pressure–volume relationship, and the pressure–volume relationship at the start of diastole. Curves are fitted through these three points. Also shown is the average volume at the x-axis intercept of the end systolic pressure–volume line (ESPVR line) at baseline,  $V_0$ . The slope of the ESPVR line is the right ventricular elastance ( $E_{es}$ ) and the slope from the maximum systolic pressure–volume point to the X-axis intercept of the end diastolic volume is the pulmonary arterial elastance ( $E_a$ ). Error bars are standard deviation for pressures and volumes.  $N = 6$

subsequent disruption of the ventriculoarterial matching by elevated afterload without a concomitant increase in contractility (Nordhaug et al., 2004). The maximum stroke work at a given end-diastolic volume will occur when  $E_{es}$  equals  $E_{ea}$  (Figure 6). Stroke work efficiency (the fraction of total cardiac work, PVA, delivered to the circulation as stroke work), on the other hand, increases as the  $E_{es}/E_{ea}$  ratio increases (Burkhoff & Sagawa, 1986). In these efficient states, a lower proportion of oxygen utilization is metabolized as potential energy (PE), where potential energy is the metabolism necessary to preserve the wall tension of the heart at end-systole. This means that a higher proportion of metabolic oxygen consumption is used for energy transfer to the aorta, and the oxygen cost of stroke work is, therefore, lower (De Tombe, Jones, Burkhoff, Hunter, & Kass, 2017). The correlation between oxygen consumption and ventriculoarterial matching is well

established (Hayashida et al., 1992; Nozawa, Yasumura, & Futaki, 1987), and also holds true in our study with a linear correlation between measured oxygen consumption and PVA.

In addition, NO has a distinct metabolic effect independent of loading conditions (Recchia et al., 1999). Various metabolic studies, as reviewed by Chang, Diers, and Hogg (2015), have demonstrated that the normal NO-tone in tissues reduces the mitochondrial oxygen consumption by reducing the oxygen interaction with cytochrome c oxidase/complex I. However, there is only one study demonstrating a decrease in non-contractile oxygen utilization combined with an unchanged contractile efficiency ( $MVO_2/PVA$ ) after infusion of the NO-precursor l-arginine. In that study the authors also observed the predicted opposite effect by infusion of a NO synthetase inhibitor (Suto et al., 1998). By employing a large animal model (pigs) in our laboratory, we have not been able to reproduce a

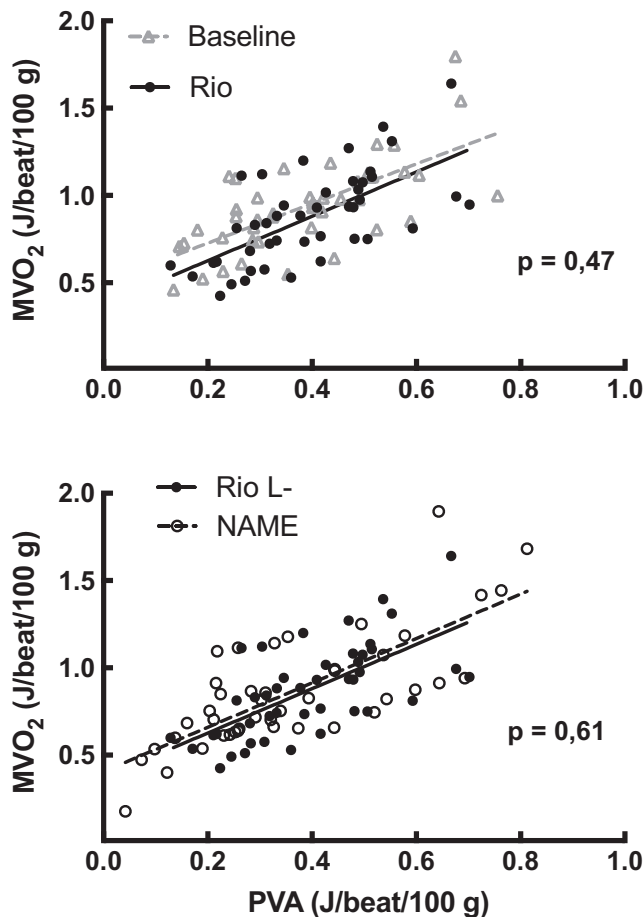


**FIGURE 7** Mechanoenergetic efficiency of the left ventricle. Mechanoenergetic efficiency was calculated as the pressure–volume area (PVA) related to myocardial oxygen consumption ( $MVO_2$ ) at a range of workloads. The panels display the pooled scatter and linear regression of  $MVO_2$ /PVA recordings from six pigs

decrease in basal oxygen requirements in the post ischemic, stunned heart after infusion of l-arginine, even though biochemical assessments demonstrated a substantial turnover of l-arginine to l-citrulline and thus a concomitant production of NO (Andersen, Igumnova, Kildal, & Myrmel, 2012). When studying experimental cardiogenic shock study in our lab, however, L-NAME was shown to increase the basal oxygen requirements in the heart (Nordhaug et al., 2004). The impaired stroke work efficiency induced by L-NAME was not mirrored in our present study, since there was no surplus  $MVO_2$  when L-NAME was given after Riociguat. This is in contrast to the effect of L-NAME given alone in other studies, as this compound has been shown to induce increased unloaded oxygen consumption (Nordhaug et al., 2004; Suto et al., 1998). Of notice, in this study we have not included a separate group of NO-blockade alone (L-NAME) due to the consistent energetic effect observed with this intervention.

Our study shows that Riociguat given to healthy animals has only a minor effect in the pulmonary circulation with no impact on the right ventriculo-pulmonary arterial coupling.

Riociguat (Adempas®) has been approved for treatment in pulmonary hypertension based on pulmonary vasodilatory effects in animal disease models and human studies. The effect of this sGC stimulator is therefore different in healthy and diseased lung vasculature.

## 5 | CONCLUSION

Riociguat alone has no effect on myocardial oxygen consumption in the healthy heart. Both ventriculoarterial coupling and basal myocardial oxygen metabolism are unaffected by infusion of 100  $\mu\text{g}/\text{kg}$  Riociguat. However, the subsequent administration of L-NAME did not increase the relative oxygen consumption in the myocardium, and this suggests that the expected surplus basal  $MVO_2$  in the heart after blocking the endogenous NO-tone by L-NAME was attenuated by this dose of Riociguat. This oxygen-conserving effect during L-NAME stimulation indicates that Riociguat can induce “metabolic protection” in stressed myocardium and potentially also in pathological states. Such a potential should be explored in experimental disease models and during various pharmacological combinations.

## 6 | DATA SHARING NOTICE

The data used for the study can be shared upon personal contact with the authors.

## ACKNOWLEDGMENTS

Thanks to the laboratory technicians in the cardiovascular research laboratory at the Arctic University in Tromsø.

## CONFLICT OF INTEREST

None of the authors has any conflicts of interest.

## AUTHOR CONTRIBUTIONS

Torvind Næsheim: Drafting protocol, sourcing medications, setting up the lab, instrumentation, data collection, analysis, and authoring; Ole-Jakob How: Idea, analysis, authoring; Truls Myrmel: Idea, drafting protocol, instrumentation, data collection, analysis, and authoring.

## ETHICAL STATEMENT

The research complies with the ethical guidelines of animal research as given by the the Norwegian Animal Research Authority. The protocol was approved in advance with the reference number FDF 2012/55972.

## ORCID

Torvind Næsheim  <https://orcid.org/0000-0002-6294-3667>

Ole-Jakob How  <https://orcid.org/0000-0003-1495-0413>

Truls Myrmel  <https://orcid.org/0000-0002-4148-9223>

## REFERENCES

- Aghajani, E., Korvald, C., Nordhaug, D., Revhaug, A., & Myrmel, T. (2004). Increased oxygen cost of contractility in the endotoxemic porcine left ventricle. *Scandinavian Cardiovascular Journal*, 38(3), 187–192. <https://doi.org/10.1080/14017430410031164>
- Aghajani, E., Nordhaug, D., Korvald, C., Steensrud, T., Husnes, K., & Ingebretsen, O. ... Myrmel, T. (2004). Mechanoenergetic inefficiency in the septic left ventricle is due to enhanced oxygen requirements for excitation-contraction coupling. *Cardiovascular Research*, 63(2), 256–263. <https://doi.org/10.1016/j.cardiores.2004.04.019>
- Andersen, I. A., Igumnova, E., Kildal, A. B., & Myrmel, T. (2012). Reassessment of a suggested pharmacological approach to heart failure: L-arginine is only a marginal NO donor in pigs. *Journal of Cardiovascular Pharmacology*, 60(3), 262–268. <https://doi.org/10.1097/FJC.0b013e31825de0bf>
- Braunwald, E. (1969). Thirteenth bowditch lecture the determinants of myocardial oxygen consumption. *Physiologist*, 12(2), 65–93.
- Burkhoff, D., & Sagawa, K. (1986). Ventricular efficiency predicted by an analytical model. *American Journal of Physiology-Regulatory, Integrative and Comparative Physiology*, 250(6), R1021–R1027. <https://doi.org/10.1152/ajpregu.1986.250.6.R1021>
- Chang, C.-F., Diers, A. R., & Hogg, N. (2015). Cancer cell metabolism and the modulating effects of nitric oxide. *Free Radical Biology and Medicine*, 79, 324–336. <https://doi.org/10.1016/j.freeradbiomed.2014.11.012>
- Chen, Y., Traverse, J. H., Du, R., Hou, M., & Bache, R. J. (2002). Nitric oxide modulates myocardial oxygen consumption in the failing heart. *Circulation*, 106(2), 273–279. <https://doi.org/10.1161/01.CIR.0000021120.90970.B9>
- De Tombe, P. P., Jones, S., Burkhoff, D., Hunter, W. C., & Kass, D. A. (2017). Ventricular stroke work and efficiency both remain nearly optimal despite altered vascular loading. *American Journal of Physiology-Heart and Circulatory Physiology*, 264(6), H1817–H1824. <https://doi.org/10.1152/ajpheart.1993.264.6.H1817>
- Douglas W. W. (1952). The effect of a ganglion-blocking drug, hexamethonium, on the response of the cat's carotid body to various stimuli. *The Journal of Physiology*, 118, (3), 373–383. <http://dx.doi.org/10.1113/jphysiol.1952.sp004801>
- Elvenes, O. P., Korvald, C., Ytrebø, L. M., Irtun, Ø., Myrmel, T., & Larsen, T. S. (2000). Myocardial metabolism and efficiency after warm continuous blood cardioplegia. *The Annals of Thoracic Surgery*, 69(6), 1799–1805. [https://doi.org/10.1016/S0003-4975\(00\)01107-3](https://doi.org/10.1016/S0003-4975(00)01107-3)
- Farber, H. W., Miller, D. P., Poms, A. D., Badesch, D. B., Frost, A. E., Rouzic, E. M. -L., ... Benza, R. L. (2015). Five-Year outcomes of patients enrolled in the REVEAL Registry. *Chest*, 148(4), 1043–1054. <https://doi.org/10.1378/chest.15-0300>
- Feneley M. P., Elbeery J. R., Gaynor J. W., Gall S. A., Davis J. W., Rankin J. S. (1990). Ellipsoidal shell subtraction model of right ventricular volume. Comparison with circular free wall dimensions as indexes of right ventricular function. *Circulation Research*, 67, (6), 1427–1436. <http://dx.doi.org/10.1161/01.res.67.6.1427>
- Galiè, N., Ghofrani, H. A., Torbicki, A., Barst, R. J., Rubin, L. J., Badesch, D., ... Simonneau, G. (2005). Sildenafil citrate therapy for pulmonary arterial hypertension. *New England Journal of Medicine*, 353(20), 2148–2157. <https://doi.org/10.1056/NEJMoa050010>
- Ghofrani, H.-A., Humbert, M., Langleben, D., Schermuly, R., Stasch, J.-P., Wilkins, M. R., & Klinger, J. R. (2017). Riociguat: Mode of action and clinical development in pulmonary hypertension. *Chest*, 151(2), 468–480. <https://doi.org/10.1016/j.chest.2016.05.024>
- Hare, J. M., Givertz, M. M., Creager, M. A., & Colucci, W. S. (1998). Increased sensitivity to nitric oxide synthase inhibition in patients with heart failure: Potentiation of  $\beta$ -adrenergic inotropic responsiveness. *Circulation*, 97(2), 161–166. <https://doi.org/10.1161/01.CIR.97.2.161>
- Hayashida, K., Sunagawa, K., Noma, M., Sugimachi, M., Ando, H., & Nakamura, M. (1992). Mechanical matching of the left ventricle with the arterial system in exercising dogs. *Circulation Research*, 71(3), 481–489. <https://doi.org/10.1161/01.RES.71.3.481>
- Hoepfer, M. M., Simonneau, G., Corris, P. A., Ghofrani, H.-A., Klinger, J.R., Langleben, D., ... Benza, R.L. (2017). RESPITE: Switching to riociguat in pulmonary arterial hypertension patients with inadequate response to phosphodiesterase-5 inhibitors. *European Respiratory Journal*, 50(3). <https://doi.org/10.1183/13993003.02425-2016>
- How, O., Aasum, E., Kunnathu, S., Severson, D. L., Myhre, E. S. P., & Larsen, T. S. (2005). Influence of substrate supply on cardiac efficiency, as measured by pressure-volume analysis in ex vivo mouse hearts. *American Journal of Physiology-Heart and Circulatory Physiology*, 288(6), H2979–H2985. <https://doi.org/10.1152/ajpheart.00084.2005>
- Korvald C., Elvenes O. P., & Myrmel T. (2000). Myocardial substrate metabolism influences left ventricular energetics in vivo. *American Journal of Physiology-Heart and Circulatory Physiology*, 278, (4), H1345–H1351. <http://dx.doi.org/10.1152/ajpheart.2000.278.4.h1345>
- Korvald C, Elvenes O. P., Ytrebø L. M., Sørliie D. G., & Myrmel T. (1999). Oxygen-wasting effect of inotropy in the “virtual work model”. *American Journal of Physiology-Heart and Circulatory Physiology*, 276, (4), H1339–H1345. <http://dx.doi.org/10.1152/ajpheart.1999.276.4.h1339>
- Kylhammar, D., Kjellström, B., Hjalmarsson, C., Jansson, K., Nisell, M., Söderberg, S., ... Rådegran, G. (2018). A comprehensive risk stratification at early follow-up determines prognosis in pulmonary arterial hypertension. *European Heart Journal*, 39(47), 4175–4181. <https://doi.org/10.1093/eurheartj/ehx257>
- Lang, M., Kojonazarov, B., Tian, X., Kalymbetov, A., Weissmann, N., Grimminger, F., ... Schermuly, R. T. (2012). The soluble guanylate cyclase stimulator riociguat ameliorates pulmonary hypertension induced by hypoxia and SU5416 in rats. *PLoS One*, 7(8), 1–9. <https://doi.org/10.1371/journal.pone.0043433>
- Loke K. E., McConnell P. I., Tuzman J. M., Shesely E. G., Smith C. J., Stackpole C. J., ... Hintze T. H. (1999). Endogenous Endothelial Nitric Oxide Synthase-Derived Nitric Oxide Is a Physiological Regulator of Myocardial Oxygen Consumption. *Circulation Research*, 84, (7), 840–845. <http://dx.doi.org/10.1161/01.res.84.7.840>
- Mohan, P., Brutsaert, D. L., Paulus, W. J., & Sys, S. U. (1996). Myocardial contractile response to nitric oxide and cGMP. *Circulation*, 93(6), 1223–1229. <https://doi.org/10.1161/01.CIR.93.6.1223>
- Morimont, P., Lambermont, B., Ghuysen, A., Gerard, P., Kolh, P., Lancellotti, P., ... D'Orto, V. (2008). Effective arterial elastance as an index of pulmonary vascular load. *American Journal of Physiology-Heart and Circulatory Physiology*, 294(6), 2736–2742. <https://doi.org/10.1152/ajpheart.00796.2007>
- Müller S, How O.-J., Jakobsen Ø., Hermansen S. E., Røsner A., Stenberg T. A., & Myrmel T. (2010). Oxygen-Wasting Effect of Inotropy. *Circulation: Heart Failure*, 3, (2), 277–285. <http://dx.doi.org/10.1161/circheartfailure.109.865519>



- Myrmel, T., & Korvald, C. (2000). New aspects of myocardial oxygen consumption. Invited review. *Scandinavian Cardiovascular Journal*, 34(3), 233–241. <https://doi.org/10.1080/713783125>
- Næsheim, T., O. J. How, and T. Myrmel. 2020. Hemodynamic effects of a soluble guanylate cyclase stimulator, riociguat, and an activator, cinaciguat, during NO-modulation in healthy pigs. *Journal of Cardiovascular Pharmacology*. <https://doi.org/10.1177/1074248420940897>.
- Nordhaug D., Steensrud T., Aghajani E., Korvald C., & Myrmel T. (2004). Nitric oxide synthase inhibition impairs myocardial efficiency and ventriculo-arterial matching in acute ischemic heart failure. *European Journal of Heart Failure*, 6, (6), 705–713. <http://dx.doi.org/10.1016/j.ejheart.2003.11.010>.
- Nordhaug, D., Steensrud, T., Korvald, C., Aghajani, E., & Myrmel, T. (2002). Preserved myocardial energetics in acute ischemic left ventricular failure – studies in an experimental pig model. *European Journal of Cardio-Thoracic Surgery*, 22(1), 135–142. [https://doi.org/10.1016/S1010-7940\(02\)00201-4](https://doi.org/10.1016/S1010-7940(02)00201-4)
- Nozawa, T., Yasumura, Y., Futaki, S., Tanaka, N., Igarashi, Y., Goto, Y., & Suga, H. (1987). Relation between oxygen consumption and pressure-volume area of in situ dog heart. *American Journal of Physiology-Heart and Circulatory Physiology*, 253(1), H31–H40. <https://doi.org/10.1152/ajpheart.1987.253.1.H31>
- Recchia F (1999). Nitric oxide controls cardiac substrate utilization in the conscious dog. *Cardiovascular Research*, 44, (2), 325–332. [http://dx.doi.org/10.1016/s0008-6363\(99\)00245-x](http://dx.doi.org/10.1016/s0008-6363(99)00245-x).
- Rees, D. D., Palmer, R. M. J., Schulz, R., Hodson, H. F., & Moncada, S. (1990). Characterization of three inhibitors of endothelial nitric oxide synthase in vitro and in vivo. *British Journal of Pharmacology*, 101(3), 746–752. <https://doi.org/10.1111/j.1476-5381.1990.tb14151.x>
- Suto N., Mikuniya A., Okubo T., Hanada H, Shinozaki N, & Okumura K. (1998). Nitric oxide modulates cardiac contractility and oxygen consumption without changing contractile efficiency. *American Journal of Physiology-Heart and Circulatory Physiology*, 275, (1), H41–H49. <http://dx.doi.org/10.1152/ajpheart.1998.275.1.h41>.
- Thoonen, R., Cauwels, A., Decaluwe, K., Geschka, S., Tainsh, R. E., Delanghe, J., ... Brouckaert, P. (2015). Cardiovascular and pharmacological implications of haem-deficient NO-unresponsive soluble guanylate cyclase knock-in mice. *Nature Communications*, 6, 8482. <https://doi.org/10.1038/ncomms9482>
- Vanderpool, R. R., Pinsky, M. R., Naeije, R., Deible, C., Kosaraju, V., Bunner, C., ... Simon, M. A. (2015). RV-pulmonary arterial coupling predicts outcome in patients referred for pulmonary hypertension. *Heart*, 101(1), 37–43. <https://doi.org/10.1136/heartjnl-2014-306142>
- Vasu M. A., O'Keefe D. D., Kapellakis G. Z., Vezeridis M. P., Jacobs M. L., Daggett W. M., & Powell W. J. (1978). Myocardial oxygen consumption: effects of epinephrine, isoproterenol, dopamine, norepinephrine, and dobutamine. *American Journal of Physiology-Heart and Circulatory Physiology*, 235, (2), H237–H241. <http://dx.doi.org/10.1152/ajpheart.1978.235.2.h237>.
- Vonk-Noordegraaf A., Haddad F., Chin K. M., Forfia P. R., Kawut S. M., Lumens J., ... , Hassoun P. M. (2013). Right Heart Adaptation to Pulmonary Arterial Hypertension. *Journal of the American College of Cardiology*, 62, (25), D22–D33. <http://dx.doi.org/10.1016/j.jacc.2013.10.027>.
- Yao, L., Xue, X., Yu, P., Ni, Y., & Chen, F. (2018). Evans blue dye: A revisit of its applications in biomedicine. *Contrast Media & Molecular Imaging*, 2018, 18–24. <https://doi.org/10.1155/2018/7628037>

**How to cite this article:** Næsheim T, How O-J, Myrmel T. The effect of Riociguat on cardiovascular function and efficiency in healthy, juvenile pigs. *Physiol Rep*. 2020;8:e14562. <https://doi.org/10.14814/phy2.14562>

## 13.2 Paper 4



The effect of Riociguat and Cinaciguat on liver blood flow during NO-modulation

The effect of Riociguat and Cinaciguat on liver blood flow in healthy anesthetized pigs during NO-modulation

Authors

Torvind Næsheim: Drafting protocol, sourcing medications, setting up the lab, instrumentation, data collection, analysis, authoring

Ole-Jakob How: Analysis, authoring

Truls Myrmel: Idea, drafting protocol, instrumentation, data collection, analysis, authoring

Affiliation

Cardiovascular Research Group, Department of Clinical Medicine (TN, TM), and Department of Medical Biology (OJH), Faculty of Health Sciences, UiT The Arctic University of Norway, Tromsø, Norway.

Department of Cardiothoracic and Vascular Surgery, Heart and Lung Clinic, University Hospital of North Norway, Tromsø, Norway (TM). Department of Anesthesiology, University Hospital of North Norway, Tromsø, Norway (TN).

Address for Correspondence

Truls.Myrmel@uit.no



## Abstract

This study investigates the effect of Riociguat, a soluble guanylate cyclase stimulator, and Cinaciguat, a soluble guanylate cyclase activator, on the blood flow through the liver in healthy, juvenile pigs (n=22). To unmask a potentially direct hepatovascular effect of the drugs, NO-tone was blocked using the NO-synthetase inhibitor L-NAME. Flow measurements in the hepatic artery and portal vein, and pressure measurements in the same vessels in addition to the caval vein and lobular liver veins allowed us to evaluate specific resistances in the different parts of the liver circulation. Using microsonometric measurements of liver dimensions and integration of liver blood inflow during occlusion of liver blood outflow, liver compliance and capacitance could be calculated. The pigs were treated with the ganglion blocker hexamethonium to avoid reflectory tachcardia.

Cinaciguat, but not Riociguat given in the highest tolerable doses to avoid hypotension in these healthy juvenile, anesthetized pigs, reduced the arterio-venous resistance through the liver, and reversed the increase in arterio-venous resistance induced by L-NAME. None of the drugs altered the porto-venous resistance, but pre-treatment with Cinciguat or Riociguat blocked the vasoconstrictive effect of NO-blockade on the portal vein flow. None of the drugs changed liver compliance, but Riociguat resulted in a slight reduction of liver capacitance.

The results demonstrates the known systemic arterial effect of these drugs. Also, their anagonistic effect on NO-blocade in the portal circulation show that these vessels do have a pharmacological response to both Riociguat and Cinaciguat.

## Introduction

Soluble guanylate cyclase activators and stimulators represent a new class of vasodilators working independently or in concert with NO to stimulate soluble guanylate cyclase. The effect of these drugs on venous vascular tone is unknown. Previous studies have shown a physiological NO tone in the portal vein, indicating that drugs acting through cGMP might alter liver blood flow<sup>1,2</sup>. We have previously demonstrated that the soluble guanylate cyclase stimulator Riociguat and the activator Cinaciguat both have vasodilating effects in healthy pigs, mainly in the systemic arterial vasculature<sup>3</sup>. Here we addressed their potential impact on both the hepatic arterial and portal liver circulation. From our previous studies, we hypothesized an apparent vasodilating effect on the hepatic artery and no or modest impact on the portal vein. To assess their interaction with NO, we addressed both drugs' effects in concert with the NO-blocker L-NAME. Finally, we have used a liver outflow occlusion model<sup>4</sup> to assess their effect on liver compliance and capacitance i.e. their potential effect on the blood reservoir in the liver.

## Material and methods

### Experimental animals

Twenty-two castrated male domestic pigs weighing  $30 \pm 5$  kg were adapted to the Animal Department for 5–7 days and fasted overnight before experiments, with free access to water.

The experimental protocol was approved by the local steering committee of the National Animal Research Authority located at the Faculty of Health Sciences, UIT, The Arctic University of Norway. The FDF reference is 2012/55972.

### Surgical preparation and instrumentation

The pigs were premedicated with an intramuscular injection of 20 mg/kg ketamine (Pfizer AS, Oslo, Norway) and 1 mg of atropine (Nycomed Pharma, Oslo, Norway). Anesthesia was induced by intravenous injection of 10 mg/kg pentobarbital sodium (Abbott, Stockholm, Sweden) and 0.01 mg/kg fentanyl (Hameln Pharmaceuticals, Hameln, Germany). The animals were normo ventilated after intubation. Normo ventilation was defined as an arterial PaCO<sub>2</sub> of  $40 \pm 2$  mmHg. A central venous catheter was placed through the left internal jugular vein. Anesthesia was maintained throughout the experiment by a continuous infusion of 4mg/kg/h pentobarbitone sodium, 0.02 mg/kg/h fentanyl, and 0.3 mg/kg/h midazolam (B. Braun, Melsungen, Germany). The circulating volume was maintained by a 20 mL/kg/h continuous infusion of 0.9% NaCl supplemented with 1.25 g/L glucose. The animals received 2500 IU of heparin and 5mg/kg amiodarone (Sanofi-Synthelabo, Stockholm, Sweden) to avoid blood clotting of catheters and to prevent cardiac arrhythmias. Hexamethonium chloride (Sigma-Aldrich, Missouri, USA, 15 mg/kg) was administered to prevent autonomous reflexes and single out vascular effects during interventions and measurements <sup>5</sup>.

Central venous pressure was measured by a vascular catheter placed in the right atrium. The systemic arterial pressure was assessed from a vascular catheter in the abdominal aorta. A 50 cc IABP (Intra Aortic Balloon Pump) balloon catheter (Teleflex, North Carolina, USA) was introduced into the inferior caval vein and positioned just below the right atrium for intermittent preload reduction and

## The effect of Riociguat and Cinaciguat on liver blood flow during NO-modulation

occlusion of hepatic venous outflow (Figure 1). The pigs then underwent laparotomy, and the hepatic artery and portal vein were isolated. Occluders were placed on these vessels for calibration of zero flow. Snug-fitting transit time flow probes (Transonic) were then placed on both vessels (Typically 12 mm on vena porta and 4 mm on arteria hepatica). Four 2-mm Tac micro sonometry crystals (Sonometrics Corporation, Ontario, Canada) were placed in a subcapsular position through a stab wound and sewn to the liver's capsule in two different lateral liver lobes. Dhep1 and Dhep2 are two hepatic dimensions (C1 to C2 and C3 to C4 in figure 1), measured in lobes in the hepatic lobar vein catheter in the region the thickest parts of these lobes.

Through an introducer in the internal jugular vein on the right side, a general-purpose 6 Fr angiography catheter (Cordis, California, USA) was placed with the guidance of contrast fluoroscopy into the hepatic vein in the area of the micro sonometric crystals. The catheter was wedged and then retracted 5-7 centimeters to a position close to the division to the inferior caval vein. Free flow around the catheter was confirmed through contrast injection. A 2 Fr micro manometric catheter (ADI instruments, Colorado, USA) was then placed through the angiography catheter ending 5 cm distal to the tip of this catheter. Total occlusion of hepatic venous flow was confirmed through injection of contrast in the hepatic vein during inflation of the IABP balloon.

At the end of the experiment, the heart was stopped by injection of 20 mmol KCl (1 mmol/ml).

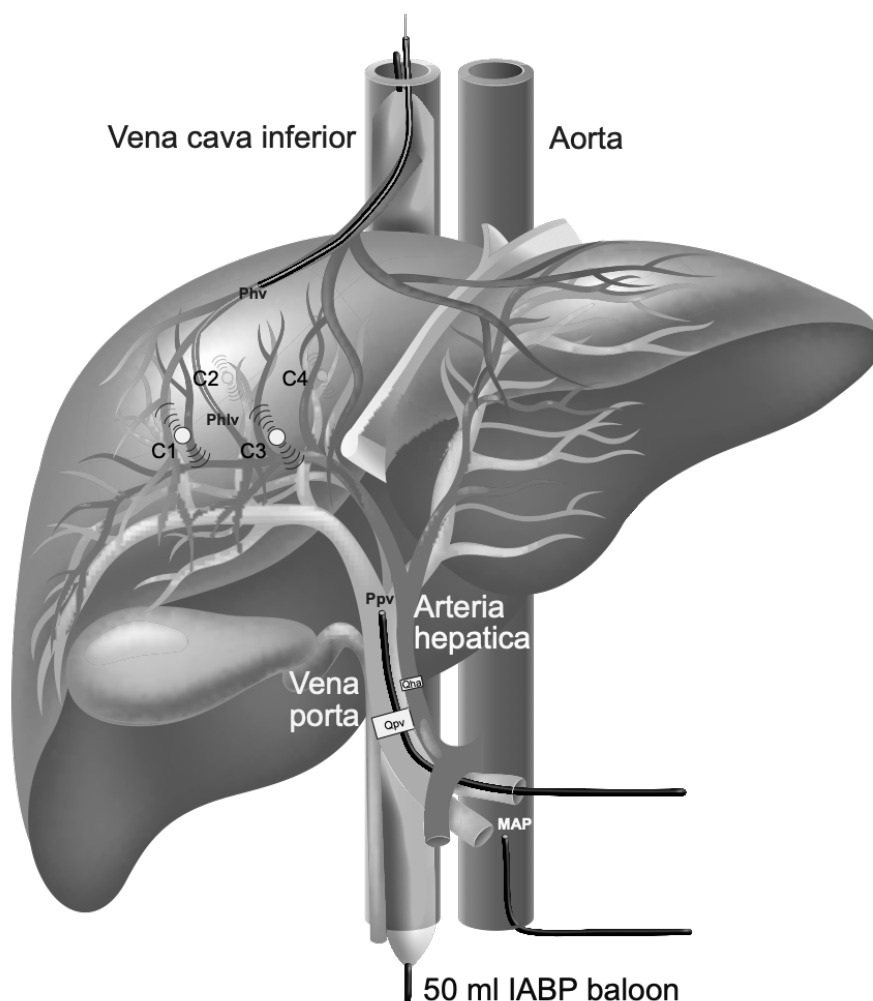


Figure 1. C1, C2, C3, and C4 are microsonometric crystals,  $Q_{pv}$  is the flow in the portal vein,  $Q_{ha}$  is the flow in the hepatic artery.  $P_{pv}$  is the pressure in the portal vein,  $P_{hv}$  is the pressure in the hepatic veins,  $P_{hlv}$  is the pressure in a hepatic lobulus vein. MAP (Mean arterial pressure) is the pressure in aorta.

## Calculations

$P_{pv}$  is the portal vein pressure measured by the catheter in the portal vein just proximal to the liver boundary.  $P_{hv}$  is the pressure of a hepatic vein just proximal to the inlet in the inferior caval vein.  $P_{hlv}$  is the pressure in the hepatic lobar vein measured by the micro-manometry catheter in a hepatic lobulus close to the placements of the micro sonometric crystals.  $Q_{ha}$  is the hepatic arterial flow,  $Q_{pv}$  is the flow in the portal vein.

Portal venous resistance is calculated as

$$PVR_{ResHep} = \frac{P_{pv} - P_{hv}}{Q_{pv}}$$

## The effect of Riociguat and Cinaciguat on liver blood flow during NO-modulation

Hepatic arterial resistance is calculated as

$$AVResHep = \frac{MAP - P_{hv}}{Q_{ha}}$$

Liver compliance was calculated as the linear regression between liver volume change and liver lobular pressure change during liver vein occlusion.

$$Compliance_n = \frac{\int_0^n (Q_{pv} + Q_{ha})}{Phlv_n - Phlv_0}$$

Baseline hepatic blood volume is set arbitrarily to 17,5 ml/kg BW<sup>6</sup>. All calculations of subsequent blood volumes are relative to this baseline value. During occlusion of liver outflow, the increase in hepatic dimensions is considered to represent hepatic blood volume increase. By plotting the change in dimensions against the integral of the hepatic inflow via vena porta and the hepatic artery, the calibration factor between liver thickness changes and liver blood volume changes is obtained. The constant between hepatic dimensions and the integral of hepatic inflow during venous occlusion (liver compliance),  $k$  was calculated by linear regression of  $k_n$  for the duration of venous occlusion.  $D_n$  is the mean of the two liver dimensions at timepoint  $n$ ,  $D_0$  is the mean of the two liver dimensions at the baseline of the experiment.

$$k_n = \frac{D_n - D_0}{\int_0^n (Q_{pv} + Q_{ha})}$$

The instantaneous liver blood volume per kg at the timepoint  $n$  ( $LBV_n$ ) was calculated as:

$$LBV_n = 17,5 + \frac{(D_n - D_0)k}{W}$$

$W$  is the pigs' body weight at baseline.

The liver blood volumes based on sonometric measurements of the dimensions could then be used to construct pressure-volume curves of liver volume against hepatic liver lobulus pressure ( $Phlv$ ) during

## The effect of Riociguat and Cinaciguat on liver blood flow during NO-modulation

liver vein occlusions. The slope (compliance) and y-intercept (capacitance) of these curves were then calculated by logistic regression.

### Experimental drugs

Riociguat was obtained from ChemOKI (Synthesi-TECH, Jiangsu, China) as a dry powder. pH neutral solutions were prepared with DMSO (dimethylsulfoxide) and a 1:1 solution of Transcutol, Diethylene glycol ethyl ether (Sigma-Aldrich, Missouri, USA), and Cremophor, macrogolglycerol ricinoleate (Sigma-Aldrich Missouri, USA). We used 5% Transcutol and Chremophor solutions, and the volume ratio between DMSO, Transcutol, and Chremophor was 0,05:2,5:2,5. This solution was then further diluted with 0,9 mg/mL NaCl to a final concentration of test drug of 0,01 to 0,1 mg/mL depending on the dose to be given. The maximum DMSO concentration was 0,02%. L-NAME, N-omega-nitro-L-arginine methyl ester, was used as a nitric oxide synthetase inhibitor<sup>7</sup>. Doses were chosen on the basis of a previous dose-response-study to yield a maximum tolerated fall in systemic pressure to MAP 50 mmHg<sup>8</sup>.

## Experimental protocol

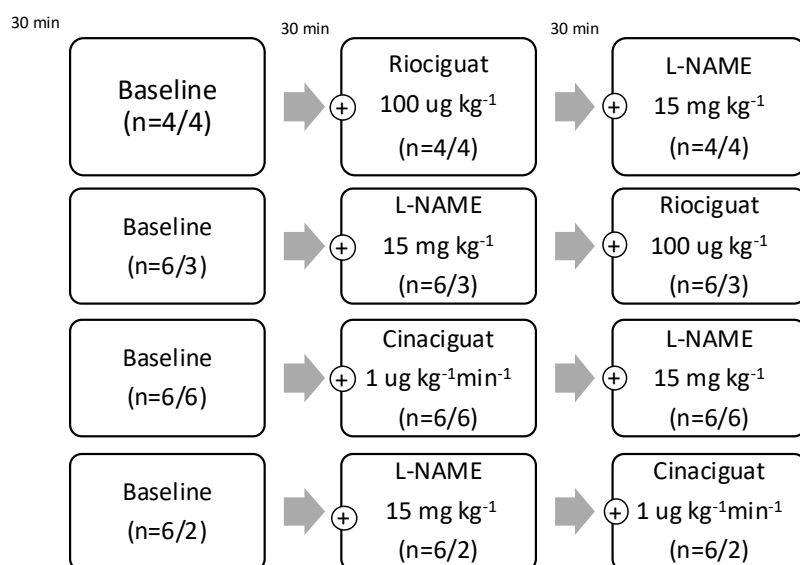


Figure 2. Experimental protocol. The first number of *n* is the number of animals with hepatic flow and pressure data. The second number after *n* is the number of animals with additional micro sonometry data and estimation of hepatic capacitance and compliance. Thirty minutes was allowed for stabilization after instrumentation and between interventions and data sampling.

The experiments were conducted using a repeated measurement design. Following surgery, the pigs were allowed to rest for 30 min before baseline measurements. Drugs were then given per protocol with time to equilibration between each measurement. At each time point, basic hemodynamic data, data on liver dimensions, pressures, and flows were sampled. Inflation of the IABP balloon provided data for analysis of integrated liver inflow and dimension data during liver vein occlusion.

## Registration of data and analysis

Data were sampled, digitized, and analyzed (using ADI LabChart Pro software v 8.1.8, Dunedin, New Zealand). Cardiac output (CO) was obtained from thermodilution with the hardware Vigilance (Medtronic, Minnesota, USA)

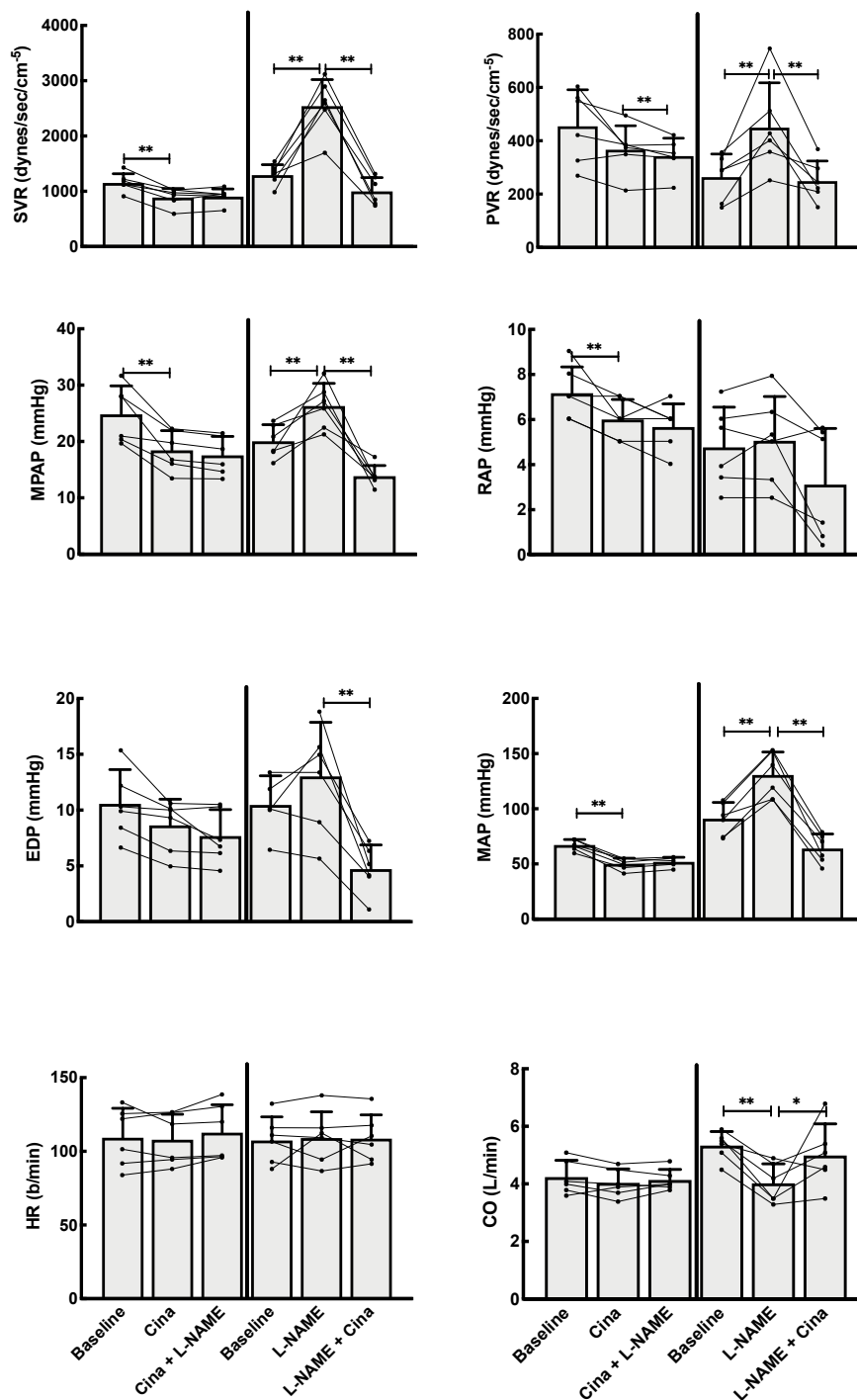


The effect of Riociguat and Cinaciguat on liver blood flow during NO-modulation

### Statistical analysis

The data are expressed as the mean and standard deviation (SD). A linear mixed model<sup>9</sup> with pig identity as random effect and combinations of medications as the fixed effect was used to compare physiological values. The autoregressive correlation structure was modeled to have the best fit. P-values <0.05 were regarded as statistically significant. All statistical analyses were conducted in SPSS 25.0 (Chicago, IL, USA).

## Results



dru

Figure 3. General hemodynamics in 12 pigs after Cinaciguat (Cina) in combination with N omega-Nitro-L-arginine methyl ester hydrochloride (L-NAME). SVR is systemic vascular resistance, PVR is pulmonary vascular resistance, MAP is mean arterial pressure, MPAP is mean pulmonary arterial pressure, EDP is the end-diastolic pressure in the left ventricle, RAP is the right atrial pressure, HR is heart rate, and CO is cardiac output. \* is p-value < 0,05 and \*\* is p-value < 0,005 after mixed models regression with pig identity as random effect.

The effect of Riociquat and Cinaciguat on liver blood flow during NO-modulation

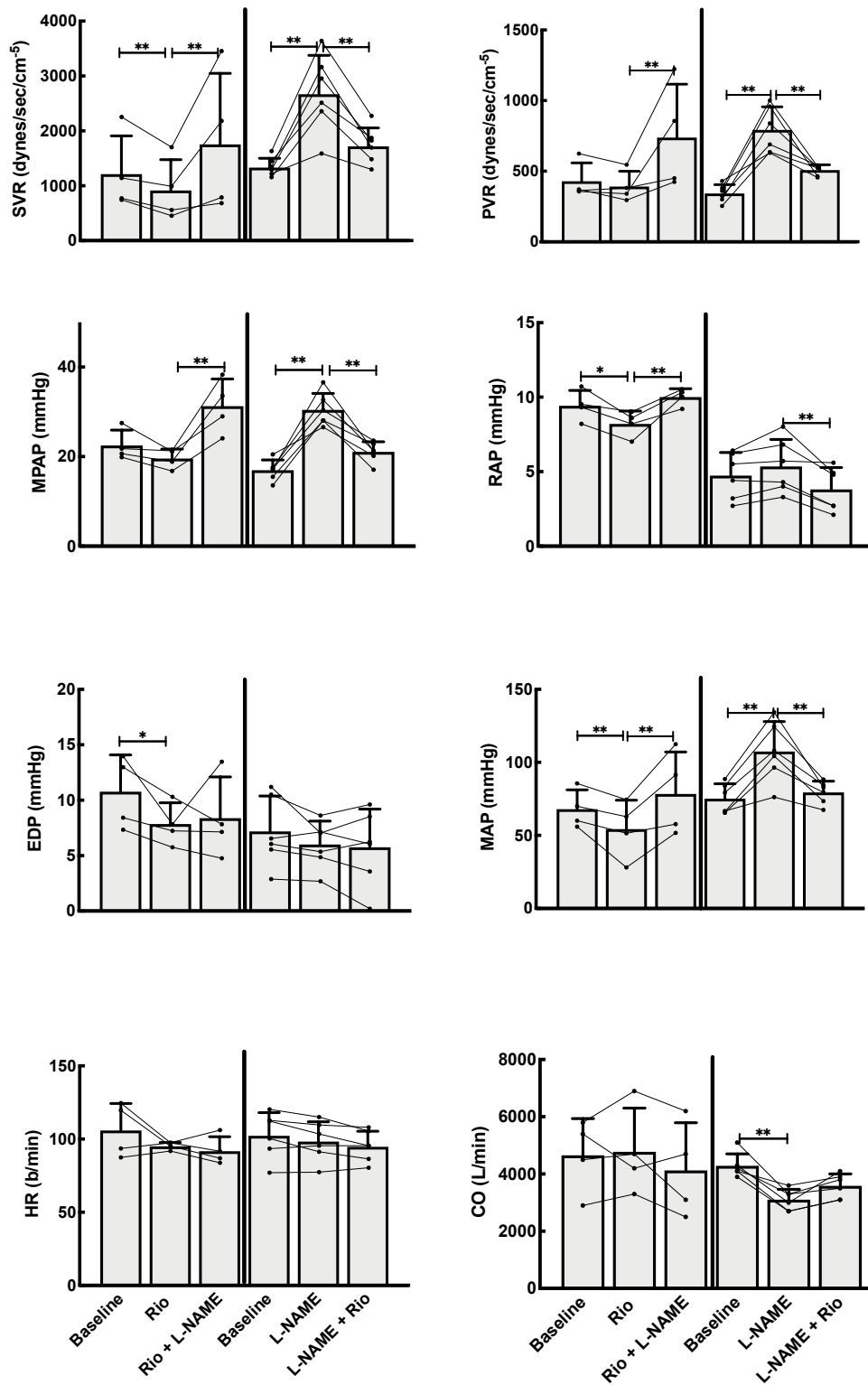


Figure 4. General hemodynamics in 10 pigs after Riociquat (Rio) in combination with N omega-Nitro-L-arginine methyl ester hydrochloride (L-NAME). SVR is systemic vascular resistance, PVR is pulmonary vascular resistance, MAP is mean arterial pressure, MPAP is mean pulmonary arterial pressure, EDP is the end-diastolic pressure in the left ventricle, RAP is the right atrial pressure, HR is heart rate, and CO is cardiac output. \* is p-value < 0,05 and \*\* is p-value < 0,005 after mixed models regression with pig identity as random effect.

## The effect of Riociguat and Cinaciguat on liver blood flow during NO-modulation

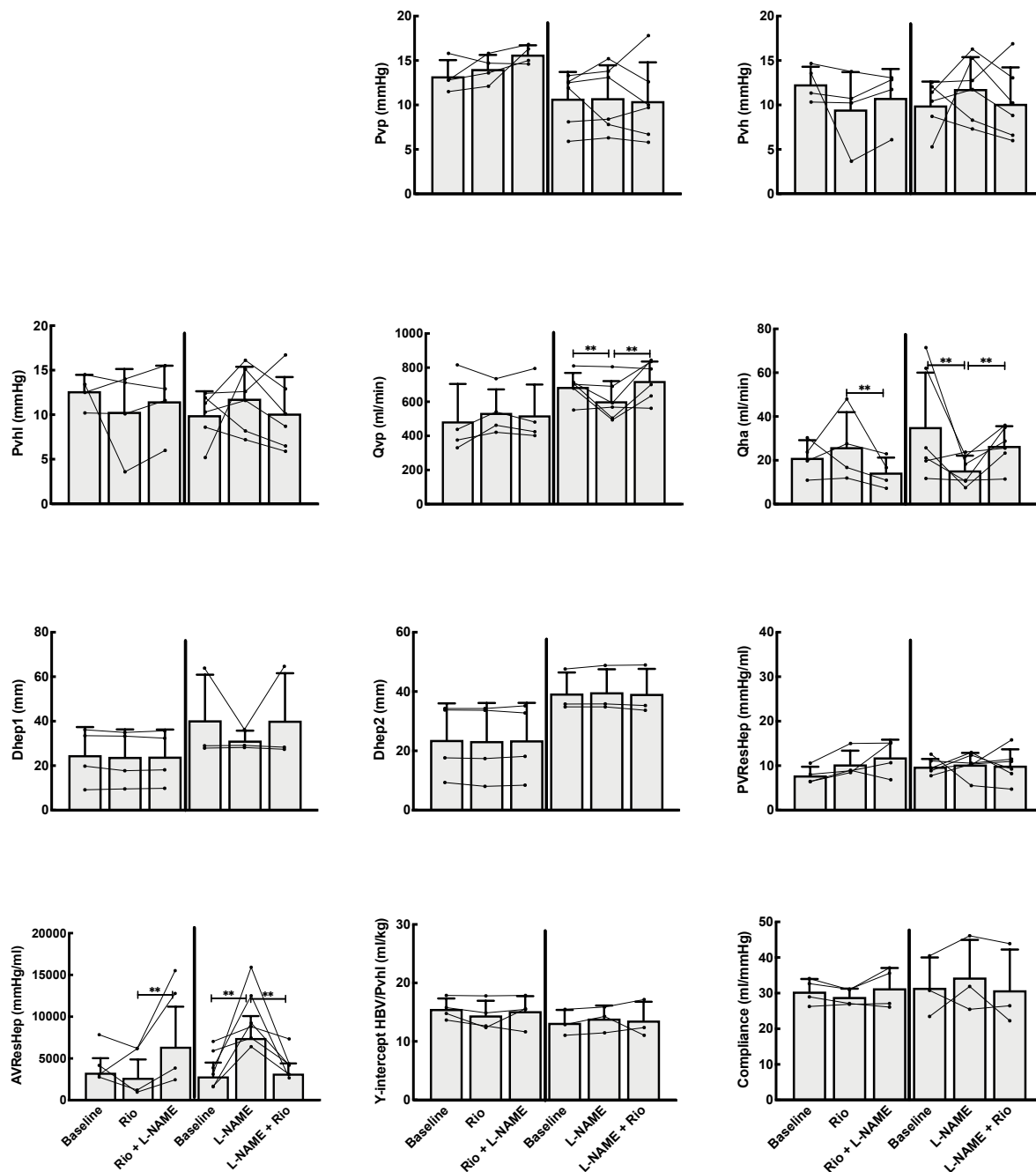


Figure 5. Liver hemodynamics in 10 pigs after Riociguat (Rio) in combination with *N* omega-Nitro-L-arginine methyl ester hydrochloride (L-NAME). Pvp is portal vein pressure, Pvh is the pressure in the hepatic vein close to the division from vena cava inferior, Phlv is the pressure in a hepatic lobulus vein close to the sites of measurement of the hepatic diameters Dhep1 and Dhep2. Qvp is the flow in the portal vein, Qha is the flow in the hepatic artery, PVResHep is the porto-venous resistance and AVResHep is the arterio-venous resistance of the liver. In 7 of the pigs additional micro sonometric data was collected for estimation of liver compliance and capacitance. Compliance is the linear regression slope between liver blood volume increase and Phlv during occlusion of the liver veins. The Y-intercept HBV/Pvhl is the crossing of the y-axis of the linear regression between calculated absolute liver blood volume and Phlv. \* is p-value < 0,05 and \*\* is p-value < 0,005 after mixed models regression with pig identity as random effect.

The effect of Riociguat and Cinaciguat on liver blood flow during NO-modulation

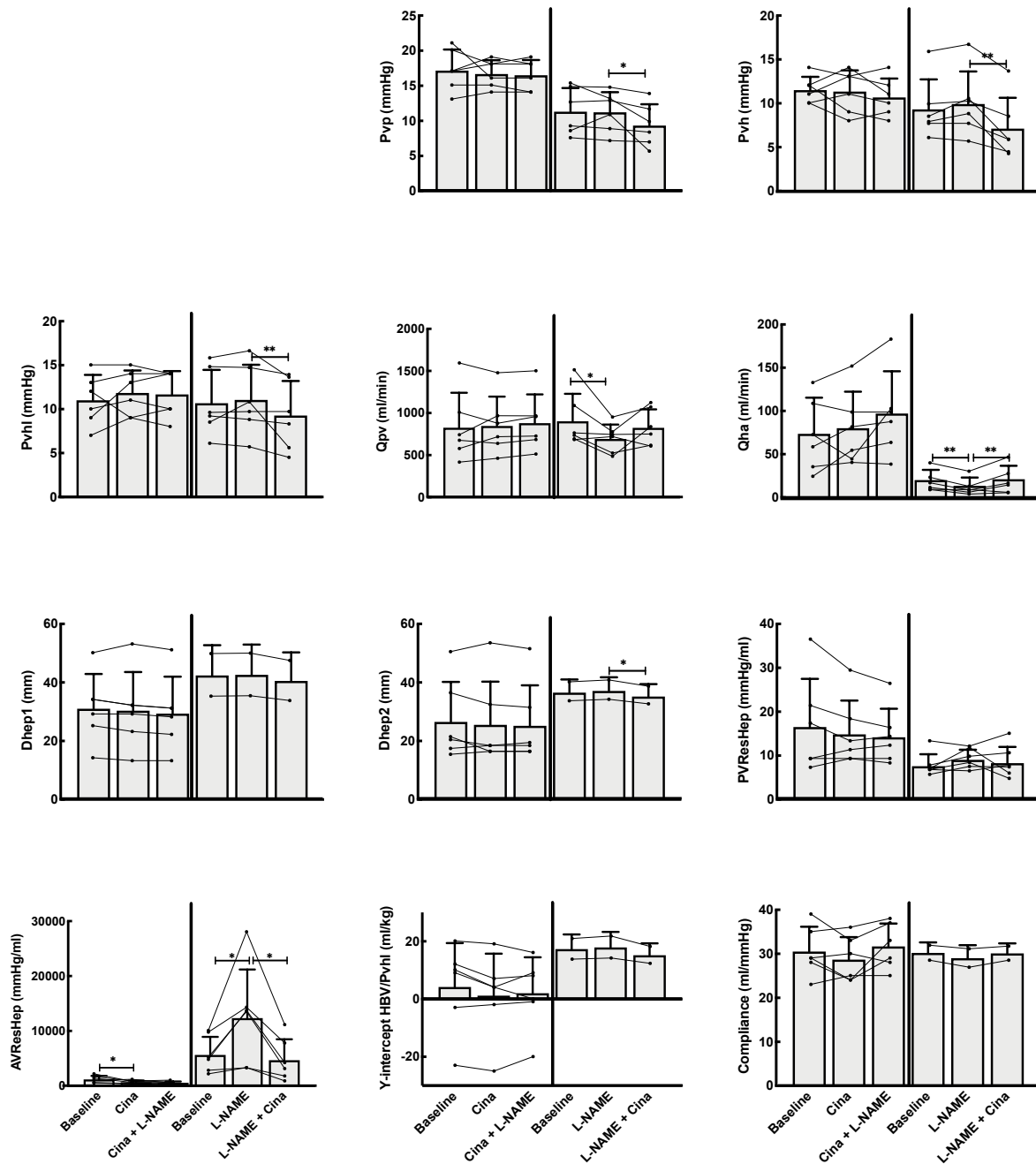


Figure 6. Liver hemodynamics in 12 pigs after Cinaciguat (Cina) in combination with N omega-Nitro-L-arginine methyl ester hydrochloride (L-NAME). Pvp is portal vein pressure, Pvh is the pressure in the hepatic vein close to the division from vena cava inferior, Pvlh is the pressure in a hepatic lobulus vein close to the sites of measurement of the hepatic diameters Dhep1 and Dhep2. Qpv is the flow in the portal vein, Qha is the flow in the hepatic artery, PVResHep is the porto-venous resistance, and AVResHep is the arterio-venous resistance of the liver. In 8 of the pigs, additional micro sonometric data was collected to estimate liver compliance and capacitance. Compliance is the linear regression slope between liver blood volume increase and Phlv during occlusion of the liver veins. The Y-intercept HBV/Phvl is the crossing of the y-axis of the linear regression between calculated absolute liver blood volume and Phlv. \* is p-value < 0,05 and \*\* is p-value < 0,005 after mixed models regression with pig identity as random effect.

## The effect of Riociguat and Cinaciguat on liver blood flow during NO-modulation

### Effects of Cinaciguat and Riociguat on hepatic flows and pressures

Cinaciguat and Riociguat did not affect the portal or arterial liver blood flows. No difference could be found in portal pressure or liver venous pressures. Cinaciguat, however, resulted in a 43% ( $\pm 84\%$ ) fall in arterio-venous resistance from baseline, while no such effect was seen for Riociguat. L-NAME caused a decrease in portal and arterial flows through the liver and increased the arterio-venous resistance by 140% ( $\pm 98\%$ ) but did not affect the porto-venous resistance. Both Cinaciguat and Riociguat reversed the increased arterio-venous resistance induced by L-NAME. Also, pre-treatment with Cinaciguat but not Riociguat prevented the arteriolar vasoconstriction caused by NO-blockade (L-NAME).

### Effects of Riociguat and Cinaciguat on liver compliance and capacitance

Neither Riociguat nor Cinaciguat or L-NAME had any influence on hepatic micro sonometric dimensions or liver compliance. The liver's venous capacitance (the unstressed volume or y-intercept of the liver volume-pressure-curve) did not change by Riociguat, Cinaciguat, or L-NAME.

The effect of Riociguat and Cinaciguat on liver blood flow during NO-modulation

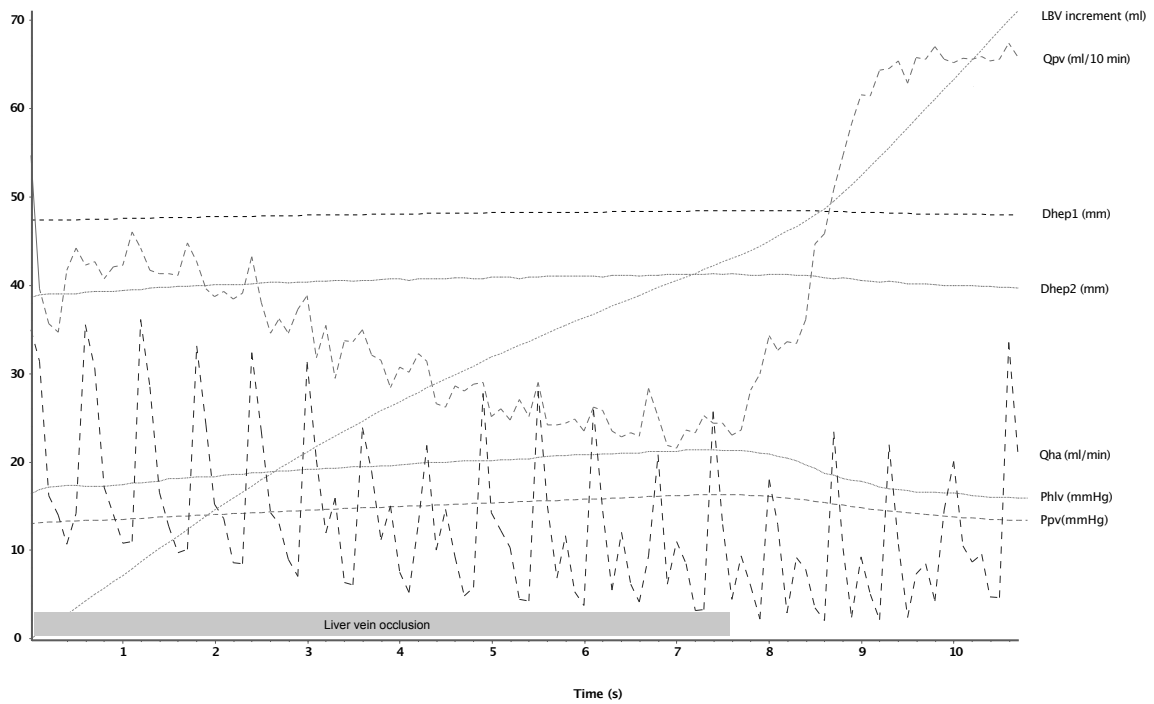


Figure 7. Data from one pig during occlusion of the liver veins.  $Q_{pv}$  is the vena porta flow,  $Q_{ha}$  is the hepatic artery flow, LBV increment is the time integral of these two flows from the start of liver vein occlusion. Dhep1 and Dhep2 are the two liver diameters measured in proximity to the pressure measurement in a hepatic lobulus vein, Phlv. Ppv is the pressure in vena porta.

Figure 2

## The effect of Riociguat and Cinaciguat on liver blood flow during NO-modulation

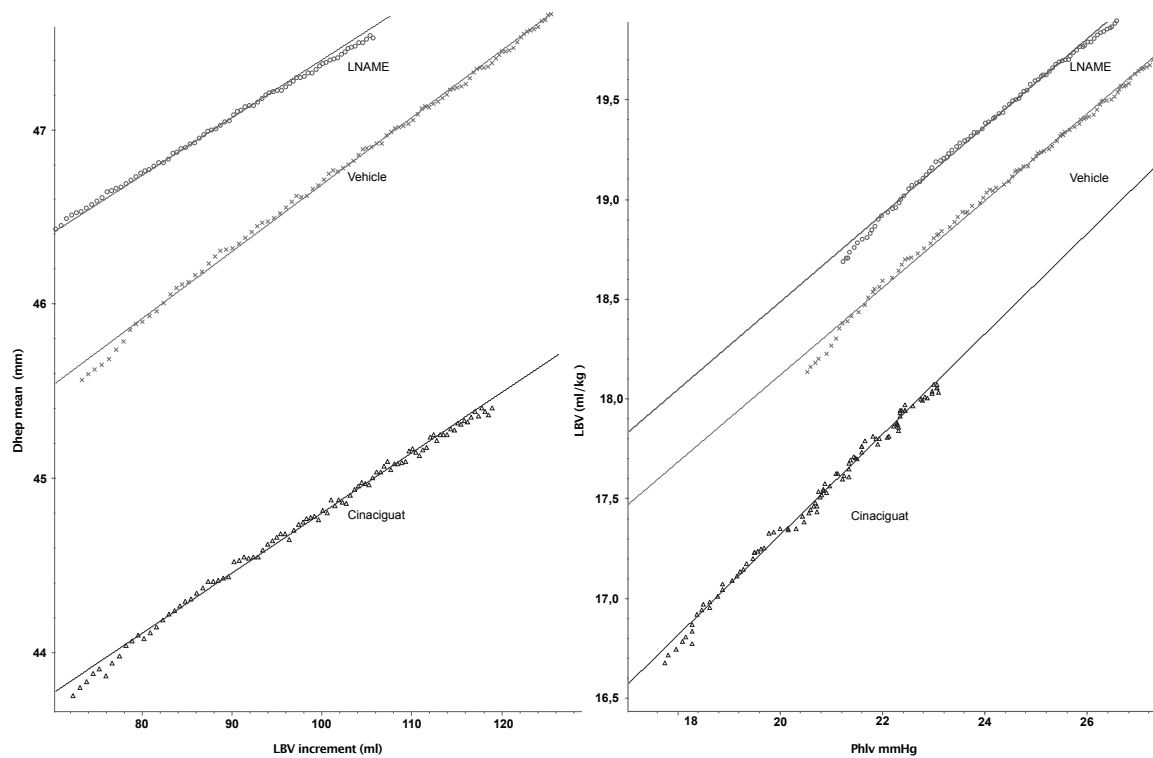


Figure 8. Data from one pig. The left panel shows the correlation of the mean (Dhep mean) of the measured hepatic diameters Dhep1 and Dhep2. LBV increment is the time integral of the hepatic arterial and portal flows during liver vein occlusion. Based on this curve slope and an arbitrary liver blood volume of 17,5 ml/kg at baseline, the relationship between absolute liver blood volume, LBV and hepatic lobulus pressure, Phlv is constructed in the right panel. The y-intercept of this curve is the theoretical liver blood volume at zero liver lobulus vein pressure.

## Discussion

In this study using healthy juvenile pigs, Riociguat and Cinaciguat infusions were given in the highest tolerable doses still avoiding systemic hypotension<sup>10</sup>. Taken together, the results indicate that neither the sGC stimulator nor the activator had any influence on the portal or venous hepatic circulation. Still, their effect could be detected in the arterial flow to the liver. A minor reversal effect of the L-NAME induced flow-reduction in the portal vein could be detected using Riociguat.



## The effect of Riociguat and Cinaciguat on liver blood flow during NO-modulation

Venous congestion is one of the mechanisms of reduced organ perfusion during cardiac failure. This congestion can happen in the absence of overt weight gain, as would be expected if venous congestion was caused by fluid retention and fluid overload. The CHAMPION trial showed that heart failure symptoms and an increase in filling pressure were observed before an increase in total body weight <sup>11</sup>. Furthermore, treatment at the time of increased filling pressure rather than an increase in weight resulted in fewer hospitalizations. In intervention studies like the UNLOAD-trial (ultrafiltration) and EVEREST trial (Tolvaptan), clinical improvement has not been linked to fluid loss or weight reduction <sup>12,13</sup>. These observations suggest that the correlation between circulating blood volume and venous filling pressures is not necessarily a parallel phenomenon. Indeed, the sympathetic nervous system has profound effects also on the venous part of the circulation, modulating the relation between volume and pressure in the highly compliant and high capacitance venous system <sup>14</sup>. The venous system has 30 times the compliance and obtains 70% of the total blood volume <sup>14</sup>. Of particular interest is the splanchnic veins because of their superior capacitance controlled by a high number of alfa-adrenergic receptors and rich sympathetic innervation. Therefore, sympathetic stimulation results in a combined effect with increased arterial pressures due to arteriole vasoconstriction and elevated venous filling pressures due to constriction of splanchnic venous capacitance vessels <sup>14</sup>.

Rapid recruitment of the venous volume reservoir is useful under bleeding or vasodilatation conditions but can lead to congestion during cardiac decompensation. Dysregulation of renal fluid homeostatic mechanisms contributes to the slow development of weight and fluid gain <sup>15</sup>. It is therefore of interest to explore treatment options to attenuate decompensatory reflexes in the venous system. Possible pharmacological modulators are adrenergic blockers, particularly alfa-adrenergic blockers, and blocking of sympatico-stimulation with loop diuretics and parasympathetic stimulation or renal denervation <sup>16,17</sup>. Of particular interest, nitroprusside has been shown to reduce the circulating volume <sup>18</sup>. In this context, the effect of sGC- activators and stimulators on venous capacitance and compliance can potentially interact with such NO-modulators.

## The effect of Riociguat and Cinaciguat on liver blood flow during NO-modulation

We have used the framework of Smiseth and co-workers<sup>4,19-21</sup> with sonometric measurements of the liver calibrated to liver blood inflow during occlusion of the liver veins to evaluate the effects of Riociguat and Cinaciguat. This method has been challenging to operate in various studies, mainly due to high spatial variability in liver dimension changes during blood volume change<sup>22</sup>. In our study, we calibrated the sonometric dimensions against the integral of flow in the portal vein and hepatic artery after occluding the liver veins and thus eliminating the uncertainties of a cubic volumetric model. Even so, the changes in liver dimensions using sonomicrometry are in the submillimetre range, and using the spleen as a marker of venous capacitance and compliance rather than the liver have been shown to increase the accuracy of such calculations<sup>23</sup>. At all registered points, the relationship between liver dimensions and increase in liver volume had a high linear correlation mainly driven by the change in calculated liver volume.

In our hexamethonium-treated, healthy pigs, the sympathetic tone is expected to be low. The unstressed liver volume is therefore expected to be at the upper part of the volume curve. The effects of Riociguat and Cinaciguat in a state of sympathetic vasoconstriction could predictably be different. Kjekshus et al.<sup>20</sup> have investigated the impact of nitroprusside given directly in vena porta in a pig model with no sympathetic blockade but instead using lightly sedated animals with muscular blockade. They observed that nitroprusside in this pharmacological state did increase the unstressed liver volume without changing the compliance. Norepinephrine had the opposite effect. Of notice, the average heart rate in their animal at baseline was  $131 \pm 7$  beats/min with a mean systemic blood pressure of  $110 \pm 5$  mmHg. In comparison, our pigs under continuous sedation had a heart rate of 100 and a mean systemic blood pressure of 79. Riociguat and Cinaciguat's minor effects in our study may reflect that our pigs are already at a low sympathetic level and that the liver already is near its maximum blood volume capacity at baseline. Indeed systemic administration of L-NAME in healthy, anesthetized rats has been shown to increase hepatic arterio-venous resistance, but not porto-venous resistance. On the other hand, administration of a CO-donor in the same rats had the opposite effects, pointing to differential regulation of arterio-venous and porto-venous flow in the liver<sup>24</sup>.

## The effect of Riociguat and Cinaciguat on liver blood flow during NO-modulation

Limitations: The volumetry of the liver with micro sonometry is uncertain, and our results should be validated in future studies using the spleen as an indicator of venous dilation or constriction.

Furthermore, the statistic power of this study is low with a limited number of animals used. This study was performed in healthy, juvenile animals, and the translational value to pathology is uncertain.

## Conclusion

Cinaciguat, but not Riociguat given in the highest tolerable doses to avoid hypotension in healthy juvenile, anesthetized pigs, reduced the arterio-venous resistance through the liver, and reversed the increase in arterio-venous resistance induced by L-NAME. None of the drugs altered the porto-venous resistance, but pre-treatment with Cinciguat or Riociguat blocked the vasoconstrictive effect of NO-blockade on the portal vein flow. None of the drugs changed liver compliance, but Riociguat resulted in a slight reduction of liver capacitance.

## Reference list

1. Ming Z, Han C, Lautt WW. Nitric oxide mediates hepatic arterial vascular escape from norepinephrine-induced constriction. *Am J Physiol - Gastrointest Liver Physiol.* 1999;277(6 40-6):1200-1206.
2. Paula Macedo M, Wayne Lautt W. Shear-induced modulation of vasoconstriction in the hepatic artery and portal vein by nitric oxide. *Am J Physiol - Gastrointest Liver Physiol.* 1998;274(2 37-2):253-260.
3. Næsheim T, How OJ, Myrmel T. Hemodynamic Effects of a Soluble Guanylate Cyclase Stimulator, Riociguat, and an Activator, Cinaciguat, During NO-Modulation in Healthy Pigs. *J Cardiovasc Pharmacol Ther.* 2020.
4. Kjekshus H, Risoe C, Scholz T, Smiseth O a. Methods for assessing hepatic distending pressure and changes in hepatic capacitance in pigs. *Am J Physiol Heart Circ Physiol.* 2000;279(4):H1796-803.
5. Douglas WW. The effect of a ganglion-blocking drug, hexamethonium, on the response of the cat's carotid body to various stimuli. *J Physiol.* 1952;118(3):373-383.
6. Lautt WW. Hepatic Circulation. *Colloq Ser Integr Syst Physiol From Mol to Funct.* 2009;1(1):1-174.

7. Rees DD, Palmer RMJ, Schulz R, Hodson HF, Moncada S. Characterization of three inhibitors of endothelial nitric oxide synthase in vitro and in vivo. *Br J Pharmacol*. 1990;101(3):746–752.
8. Næsheim T, How OJ, Myrmet T. Hemodynamic Effects of a Soluble Guanylate Cyclase Stimulator, Riociguat, and an Activator, Cinaciguat, During NO-Modulation in Healthy Pigs. *J Cardiovasc Pharmacol Ther*. 2021;26(1):75-87.
9. Wang and L. A. Goonewardene Z. The use of MIXED models in the analysis of animal experiments with repeated measures data. *Can J Anim Sci*. 2004;84(1):1-11.
10. Næsheim T, How O-J, Myrmet T. Hemodynamic Effects of a Soluble Guanylate Cyclase Stimulator, Riociguat, and an Activator, Cinaciguat, During NO-Modulation in Healthy Pigs. *J Cardiovasc Pharmacol Ther*. 2020.
11. Ritzema J, Troughton R, Melton I, et al. Physician-directed patient self-management of left atrial pressure in advanced chronic heart failure. *Circulation*. 2010;121(9):1086-1095.
12. Konstam MA, Gheorghiade M, Burnett JC, et al. Effects of oral tolvaptan in patients hospitalized for worsening heart failure: The EVEREST outcome trial. *J Am Med Assoc*. 2007;297(12):1319-1331.
13. Costanzo MR, Guglin ME, Saltzberg MT, et al. Ultrafiltration Versus Intravenous Diuretics for Patients Hospitalized for Acute Decompensated Heart Failure. *J Am Coll Cardiol*. 2007;49(6):675-683.
14. Gelman S. Venous Function and Central Venous Pressure. *Anesthesiology*. 2008;108(4):735-748.
15. Burkhoff D, Tyberg J V. Why does pulmonary venous pressure rise after onset of LV dysfunction: a theoretical analysis. *Am J Physiol Circ Physiol*. 1993;265(5):H1819-H1828.
16. Missouriis CG, Grouzmann E, Buckley MG, Barron J, MacGregor GA, Singer DRJ. How Does Treatment Influence Endocrine Mechanisms in Acute Severe Heart Failure? Effects on Cardiac Natriuretic Peptides, the Renin System, Neuropeptide Y and Catecholamines. *Clin Sci*. 1998;94(6):591-599.
17. Renal sympathetic denervation in patients with treatment-resistant hypertension (The Symplicity HTN-2 Trial): a randomised controlled trial. *Lancet*. 2010;376(9756):1903-1909.
18. Pouleur H, Covell JW, Ross J. Effects of nitroprusside on venous return and central blood volume in the absence and presence of acute heart failure. *Circulation*. 1980;61(2):328-337.
19. Risøe C, Hall C, Smiseth OA. Splanchnic vascular capacitance and positive end-expiratory pressure in dogs. *J Appl Physiol*. 1991;70(2):818-824.
20. Kjekshus H, Risoe C, Scholz T, Smiseth OA. Regulation of Hepatic Vascular Volume : Contributions From Active and Passive Mechanisms During Catecholamine and Sodium Nitroprusside Infusion. *Circulation*. 1997;96(12):4415-4423.
21. Smith ER, Smiseth O a, Kingma I, Manyari D, Belenkie I, Tyberg J V. Mechanism of action of nitrates. Role of changes in venous capacitance and in the left ventricular diastolic pressure-volume relation. *Am J Med*. 1984;76(6A):14-21.
22. Greenway C V., Rothe CF. Ultrasonic crystal measurement of blood volume changes in liver and spleen. *Am J Physiol - Gastrointest Liver Physiol*. 1992;262(5 25-5).
23. Greenway C V, Rothe CF. Ultrasonic crystal measurement of blood volume changes in liver and spleen. *Am J Physiol*. 1992;262(5 Pt 1):G934-9.

The effect of Riociguat and Cinaciguat on liver blood flow during NO-modulation

24. Pannen BHJ, Bauer M. Differential regulation of hepatic arterial and portal venous vascular resistance by nitric oxide and carbon monoxide in rats. *Life Sci.* 1998;62(22):2025-2033.





